Experimental Studies on Plate Fin Heat Exchangers

A Thesis Submitted for Award of the Degree of

Doctor of Philosophy

Sidramappa Alur

Mechanical Engineering Department
National Institute of Technology
Rourkela

Dedicated to

The Memory of My Parents

NATIONAL INSTITUTE OF TECHNOLOGY

ROURKELA—769008
INDIA

Ranjit Kr Sahoo
Professor
Mechanical Engg. Department
NIT Rourkela

Sunil Kr Sarangi
Director
NIT Rourkela

CERTIFICATE

This is to certify that the thesis entitled "Experimental Studies on Plate Fin Heat Exchangers", being submitted by Shri Sidramappa Alur, is a record of bonafide research carried out by him at Mechanical Engineering Department, National Institute of Technology, Rourkela, under our guidance and supervision. The work incorporated in this thesis has not been, to the best of our knowledge, submitted to any other university or institute for the award of any degree or diploma.

(Ranjit Kr Sahoo) (Sunil Kr Sarangi)

Date: January 6, 2012

Acknowledgements

I would like to express my deep sense of gratitude and respect to my supervisors Prof S.K.Sarangi and Prof R.K.Sahoo for their excellent guidance, suggestions and constructive criticism. I feel proud that I am one of their doctoral students. The charming personality of Prof Sarangi has been unified perfectly with knowledge that creates a permanent impression in my mind. It is my proud privilege to work under not only a wonderful supervisor but also a sympathetic person, who always stood on my side at tough times during my stay at N.I.T,Rourkela. I and my family members also remember the affectionate love and kind support extended by Madam Sarangi during our stay at Rourkela.

I also feel lucky to get Prof R.K.Sahoo as one of my supervisors. His invaluable academic and family support and creative suggestions helped me a lot to complete the task successfully. His liberal attitude encouraged me to have a friendly interaction, which never made me feel the burden of work. I record my deepest gratitude to Madam Sahoo for family support all the times during our stay at Rourkela.

I record my gratitude to cryogenic division of Bhabha Atomic research centre,Mumbai for giving us the heat exchanger for testing in our laboratory. I am grateful to Mr. Tilok Singh, Head, the Cryogenic Division of Bhabha Atomic Research Centre (BARC), Mumbai ,Mr. Mukesh Goyal and Dr Anindya Chakravarty for sharing their knowledge and experience on plate fin heat exchangers and for the encouragement throughout this work. I take this opportunity to express my heartfelt thanks to the members of my doctoral scrutiny committee for thoughtful advice and useful suggestions.

I take this opportunity to express my heartfelt gratitude to all the staff members of Mechanical Engineering Department, NIT, Rourkela for their valuable suggestions and timely support. I am deeply indebted to Mr. Biswanath Mukherjee, technical assistant, for the fabrication of the heat exchanger test rig. The hard work put in by Mr. Jitendra Kumar and Mr. Akash Pandey, M.Tech students for making the test rig leak proof and insulated deserves special appreciation. I am also thankful to Raman, Ajay Sutar and Rohit Mukare for their help in organising the seminars. I am also thankful to Mr. Binay Kar, technical assistant, Refrigeration laboratory, for his helping hand during the calibration of the instruments.

I feel lucky to have Mr. Balaji Kumar Choudhury as my co-research fellow. Working with him was really a wonderful and fascinating experience. He has been with me for four years of my research at N.I.T, Rourkela. I am thankful to Mr. Sachindra Kumar Rout, Mr. L.N.Patra, Mr. Prakash , research Scholars for their kind help and valuable suggestions. I am also grateful to Mr. Tapas Sarangi and Mr. Harihar Barkey for the kind help extended in academic matters.

I record my sincere apologies to those whose names I have inadvertently missed despite their meaning contribution during the course of this work.

I am really grateful to my brother and my sisters, in laws and my relatives for their perseverance, encouragement with support of all kinds and their unconditional affection. With a smile on their faces but anxiety in their minds, they stood by my side in times of need. Their presence itself came as a soothing solace. My beloved wife had to manage all kinds of difficult situations all alone during the correction and submission of my thesis. I am sorry for this but feel proud of her. I feel sorry for my kids, Vaibhav and Vaishnavi for disturbing their education in the beginning of my research at N.I.T, Rourkela. I feel proud of their understanding of my situation, their preservance and their adaptability which is beyond their age. They filled my life with joy and laughter. I never felt the burden of the work in their company.

I am grateful to Dr U.C.Kapale, our beloved Principal, for his encouragement and cooperation throughout my research. I wholeheartedly thank my colleagues at H.I.T, Nidasoshi for their well wishes and encouragement. I thank Mr. S.N.Toppannavar, for his kind cooperation and assistance during the correction and submission of the thesis.

I am very grateful to the Boarders of S.S.B. Hall of residence for their love and affection during our stay at N.I.T, Rourkela. Special thanks to Mr. Nimain, for attending to all the essential requirements in the hall.

Sidramappa Alur

(January 6, 2012)

Abstract

Heat exchangers used in cryogenic applications need to have very high effectiveness to preserve the refrigerating effect produced. Normally the heat exchangers used in cryogenic refrigerators and liquefiers have effectiveness of the order of 0.95 or higher. If the effectiveness of the heat exchangers falls below the design value, there may not be any liquid yield. Plate fin heat exchangers, because of their compactness, low weight and high effectiveness, are widely used in aerospace and cryogenic applications. Such heat exchangers have closely spaced fins and offer narrow and intricate passages for the fluid flow which often leads to significant pressure drop. The stringent requirement of high effectiveness in cryogenic refrigerators and liquefiers and high pressure drop occurring in plate fin heat exchangers make it necessary to test the heat exchanger before putting into operation in a liquefier.

Plate fin heat exchanger (PFHE) is a type of compact exchanger that consists of a stack of alternate flat plates called parting sheets and corrugated fins, both being brazed together as a block. Streams exchange heat by flowing along the passages made by the fins between the parting sheets. Separating plates act as the primary heat transfer surfaces and the appendages known as fins act as the secondary heat transfer surfaces intimately bonded to the primary surface. Aluminum is the most commonly used material and stainless steel is employed in high pressure and high temperature applications.

Extensive research has been done on plate and fin heat exchangers over the last eight decades to understand the heat transfer phenomena occurring therein and to determine the dimensionless heat transfer coefficient, j and the friction factor, f. Though experimental investigations predominate in the literature, analytical modeling and numerical solutions have also been carried out. The theoretical solutions often suffer from oversimplification of fin channel geometry and simplifying assumptions made. Experiments on heat transfer over plate fin surfaces are expensive and difficult. Experimental results generated by reputed international laboratories are limited and have remained almost totally proprietary. With successful fabrication of plate and fin heat exchangers, it became necessary for us to devolp the methodology for the design, fabrication and testing of plate fin heat exchangers. An experimental set up has been built in the laboratory to test the plate fin heat exchanger. The validity of the existing correlations is checked by conducting performance test on a counter flow heat exchanger.

One of the earliest and most comprehensive works on compact heat exchangers was carried out by Kays and London at Stanford University in late 1940's. Their report published in 1948 is the most authoritative and reliable source for j and f factors and they are still used today for the geometries tested by the authors. The set-up of the test bench at Stanford was used for accurate measurement of the basic heat transfer and flow friction characteristics of the plate fin surfaces. Several researchers used the experimental technique of Kays and London to develop j and f data for many other surfaces. Several empirical correlations were generated from the data base of Kays and London and other experimental works.The description of the experimental set up used and methodology adopted at that time is described in chapter-II for comparison with the experimental work carried out in this thesis.

The experimental set adopted in this investigation consists of a counter flow heat exchanger. High pressure cold air from a compressor is made to flow through one channel of the heat exchanger. On exit from channel-I, the stream of air is heated in a heating unit and is made to flow through the other channel in the reverse direction. The pressures at the inlet of both the fluids are noted from the pressure gauges. The temperatures at inlet and outlet of both the fluid streams are measured by resistance temperature detectors. Mass flow rate is measured by a rotameter placed at the exit of the hot fluid. The effectiveness is calculated from the measured temperature values for balanced flow. Predicted value of the effectiveness considering longitudinal heat conduction loss is calculated by the rating procedure. Pressure drop across the core for both the fluids is measured by a U- tube manometer. Minor losses such as loss due to bends and pressure losses in the headers are subtracted from the measured pressure drop to get the core loss. The effect of heat loss to the ambient on the effectiveness is obtained by the difference of energy unbalance between the streams.

The temperature difference is a measure of effectiveness of heat exchanger directly from the experiment. The effectiveness of plate fin heat exchanger is an important parameter for the heat exchanger used for cryogenic applications and is used for the calculation of other process parameters. Hence results are expressed as effectiveness and pressure drop versus mass flow rate. On the contrary, representation of effectiveness versus NTU requires estimation of two major parameters; heat transfer coefficient and effective area of heat transfer. These parameters are to be estimated from the correlations. Since there are four such correlations it will be difficult to use any one of them.

Values of heat exchanger effectiveness and pressure drop obtained from experiments are compared with those evaluated by using correlations developed by various investigators. The experimental effectiveness is also compared with the value obtained by simulation software, Aspen MUSE. Heat loss to the ambient leads to two values of effectiveness - ε_h, the effectiveness based on the hot fluid and ε_c, the effectiveness based on the cold fluid. These effectiveness values are compared with the respective effectiveness values obtained by simulation software, Aspen MUSE. The comparison shows that the two effectiveness values agree within $\pm 2.75\,\%$. The mean effectiveness values are compared with the theoretical values obtained (without considering the heat loss) by using the correlations. Comparison shows that correlations developed by Maiti and Sarangi are in better agreement with the experimental data compared to the other correlations where percentage deviation varies from 6.42 to 4.57%.

A large amount of deviation is observed between the measured pressures drop and that computed from various correlations. The difference between the pressure drop values obtained from experiments and by simulation using Aspen MUSE is also significant. Comparison is made between the experimental arrangements used in the present work and that used by Kays and London to explore the possible causes of this deviation.

Uncertainty analysis of results is an essential component in experimental procedure. The uncertainty in the effectiveness of heat exchangers arises from those in mass flow and temperature measurements. Gas volume flow rates are measured with a rotameter and temperature is measured with a platinum resistance thermometer. The uncertainty in experiment is estimated to be 4.8% for an effectiveness of 89%.

Contents

List of Figures

List of Tables

Nomenclature

A Heat transfer area of the heat exchanger with subscripts h or c denoting hot and cold fluid, m^2

A_{ff} Free flow area available for hot or cold fluid with subscripts h or c respectively, m^2

A_{fr} Frontal area available for hot or cold fluid with subscripts h or c respectively, m^2

A_w Total wall area for transverse heat conduction from the hot fluid to cold fluid, m2

a Plate thickness, m

a_f Fin surface area, m^2

a_{ff} Free flow area/fin, m^2

a_{fr} Frontal area/fin, m^2

a_s Heat transfer area/fin, m^2

a_w Total wall cross sectional area for longitudinal conduction, m^2

C Flow stream heat capacity rate with subscript h or c for hot and cold fluids, W/K.

C_d Coefficient of discharge, dimensionless

$C_{\min}$ Minimum of C_c or C_h, W/K

C_p Specific heat at constant pressure, J/kg-K

C_r Heat capacity rate ratio, dimensionless

D_e Equivalent diameter of the flow passage, m

f Fin frequency, Number of fins per meter length, fins/m

f Fanning friction factor, dimensionless

G Core mass velocity, kg/m^2s

H No flow height (stack height) of the heat exchanger core, m

h Height of fins, m

h Convective heat transfer coefficient, W/m^2 K

j The Colburn factor, non-dimensional heat transfer characteristic

K_c Contraction coefficient, no units

K_e Expansion coefficient ,no units

K_f Conductivity of the fin material, W/m- K

K_w Conductivity of the wall material, W/m- K

L Fluid flow (core) length on one side of the heat exchanger, m

l Fin flow length on one side of a heat exchanger, m

l_e Effective fin length for efficiency determination with subscripts h and c denoting hot and cold fluids, m

m Mass flow rate, kg/sec.

N Total number of layers or total number of fluid passages

N_{tu} Number of heat transfer units, $UA/C_{\min}$, dimensionless

n_{tuc} Number of heat transfer units based on cold fluid side, $(\eta_0 hA)_c / C_c$

n_{tuh} Number of heat transfer units based on the hot fluid side, $(\eta_0 hA)_h / C_h$

p_f Fin pitch, $1/f$, m

$\mathrm{Pr} =$ Prandtl number of the fluid

Q = Heat load, W

Re Reynolds number, dimensionless

Re^* Critical Reynolds number with subscripts j or f for heat transfer and pressure drop considerations

s Spacing between adjacent fins, $p_f - t$, m

T Temperature of the fluid (with subscripts c, h or i, o)

t Thickness of fin, m

U_o Overall heat transfer coefficient. W/m^2 K

W Width of the core, m

Greek symbols

σ Ratio of free flow area to frontal area, a_{ff} / a_{fr}, dimensionless

λ Longitudinal conduction parameter, dimensionless

μ Fluid dynamic viscosity, pa-sec

ρ Fluid density, kg/m^3

$\eta_0 hA$ Convection conductance, W/ K

ε Effectiveness of heat exchanger, dimensionless

η_f Fin efficiency, dimensionless.

η_o Overall surface effectiveness of the extended fin surfaces (secondary surfaces) with subscripts c or h denoting cold and hot fluids, dimensionless.

Δp Pressure drops of hot and cold fluid with subscripts h or c, Pa.

δm_1 The uncertainty in mass of hot fluid, kg/sec

δm_2 The uncertainty in mass of cold fluid, kg/sec

δT The uncertainty in temperature, K

$\delta \eta$ The uncertainty in effectiveness

Subscripts:

b Bulk or mean fluid

c Cold fluid side

h Hot fluid side

i Inlet

Max Maximum

Min Minimum

m mean

o Overall

w Wall or properties at the wall temperature

Chapter 1

Introduction

Chapter I

INTRODUCTION

Heat exchangers used in cryogenic applications need to have very high effectiveness to preserve the refrigerating effect produced. Normally the heat exchangers used in liquefiers have the effectiveness of the order of 0.95 or higher. If the effectiveness of heat exchangers falls below the design value, there may not be any liquid yield [1]. The minimum effectiveness of heat exchanger devices required in regenerative refrigerators stands at 95-98%. In aircrafts where the demand on performance is not high, the volume and weight of the heat exchanger should be kept at minimum. These requirements have led to the development of a unique class of heat exchangers known as compact heat exchangers. Compact heat exchangers present a large surface area (area to volume ratio greater than 700 m^2/m^3).

1.1 Plate fin heat exchanger

Plate fin exchanger is a type of compact heat exchanger where the heat transfer surface area is enhanced by providing extended metal surface, interfaced between the two fluids and is called the fins. Out of the various compact heat exchangers, plate fin heat exchangers are unique due to their superior construction and performance. They are characterized by high effectiveness, compactness, low weight and moderate cost. As the name suggests, a plate fin heat exchanger (PFHE) is a type of compact exchanger that consists of a stack of alternate flat plates called parting sheets and corrugated fins brazed together as a block. Streams exchange heat by flowing along the passages made by the fins between the parting sheets. Separating plates act as the primary heat transfer surfaces and the appendages known as fins act as the secondary heat transfer surfaces intimately bonded to the primary surfaces. Fins not only form the extended heat transfer surfaces, but also work as structural supports against internal pressure difference. The side bars prevent the fluid from spilling over and mixing with the second fluid or leaking to outside. The fins and side bars are brazed with the parting sheets to ensure good thermal link and to provide mechanical stability. Figure 1.1 shows an exploded view of

two layers of a plate fin heat exchanger. Such layers are arranged together in a monolithic block to form a heat exchanger.

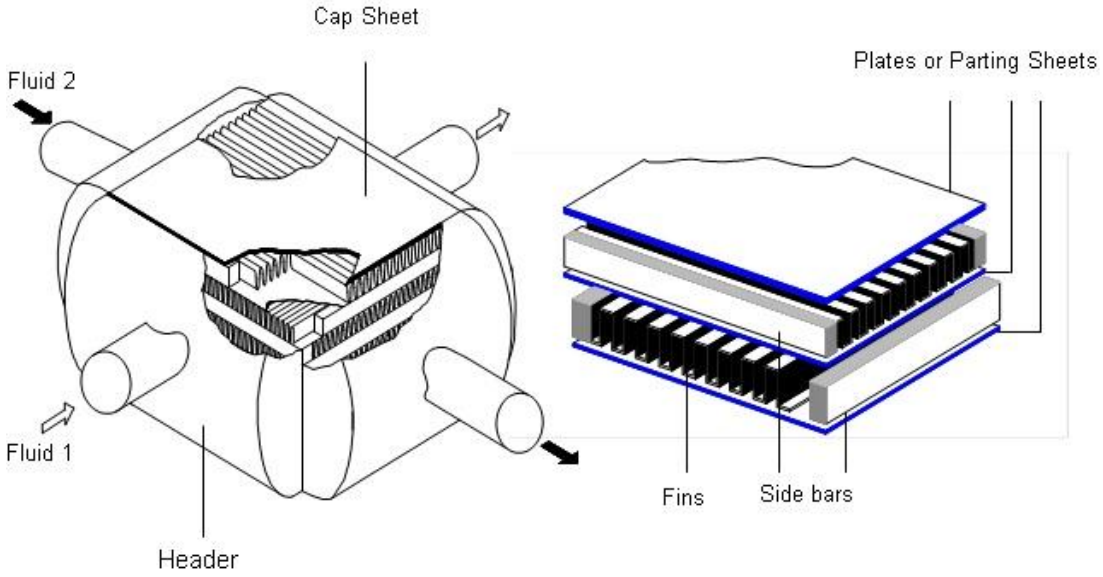

Figure 1.1: Plate fin heat exchanger assembly and details [45]

A. Advantages and disadvantages

Plate fin heat exchangers offer several advantages over the other types of heat exchanger:

i) **Compactness:** Large heat transfer surface area per unit volume (typically 1000 m^2/m^3), is usually provided by plate fin heat exchangers. Small passage size produces a high overall heat transfer coefficient because of the heat transfer associated with the narrow passages and corrugated surfaces.

ii) **Effectiveness:** Very high thermal effectiveness more than 95% can be obtained.

iii) **Temperature control:** The plate fin heat exchanger can operate with small temperature differences. A close temperature approach (temperature approach as low as 3K) is obtained for a heat exchanger exchanging heat with single phase fluid streams. This is an advantage when high temperatures need be avoided. Local overheating and possibility of stagnant zones can also be reduced by the form of the flow passage.

iv) **Flexibility:** Changes can be made to heat exchanger performance by utilizing a wide range of fluids and conditions that can be modified to adapt to various design specifications. Multi stream operation is possible up to 10 streams.

v) **Counter flow**: True counter-flow operation (Unlike the shell and tube heat exchanger, where the shell side flow is usually a mixture of cross and counter flow) is possible in a plate fin heat exchanger.

The main disadvantages of a plate fin heat exchanger are:

i) The rectangular geometry used puts a limit on operating range of pressure and temperatures
ii) Difficulty in cleaning of passages, which limits its application to clean and relatively non-corrosive fluids, and
iii) Difficulty of repair in case of failure or leakage between passages.
iv) Relatively high pressure drop due to narrow and constricted passages.

B. Manufacturing process

The basic principles of plate fin heat exchanger manufacturing process are the same for all sizes and all materials. The heat exchanger is assembled from a series of flat sheets and corrugated fins in a sandwich construction. Separating plates (i.e. parting sheets) provide the primary heat transfer surface. Separating plates are positioned alternatively with the layers of fins in the stack to form the containment between individual layers. These elements i.e., corrugations, side-bars, parting sheets and cap sheets are held together in a jig under a predefined load, and placed in a brazing furnace to form the plate fin heat exchanger block. After this, the header tanks and nozzles are welded to the block, taking care that the brazed joints remain intact during the welding process. Differences arise in the manner in which the brazing process is carried out. The methods in common use are salt bath brazing and vacuum brazing. In the salt bath process, the stacked assembly is preheated in a furnace to about 550^0 C, and then dipped into a bath of fused salt composed mainly of fluorides or chlorides of alkali metals. The molten salt works as both flux and heating agent, maintaining the furnace at a uniform temperature. In case of heat exchangers made up of aluminum, the molten salt removes grease and the tenacious layer of aluminum oxide, which would otherwise weaken the joints. Brazing takes place in the bath when the temperature is raised above the melting point of the brazing alloy. The brazed block is cleaned of the residual solidified salt by dissolving in water, and is then thoroughly dried. In the vacuum brazing process, no flux or separate pre-heating furnace is required. The assembled block is heated to brazing temperature by radiation from electric heaters and by conduction from the exposed surfaces into the interior of the block. The absence of oxygen in the brazing

environment is ensured by application of high vacuum (Pressure ≈ 10^{-6} millibar). The composition of the residual gas is further improved (lower oxygen content) by alternate evacuation and filling with an inert gas as many times as experience dictates. No washing or drying of the brazed block is required. Many metals, such as aluminum, stainless steel, copper and nickel alloys can be brazed satisfactorily in a vacuum furnace. In recent times vacuum brazing process has been used almost exclusively for manufacture of plate fin heat exchangers.

C. Applications

The plate-fin heat exchanger is suitable for use over a wide range of temperatures and pressures for gas-gas, gas-liquid and multi-phase duties. They are used in a variety of applications. They are mainly employed in the field of cryogenics for separation and liquefaction of air, natural gas processing and liquefaction, production of petrochemicals and large refrigeration systems. The exchangers that are used for cryogenic air separation and LPG fractionation are the largest and most complex units of the plate fin type and a single unit can be of several meters in length. Brazed aluminum plate fin exchangers are widely used in the aerospace industry because of their low weight to volume ratio and compactness. They are being used mainly in environment control system of the aircraft, avionics cooling, hydraulic oil cooling and fuel heating. Making heat exchangers as compact as possible has been an everlasting demand in automobile and air conditioning industries as both are space conscious. In the automobile sector they are used for making the radiators. The other miscellaneous applications are:

i) Fuel cells
ii) Process heat exchangers
iii) Heat recovery plants
iv) Pollution control systems
v) Fuel processing and conditioning plants
vi) Ethylene and propylene production plants

D. Flow arrangement

A plate fin heat exchanger can have two or more streams, which may flow in directions parallel or perpendicular to one another. When the flow directions are parallel, the streams may flow in the same or in opposite sense. So there are three primary flow arrangements for a plate fin heat exchanger – (i) parallel flow, (ii) counter-flow and (iii)

cross flow. Thermodynamically, the counter-flow arrangement provides the highest heat (or cold) recovery, while the parallel flow geometry gives the lowest. The cross flow arrangement, gives an intermediate thermodynamic performance, by offering superior heat transfer properties and easier mechanical layout. Under some circumstances, a hybrid cross – counter-flow geometry provides greater heat (or cold) recovery with superior heat transfer performance. Thus in general engineering practice, there are three main configurations for the plate fin heat exchangers: (a) cross flow, (b) counter-flow and (c) cross-counter flow.

(a) Cross flow:

Cross flow and counter flow arrangement of fluids in heat exchangers is as shown in Figure (1.2). In cross flow heat exchangers, the fluids flow in directions normal to each other. Thermodynamically the effectiveness for cross flow heat exchangers falls in between that for the counter flow and parallel flow arrangements. The largest structural temperature difference exists at the corner of the entering hot and cold fluids. Only two streams are handled in a cross flow type of a heat exchanger which eliminates the need for distributors. For this type of heat exchangers the header tanks are located on all four sides of the heat exchanger core, making this arrangement simple and cheap. If high effectiveness is not necessary, and if the two fluid streams have widely differing volume flow rates, or if either one or both streams have constant temperature, the cross flow arrangement should be preferred. Typical applications include automobile radiators and some aircraft heat exchangers.

(b) Counter flow:

In a counter flows heat exchanger the two fluids flow parallel to each other but in opposite directions. The counter-flow heat exchanger provides the most thermally effective arrangement for recovery of heat or cold from process streams. A counter flow arrangement is thermodynamically superior to any other flow arrangement. It is the most efficient flow arrangement, producing the highest temperature change in each fluid compared to any other two-fluid arrangement for a given overall thermal conductance (UA), fluid flow rates and fluid inlet temperatures. Cryogenic refrigeration and liquefaction equipment use this geometry almost exclusively. But these type of heat exchangers demand proper design because of the complex geometry of headers.

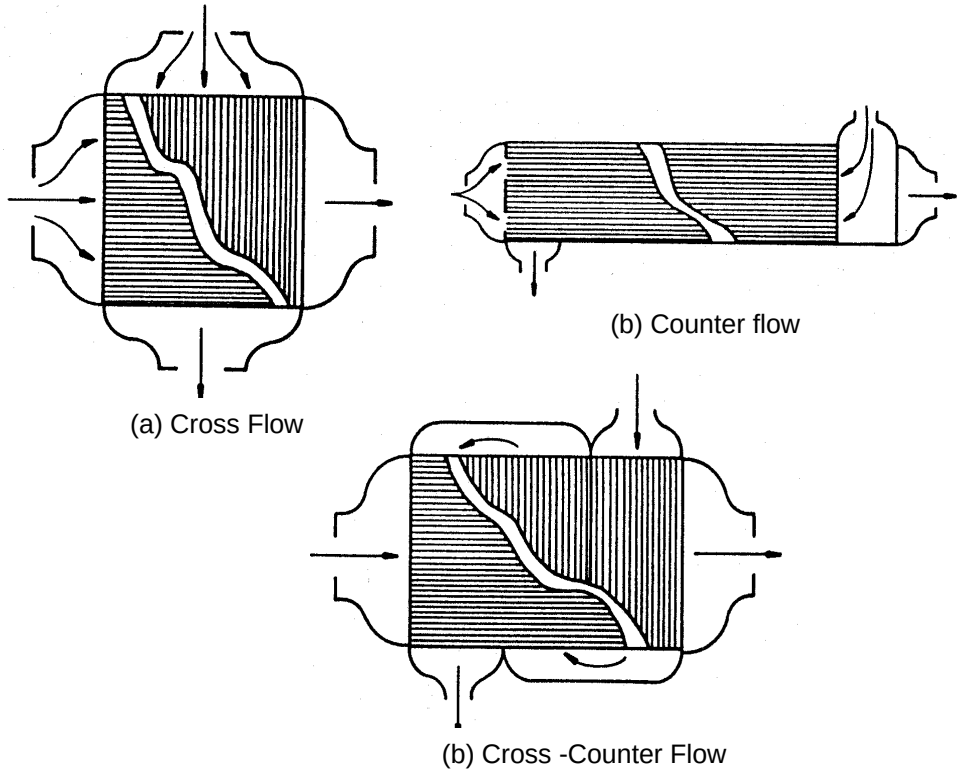

Figure 1.2: Cross flow and counter flow arrangement[45]

(c) Cross-counter flow:

The cross-counter flow geometry is a hybrid of counter-flow and cross flow arrangements, delivering the thermal effectiveness of counter-flow heat exchanger with the superior heat transfer characteristics of the cross flow configuration. In this arrangement, one of the streams flows in a straight path, whereas the second stream follows a zigzag path normal to that of the first stream. While moving along the zigzag path, the second fluid stream covers the length of the heat exchanger in a direction opposite to that of the direct stream. Thus the flow pattern can be assumed to be globally counter flow while remaining locally cross flow. Cross-counter flow PFHEs are used in applications similar to those of simple cross flow exchangers, but they allow more flexibility in design and fabrication. They are particularly suited for the applications where the two streams have considerably different volume flow rates, or permit significantly different pressure drops. The fluid with the larger volume flow rate or that with the smaller value of allowable pressure drop is made to flow through the straight channel, while the other stream follows the zigzag path. For example, in a liquid-to-gas heat exchanger, the gas stream with a large volume flow rate and low allowable pressure drop is assigned the straight path, while the liquid stream with a high allowable pressure drop

flows normal to it over a zigzag path. This arrangement optimizes the overall geometry. (Figure 1.2 shows a cross-counter flow arrangement for heat exchanger)

1.2 Plate fin heat transfer surfaces

The plate fin exchangers are mainly employed for liquid-to-gas and gas-to-gas applications. Due to the low heat transfer coefficients in gas flows, extended surfaces are commonly employed in plate-fin heat exchangers. By using specially configured extended surfaces, heat transfer coefficients can also be enhanced. While such special surface geometries provide much higher heat transfer coefficients than plain extended surfaces, but at the same time, the pressure drop penalties are also high, though they may not be severe enough to negate the thermal benefits. A variety of extended surfaces like the plain trapezoidal, plain rectangular shown in Figure 1.3 can perform such function. The offset strip fin geometry is included in the present study.

In order to improve the gas side heat transfer coefficients, surface features are needed to be provided on the gas side. These features may be divided into two categories: the first, in which the surface remains continuous (wavy and herring-bone fins) and the second in which it is cut (offset, louvered). In a continuous type fin, the corrugations cause the gas to make sudden direction changes so that locally the velocity and temperature gradients are increased (Figure 1.4). This results in local enhancement of heat transfer coefficient. But an undesirable consequence of such enhancement in heat transfer coefficient is an increase in the friction factor and pressure drop whereas in a discontinuous type of fin geometry boundary layers are interrupted, otherwise this would have formed on a continuous plate. Adjacent to the leading edge of the fin, both heat transfer coefficient and friction factor are high due to generation of fresh boundary layers. But in addition to this friction drag, form drag is also formed due to the finite thickness of the fin. Although friction drag is associated with high heat transfer coefficient, form drag has no counterpart and represents one form of wasted energy. The form drag can be substantial depending on the quality of the cutting edge. However, machined-formed fins are generally free from this problem.

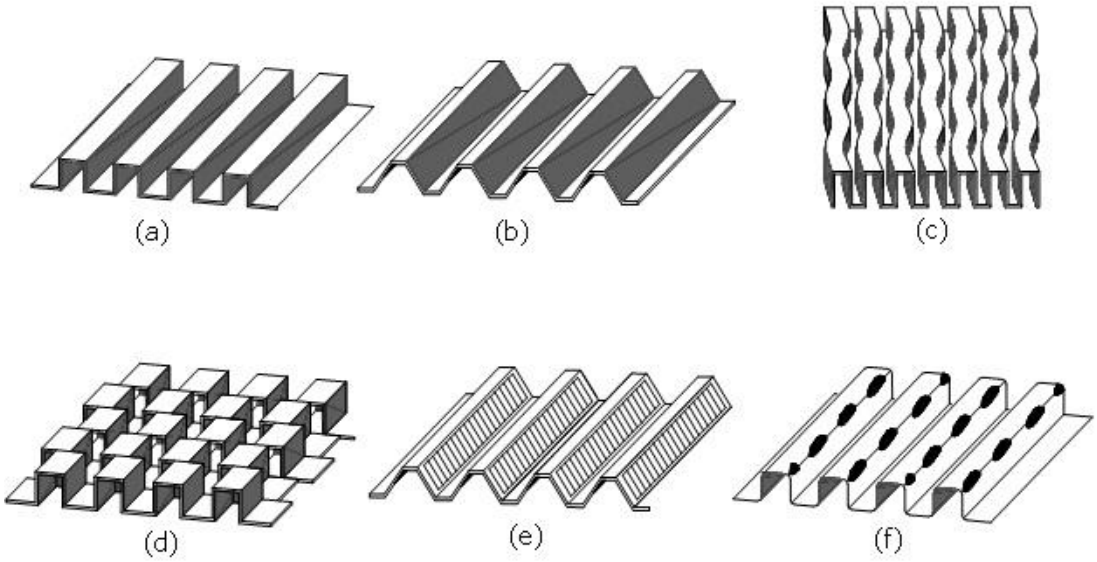

Figure 1.3: Types of plate fin surfaces: (a) Plain rectangular (b) Plain trapezoidal (c) Wavy (d) Serrated or offset strip fin (e) Louvered (f) Perforated [45]

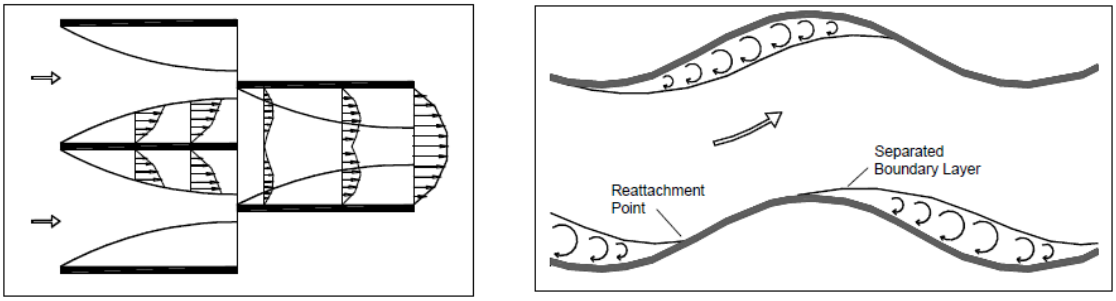

Figure 1.4: Details of boundary layer for flow across offset strip and wavy fin [44]

1.3 Heat transfer and flow friction characteristics

The heat transfer and flow friction characteristics of a heat exchanger surfaces are commonly expressed in non-dimensional form and are simply referred to as the basic characteristic or basic data of the surface. Various correlations are available in literatures which express the Colburn factor, j and friction factor, f as functions of Reynolds number and other geometrical properties**.** The Colburn and friction factors are defined by the relations:

$$j = \frac{h}{GC_P}(\mathrm{Pr})^{2/3} \tag{1.1}$$

$$\Delta p = \frac{4flG^2}{2D_h\rho} \tag{1.2}$$

Where, h =heat transfer coefficient (W/m^2-K)

$G =$ Mass velocity (kg/s-m^2) [on the basis of minimum free flow area]

$L =$ Length of flow passage (m)

$D_h =$ Hydraulic diameter (m)

$\rho =$ Mean density of fluid (kg/m^3)

1.4 The measurement principles

The experimental data given by Kays and London [2] are the most authoritative and reliable sources of heat transfer and pressure drop characteristic of the plate fin heat exchangers. The experimental set up used by Kays and London [2] consists of cross flow heat exchanger. One channel of the cross flow heat exchanger is made of the surface to be characterized. The fluid flowing over this test section should preferably be one which is likely to be used in service. A condensing steam is made to flow through the other channel giving a very high heat transfer coefficient so that thermal resistance on that side is neglected. The longitudinal heat loss through the walls is negligible and is not considered in determining the heat transfer characteristics.

The experimental set up used here consists of a counter flow heat exchanger. Cold air from the compressor is made to flow through one channel where as the hot air coming from a heating unit is made to flow through another channel in the counter flow direction. The pressures at the inlet of both the fluids are noted from the pressure gauges. The temperatures at inlet and outlet of both the fluids are measured by resistance temperature detectors. From the measurement of effectiveness, overall heat transfer coefficient and the number of transfer units are calculated. The effectiveness considering the longitudinal heat loss is calculated using Kreogers [84] equation. The effectiveness is calculated from measurement of the temperature and mass flow rates.

1.5 Objectives of the study

In open literature many correlations of heat transfer coefficient and friction factor are available for design and rating of PFHE. In many cases, reports on validation of these correlations with experiments are scarce. Hence the main objective of the present work is to evaluate the performance parameters of a counter flow plate and fin heat exchanger (PPHE) which includes the following steps.

i) Design of a PFHE based on a chosen correlation.
ii) Industrial fabrication of the PFHE with the above supplied design data.

iii) Fabrication of a test rig for testing.
iv) Comparison of the values of effectiveness, overall heat transfer coefficient and pressure drop obtained by experiment with the rating values of PFHE based on various other correlations.

The hot test method is adopted for this study. The correlation used for design and rating of PFHE are listed as

i) Maiti- Sarangi correlation[45]
ii) Manglik- Bergles correlation[70]
iii) Joshi-Webb correlation[68]
iv) Simulation software of Aspen-MUSE.[113]

1.6 Organization of the Thesis

The thesis has been arranged into seven chapters. Chapter I deals with general introduction to compact plate fin heat exchanger and enumerates the objective of the present investigation. In Chapter II, a brief review of relevant literature covering theoretical and experimental studies undertaken for determination of heat transfer and flow friction characteristics of surfaces, and review of various correlations available in literature for determination of heat transfer and flow friction characteristics of offset strip fin surfaces have been presented. Chapter II also covers review of literature on irreversibilities that affect heat exchanger performance.

In Chapter III, design procedure for plate fin heat exchanger is outlined. Design of the given plate fin heat exchanger using correlations developed by Maiti and Sarangi [45], Manglik and Bergles[70], Joshi and Webb [68] and simulation software, Aspen-MUSE [113] have been presented. Rating i.e., calculation of performance parameters of plate fin heat exchanger using the correlations developed by Maiti and Sarangi [45], Manglik and Bergles [70], Joshi and Webb [68] and simulation software, Aspen-MUSE [113] has been presented in Chapter IV.

A detailed description of the experimental set up and the operating procedure for the hot test has been given in Chapter V. Description of the different components of the experimental set up, instruments used and their calibration procedure are given.

Uncertainty analysis of the results has also been included in Chapter V. Experimental results have been presented in Chapter VI. Chapter VI also contains the graphs showing the comparison between the theoretical and experimental values of performance parameters and discussion on the results.

Chapter VII, the last and final chapter, is devoted to concluding remarks and for defining the scope of future work.

Chapter 2

Literature Review

Chapter II

LITERATURE SURVEY

Plate fin heat exchangers, because of their compactness, low weight and high effectiveness are widely used in aerospace and cryogenic applications. Cryogenic liquefiers need heat exchangers of very high effectiveness(of the order of 0.95 or more) and the liquefiers cease to produce any liquid if the effectiveness of heat exchangers falls below the design value[1].Correct design and quality construction of heat exchangers is essential for proper functioning of such systems.

The heat transfer coefficient and the flow resistance are expressed in non dimensional form as Colburn factor, j and the friction factor, f. Accurate prediction of the heat transfer coefficient and friction factor is essential for proper design of heat exchangers. The Colburn factor, j and the friction factor, f are expressed as functions of Reynolds number and other geometrical parameters. j and f factors can be determined by numerical modeling of the flow field through CFD.In spite of the progress in computing power, it is not possible to predict j and f data by numerical solution. This is because the models are usually based on certain simplifying assumptions. Numerical solution along with flow visualization, however, helps in understanding the flow physics associated with heat transfer enhancement. It is also possible to carry out a parametric study on the effect of geometrical parameters on the performance of finned surfaces.

Fundamental relations describing various types of heat transfer phenomena and heat exchanger design techniques have been discussed in well known text books [2-8].The book "Compact Heat Exchangers" by Kays and London [2] provides an excellent introduction to the analysis of plate fin heat exchangers, and contains a valuable database on the heat transfer and flow friction characteristics of several fin geometries. The recent work of Shah [7-8] provides the most comprehensive information on the subject, particularly on compact plate fin heat exchangers. Several specialized monographs and conference proceedings, covering basic heat transfer, heat transfer augmentation and design and simulation methodologies have further enriched the literature [9-13].

Journals on thermal engineering and heat transfer devote a sizable portion of their content to research findings on heat exchangers [14-17].Two major journals: Heat

Transfer Engineering [18] and International Journal of Heat exchangers [19] are almost exclusively dedicated to the subject of heat exchangers.

One of the earliest and most comprehensive experimental works on compact heat exchangers was carried out by Kays and London at Stanford University in late 1940.Their report [37] published in 1948 gives the complete methodology and details of the experimental set up. Several researchers used the same experimental technique for the experimental determination of non dimensional heat transfer coefficient and friction factor. Later on several empirical correlations were generated from the experimental data of Kays and London [2] and other experimental works.

Analytical determination of non dimensional heat transfer and pressure drop characteristics is difficult. This is because the heat transfer and flow friction characteristic of a surface are strong functions of geometrical parameters such as fin height, fin spacing, fin thickness, etc; each fin type needs to be characterized separately.

This literature review focuses primarily on plate fin heat exchangers, details of the experimental, numerical and analytical studies, predictions of j and f factors for offset strip fin surfaces and a brief review on the secondary irreversibilities.

2.1 Plate Fin Heat Exchangers

The plate fin heat exchanger, a member of the compact heat exchanger family, has found wide applications in various fields of engineering. They are widely used in aircraft and automobile industry, chemical process plants and cryogenic engineering.

History of Development

Early developments of compact heat exchangers were stimulated by their applications in the automobile and aircraft industries. During the 1930's,the secondary surface plate and corrugation construction became established for aero engine radiators using dip soldered copper as the material of construction [20].Development of compact heat exchangers in the automobile and air conditioning industries has been reviewed by Mori et al [21] and Cowell et al [22].In the early 1940s, the introduction of the aluminum dip-brazing process made it possible to manufacture aircraft heat exchangers with aluminum and resulted in substantial reduction in weight[23]. Subsequently, brazed aluminum heat exchangers, fabricated from plate pairs, were employed as aircraft engine intercoolers [24].Development of machines capable of producing very precise

corrugated fins with varying height and spacing lead to mass production. Continued reduction in weight, increase of surface area density, enhanced reliability and flexibility that it offers to the manufacturer have made the plate fin heat exchanger indispensable in gas to gas heat exchange applications in cryogenic and chemical industries. More recently their application has been extended to boiling and condensation duties [25, 26].Dip brazing was first employed commercially by the Trane Company in USA during World War II and the first industrial size exchangers were manufactured in 1949 [24].

No loss of strength and ductility at low temperatures made aluminum extremely suitable for cryogenic applications. Tubular heat exchangers used in cryogenic applications were replaced by aluminum plate and fin heat exchangers. Features such as compact shape, low weight, and design flexibility available with plate fin heat exchangers led the way for their application on a much wider scale.Devolpment of large aluminum plate fin heat exchangers and that of tonnage air separation plant supported each other for further growth.

Today, brazed aluminum plate fin exchangers are being designed and manufactured by several reputed companies around the globe. Information on these companies and their products are available from the web sites of the Aluminium Plate Fin Heat Exchanger Manufacturer's Association [27].The five members of the organization are Chart Heat Exchanger, USA[28], Kobe Steel Ltd, Japan [29], Linde AG, Germany [30], Nordon Cryogenie,France [31], and Sumitomo Precision Products Co Ltd,Japan [32]. In addition, several smaller but knowledge based companies manufacture heat exchangers for specialized applications. The automobile industry is another major manufacturer and user of aluminium plate fin exchangers.

Several specialized laboratories also made significant contribution to the research on plate fin heat exchangers. Most notable among them are the Heat Transfer and Fluid Flow Services (HTFS)[33] in England and Heat Transfer Research Inc (HTRI) [34] in USA. These organizations, supported by industry and institutions from around the world continue to produce most advanced and authentic information on the subject of plate fin heat exchangers.

Fabrication of heat exchangers

The basic approach to fabricate plate fin heat exchangers is to assemble the parting sheets, fins, side bars and top plates together in a fixture and to braze the assembly to form the heat exchanger core. While the side bars and the parting sheets are cut to size by milling and shearing, electro discharge machining(EDM) is employed

for cutting the preformed thin walled fins (thickness of 0.1 mm) to the required shape and size. Typical materials include alloys of aluminum or stainless steel. Manganese based 3000-series aluminium alloy (e.g Al 3003) can be easily brazed using 7 % Silicon based aluminium filler metal (e.g.4004).For stainless steel the material of construction is SS-304 and the filler material is a low melting nickel-iron alloy.

The brazing of fins to parting sheets is done either by dip brazing or, more commonly, by vacuum brazing technique. Most metals, such as stainless steel, copper and nickel alloys, can be brazed satisfactorily in a vacuum brazing furnace.Aluminium, because of the tenacious oxide layer that forms quickly on the surface, requires either a molten salt bath to dissolve the oxide or a very high vacuum [12].Detailed information on different brazing techniques is available in literature[12,35-36].

In the dip brazing technique, the stacked assembly is heated in a furnace to a temperature few tens of degrees below the melting point of the brazing alloy.The preheated assembly is then dipped into a bath of fused salt mainly composed of fluorides and chlorides of alkaline metals. The molten salt bath, with its temperature carefully controlled, acts both as a flux and as the heating agent. On entry into the salt bath, the brazing alloy melts and flows by surface tension along the joints between the separating sheets, fins and sidebars. On completion of salt-bath brazing, the unit is washed with clean water, followed by a wash with dilute nitric acid. Finally the unit is washed thoroughly with dematerialized water [35] to remove traces of the acid.

In the vacuum brazing process, the stacked assembly is heated up to the brazing temperature by radiation heating in a vacuum furnace. High vacuum (10^{-6} torr) ensures a very low partial pressure of oxygen in the atmosphere, and facilitates chemical splitting of the oxides).The size of the exchanger determines the temperature ramp and the soaking time to be employed. In case of vacuum brazing of aluminium,the narrow margin between the melting point of the brazing alloy and the parent metal (about 50 K) makes it mandatory to employ close temperature control in the furnace [36].For small heat exchangers, an independent six-zone control with 1 K variation is adopted, while large units demand still more specialized control strategy. It is done to ensure complete and uniform heating and chemical decomposition of the oxide layer. The system temperature is raised quickly to the melting temperature of the brazing alloy, held for one or two minutes, and brought down to a temperature 50 K below the brazing temperature. This is done to avoid creeping deformation of the assembly under its own weight. In stainless steel exchangers, because of the large difference in the melting temperature of the braze alloy and the parent metal, such care is not strictly necessary.

The headers and the nozzle are welded to the heat exchanger core by TIG welding. Care must be taken to ensure that remelting of the already brazed joints does not take place. This is a serious problem in stainless steel exchangers where the difference in melting temperatures of the parent metal and brazing alloy can exceed 50 K. The heat exchanger thus fabricated is then subjected to a series of tests viz. leak test, pressure test etc before final acceptance for service.

2.2 Experimental studies

The prediction of non-dimensional heat transfer coefficient, j and friction factor, f by numerical solution has not yielded accurate results because of the limitation of the computing resources and the simplifying assumptions made. Empirical relations for the j and f factors can be successfully used in less critical designs but for the more critical design such as application in cryogenic systems, experimental determination of the non dimensional heat transfer coefficient, j and the friction factor, f remains the only choice. The experimental work can be conducted to check whether a given heat exchanger meets the prescribed thermal performance and pressure drop requirement, and to analyze the various causes of degradation and malfunctioning.

The experimental methods can be broadly classified as follows:

1. Steady state technique where heat is transferred from one fluid to another through a separating wall (recuperative heat exchanger).
2. Transient technique where heat is exchanged with a solid matrix (regenerative heat exchanger). This technique is further classified as
    a. Single blow method, and
    b. Periodic test methods.

A. Steady state methods

a) Kays and London

One of the earliest and most comprehensive works on compact heat exchangers was carried out by Kays and London at Stanford University in late 1940.Their report published in 1948 is the most authoritative and reliable source for j and f factors till today. Most of the correlations developed later are reworking of these correlations. Their set up for the test bench at Stanford is used for the accurate measurement of the basic

heat transfer and flow friction characteristics. The methodology they adopted and conditions in which these correlations are derived has been discussed here for comparison with the experimental work carried out in this study.

In the steady state method, a cross flow type heat exchanger is usually employed as the test exchanger. One channel of the cross flow heat exchanger is made of the surface to be characterised.The fluid flowing over this test surface should preferably be one which is likely to be used in service. Because a majority of plate fin heat exchangers are used in gas to gas applications, and because most gases have comparable physical properties, air is conventionally used as the testing medium. The fluid flowing over the second channel must provide high heat transfer rate and low pressure drop to improve accuracy. The list of fluids with high heat transfer coefficient includes condensing steam, hot water and oil.

In a steady state experiment, measurement of temperatures and mass flow rates in the two sides provides the required information to compute the heat exchanger effectiveness. An $\varepsilon - Ntu$ relation, appropriate to the cross flow arrangement, is applied to determine the N_{tu} and hence the overall heat transfer coefficient (U), the inverse of which is related to the resistances of individual sides and that of the separating wall. Assuming that the fouling resistances are negligible; the overall thermal resistance (1/UA) is expressed by the following relation:

$$\frac{1}{UA} = \frac{1}{(\eta_0 hA)_{unknown}} + \frac{1}{(\eta_0 hA)_{known}} + R_{wall} \tag{2.1}$$

where,

$$\eta_0 = 1 - (a_f / a_s) \times (1 - \eta_f) \tag{2.2}$$

where

a_f / a_s is the ratio of fins to the total surface area, and η_f is the fin efficiency.

The fin efficiency η_f is calculated by the formula

$$n_f = \tanh(Ml\ ) / (Ml) \tag{2.3}$$

with

$$M = \sqrt{\frac{(2 \times h\ )}{(K_f \times t)}} \tag{2.4}$$

Once the surface area and the geometry are known for the extended surfaces, h and η_0 are computed iteratively from equations (2.1) to (2.4), the j factor is then calculated from its definition

$$j = \frac{h}{Gc_p}(\mathrm{Pr})^{2/3} \tag{2.5}$$

The plate-fin heat exchangers are commonly used for gas-to gas heat exchange, and the pressure drop for each stream is an important design factor. The overall pressure drop through the plate fin heat exchanger involves four components: (1) the pressure drop at the inlet, as the fluid leaves the inlet header and enters the finned section (heat exchanger core), (2) the frictional pressure drop in the finned section or core, (3) the pressure drop (or possibly a pressure rise) at the outlet, as the fluid leaves the core and enters the outlet header, and (4) the momentum pressure drop (or rise) due to the velocity changes in the heat exchanger core resulting from changes in density of the fluid. Fanning friction factor f is obtained from the following

$$f = \frac{\rho_m D_h}{4L}\left[\frac{2\Delta P}{G^2} - \frac{1}{\rho_{inlet}}(K_c - 1 - \sigma^2) - \frac{1}{\rho_{outlet}}\left\{K_e + 1 + \sigma^2(1 + 4\frac{f_d L_d}{D_d})\right\}\right] \tag{2.6}$$

Where K_c and K_e are the contraction and expansion coefficients respectively

Following points can be observed from the above experimental set up:

1. Condensing vapor (i.e., steam) is used as the heat transfer medium in the second channel. Heat transfer coefficients are very high in condensation heat transfer.Seperating walls are made thin. Thus the magnitude of the wall resistance and the thermal resistance of the second channel are minimized. This increases the accuracy in the measurement of hA over the test surface. Flow of condensing vapor in the other channel gives a thermal boundary condition of a uniform wall temperature with zero heat capacity rate (C_r). Longitudinal heat conduction is normally negligible compared to the high rate of heat transfer in the lateral direction.

   The number of transfer units can be found out from the relation:

$$N_{tu} = \ln(\frac{1}{(1-\varepsilon)} = \ln(\frac{T_s - T_{inlet}}{T_s - T_{outlet}}) \tag{2.7}$$

where

T_s is the saturation temperature of condensing fluid (steam) at its inlet condition.

2. With high N_{tu} heat exchangers, thermodynamic limitation restricts the change of outlet fluid temperatures, making them less sensitive to changes in heat transfer coefficient and making the j factor measurement less accurate. Therefore N_{tu} of the test core in the steady state experiment is restricted between 1.0 and 3.0 to minimize the error in j and f measurement.
3. The measurement of friction characteristics is rather simple. Measurement of fluid flow rate, inlet temperature, pressure and pressure drop across the core is sufficient to determine the Fanning friction factor, f. The loss of pressure due to flow through elbows and headers is to be deducted from the measured pressure drop to get the pressure drop across the core.

6) Other experimental works

In extension of the work by Kays and London, London and Shah [38] have reported measurement on eight high performance surfaces, all of the offset strip fin geometry. The third and last edition of the book by Kays and London [2] presents all available data in a systematic manner. More recently, Shah has suggested a "modified Wilson Plot technique" [39] for determining heat transfer in both sides of a heat exchanger simultaneously.

Davenport [40] conducted experiments on eight louvered fin surfaces to study the effect of louver pitch with all other geometrical properties held constant. His test core had a square crossection, 152 mm on each side, with a length of 40 mm along the flow direction. Davenport used water at 85^0C temperature on the second channel. Heat transfer coefficient on this side was found out by Dittus Boelter equation. The friction factor was derived from the relation:

$$\Delta P = \frac{(\rho_{inlet} V^2)}{2}\left[K_e + K_c + f\left(A/A_{ff}\right)\right] \tag{2.8}$$

The experimental error involved has been attributed mainly to flow measurement. Maximum errors on Stanton number (St) and friction factor (f) have been estimated at 5% and 12% respectively.

Sunden and Svantesson [41] used the same experimental scheme as adopted by Davenport [40] but they used a single channel of width 80 mm with fins of height 12.5

mm.The length of the core along the direction of air flow was 60 mm. Heat was provided to the single channel heat exchanger from a constant oil bath maintained at 60^0C.They used the Dittus Boelter equation to calculate the oil side heat transfer coefficient. The estimated uncertainties in the measurement of St and f were $\pm 15\%$ and $\pm 6\%$ respectively.

Wang et al [42] carried out heat transfer and flow friction experiments to study the role of fin frequency on heat transfer and pressure drop.Lozza et al [43] have also conducted steady state experiments on fin and tube heat exchangers having different fin geometries using air and hot water at 60^0C as working fluids.

Recently Ghosh [44] at I.I.T., Kharagpur used the experimental technique of Kays and London [2] and conducted experiments on three wavy and six offset strip fin surfaces. The details of the geometry used are given in his thesis [44]. The results so obtained were combined with the numerical results obtained in the same laboratory by Maiti and Sarangi [45] to generate separate correlations for laminar and turbulent zones. Some of the constants were obtained by multiple regressions over the numerically computed results whereas the remaining constants were obtained from the experimental data.

S.Freund and S. Kabelac[46] have used TOIRT method (Temperature oscillation IR thermography) for determining the local heat transfer coefficients for plate heat exchangers. In TOIRT method, temperature measurements are taken on outer surface of a heat transferring wall with an IR camera and temperature oscillations are generated by radiant heating. C.F.D. models for turbulent flow were correlated by using the experimental values.

B. Transient technique:

The single blow transient method is an alternative method of characterizing heat transfer surfaces. This technique is used for calculating average heat transfer coefficient of packed bed regenerator and matrix type high N_{tu} heat exchanger surfaces. In this method, a compact heat exchanger matrix, or a packed bed, is first allowed to come in equilibrium with the process fluid temperature. Another cooler fluid is then allowed to flow through the matrix. The fluid exchanges heat with the matrix. A three way valve is used to switch from one fluid stream to another flowing through the matrix. Another alternative is to employ a low thermal capacity electric heater upstream of the matrix.

Heating is continued until the core reaches a uniform temperature manifested by a negligible difference between the temperature of air stream at inlet and exit. The electricity supply is switched off instantly to generate the step change. The fluid outlet temperature is recorded during the cooling period up to the new equilibrated temperature. This measured temperature response is matched with exit fluid temperature history derived from a mathematical model of the system. From the parameters of the mathematical model and the operating condition it is possible to determine the heat transfer coefficient.

There are several computational methods to analyze the measured data for determination of N_{tu}. The most prominent among them are:(1)The maximum slope method,(2) the zero intercept method,(3) the direct curve matching method, and (4) the first moment of area method. Detailed discussions on these techniques have been given in references [47] and [48].Typical uncertainties in the final values of Colburn j factor has been reported [49] to be 13% with overall N_{tu} of 3.5 for the test core.

Though transient tests are relatively easy to perform, the data reduction procedures are significantly more complex compared to those in the steady state technique. Transient tests are ideal for large N_{tu} heat exchangers, as the data reduction procedures have substantial errors when used for low N_{tu}.The steady state technique yields more accurate results for high performance surfaces.

2.3 Analytical and numerical studies

Unlike simpler geometries, the performance of a plate and fin heat exchanger is not uniquely determined by the hydraulic diameter. Other geometrical parameters such as fin spacing(s), fin height (h), fin thickness (t), offset strip length (l), wavelength ($\wedge$), and wave amplitude (a) etc play significant roles. It will be very expensive and time consuming to fabricate heat exchanger cores and conduct experiments over reasonable ranges of all the geometric variables and Reynolds numbers. In contrast, it is relatively easy and cost effective to carry out a parametric study through numerical simulation and derive acceptable correlations for use by the heat exchanger industry. With the development of more powerful computational tools, numerical prediction of j and f factors are now feasible by solving the continuity, momentum and energy equations. Patankar [50] provides a comprehensive summary of CFD equations relevant to compact heat exchanger passages and techniques employed for their solution**.** Levent Bilir et al[51] used CFD program ‘’FLUENT ‘’ to analyze the effect of three different types of

vortex generators on the performance of fin tube heat exchangers. They found that the three vortex generators when placed suitably will increase the heat transfer with moderate increase in pressure drop. Numerical studies, supplemented by flow visualization, can definitely be a means for the understanding of the heat transfer enhancement mechanism. A detailed discussion of the physics of the heat transfer process has been given by Jacobi and Shah[52].Shah et al have also presented a comprehensive review of numerical analysis of some of the important fin geometries employed in compact heat exchangers[53]. Results of numerical studies on several plate fin geometries have been summarized. This review also contains a discussion on the physics of the flow process, as determined from experimentation and flow visualization. This information will be useful in further refinement of the numerical techniques in future.

Because of the extensive practical applications, louvered and offset strip fins have attracted the attention of researchers more than other geometries. A brief review of literature on analytical and computational studies on offset strip and louver fins is presented in the following sections.

Offset strip fin surfaces:

Sparrow, Patankar and coworkers [54] were the first to use numerical (CFD) techniques for prediction of j and f data in offset strip fin heat exchangers. Patankar and Prakash [55] extended their work further and compared their numerical results for a two dimensional heat transfer matrix having offset strip fins with the experimental results of London and Shah [38].The results indicated reasonable agreement for the f factors. But the predicted j factors were about twice as large as the experimental data.

Suzuki et al (56) took a different numerical approach by solving elliptic differential equations of momentum and energy to study the thermal performance of a staggered array of vertical flat plates at low Reynolds number. The validation of their numerical model was done by carrying out experiments on a two dimensional system, followed by those on a practical offset strip fin heat exchanger. The experimental results were in good agreement with the computed values in the Reynolds number range Re<800.Zhang et al (57) has attempted solving the unsteady Navier-Stokes and energy equations on a massively parallel computer. Their study shows that the inclusion of flow unsteadiness plays an important role in accurate prediction of j and f factors.

Louvered fins:

Louvered fins have found wide application in the aerospace industry. In the 1990s several workers devolped CFD codes based on non-orthogonal boundary fitted meshes to compute the flow over louvered fins. Others used non-orthogonal meshes in conjunction with commercial CFD codes [58-60].

Achaichia et al [58] investigated the variation in flow alignment with Reynolds number using the mean flow angle α defined by Achaichia and Cowell [61] as a measure of the local degree of alignment. They found that the maximum value reached by α was less than the louver angle, but approached it at high Reynolds number. Atkinson et al [60] analyzed two and three dimensional numerical models of louvered fin arrays on a powerful work station using a commercial CFD package. They compared their numerical results with experimental data of Achaichaia and Cowell [61] and concluded that the heat transfer predictions of the 3D model were in agreement with experimental observations. Ha et al [59] computed the overall Nusselt number and friction factor for a limited number of louver angles, fin pitches and Reynolds numbers. They found that the Nusselt number and the friction factor increase with that of louver angle and decrease with reduction of fin pitch.

Springer and Thole [62] carried out a combined experimental and computational study of flow through a louvered fin array at two different Reynolds numbers. The experiments were conducted on a 20:1 scaled up model of a 19 row louvered fin array with louver angle of 27^0 and fin pitch to louver pitch ratio of 0.76.Numerical simulation was carried out for a single row of louvers assuming periodic boundary conditions and two-dimensional, steady, laminar flow. Good agreement was found between the computational predictions and the experimental measurements made with a two component Laser Doppler Velocimeter.

All the studies discussed so far have assumed steady laminar flow and thus are incapable of predicting time depentment phenomena such as flow separation and vortex shedding. With the advent of high speed parallel computers, it has become possible to solve the time dependent CFD equations. Tafti et al [63, 64] have used an efficient time dependent calculation procedure for studying both fully developed and developing unsteady flow and heat transfer in louvered fin heat exchangers. Their result shows that, in the transitional regime, local heat transfer is strongly influenced by large-scale vortices generated at the leading edge of the louvers.

2.4 Heat transfer and flow friction characteristics

One of the earliest and the most authoritative sources of experimental j and f data on plate and fin surfaces is the monograph of compact heat exchangers by Kays and London [2].Kays and London conducted experiments on different types of plate and fin surfaces and observed from experiments that the heat transfer coefficient and friction factor f of surfaces having the same effective diameter differed mutually according to the fin geometrical properties like h/s, l/s and t/s etc. Therefore, it is imperative that the j and f factors are obtained experimentally as functions of Reynolds number and other geometrical properties. The expression for j and f data is obtained separately for each surface type. J and f so presented are applicable to surfaces of any hydraulic diameter, provided a complete geometric similarity is maintained. Different heat transfer correlations for offset strip fins are given as below:

Offset strip fin surfaces:

Manson [65] appears to have made the first attempt at developing predictive equations. However the data base he employed consisted of dissimilar geometries: scaled up and actual offset strip fins, louvered fins and finned flat tubes. Kays [66] made one of the first attempts at analytical modeling of heat transfer and friction loss in offset strip fins and proposed a modified laminar boundary layer solution that includes form drag contribution of blunt fin edges.

Wieting [67] developed an empirical correlation from experimental heat transfer and flow friction data on 22 offset strip fin surfaces of Kays and London[2], London and Shah[38], Walters[112] etc over two Reynolds number ranges:Re< 1000 and Re >2000.

For $\mathrm{Re} \le 1000$

$$j = 0.483(l/D_h)^{-0.162}(s/h)^{-0.184}(\mathrm{Re})^{-0.536} \quad (2.11)$$

$$f = 7.661(l/D_h)^{-0.384}(s/h)^{-0.092}(\mathrm{Re})^{-0.712} \quad (2.12)$$

For

$\mathrm{Re} \ge 2000$

$$j = 0.242(l/D_h)^{-0.322}(t/D_h)^{0.08}(\mathrm{Re})^{-0.368} \quad (2.13)$$

$$f = 7.661(l/D_h)^{-0.384}(s/h)^{-0.092}(\mathrm{Re})^{-0.712} \quad (2.14)$$

For predicting j and f in the transition zone, extrapolating the equations upto their respective transition zone boundaries was suggested. Although 85% of all available data were correlated within $\pm 15\%$ for friction factor and $\pm 10\%$ for heat transfer,a few points showed discrepancy as high as $\pm 40\%$.Wieting's correlation can be successfully used for the design of practical heat exchangers, but care should be taken in extrapolating the data to fins with geometrical parameters outside the recommended range.

Joshi and Webb [68] conducted flow visualization experiments to identify the transition from laminar flow. As the flow rate increases, oscillating velocities develop in the wakes, leading to vortex shedding with further increase in Re. The onset of oscillating flow and the consequent change in the wake structure were found to correspond approximately to the departure from the laminar log linear behavoiur of j and f. A wake width based equation was devolved to determine the critical Reynolds number. They developed an analytical model in the laminar zone based on the numerical solution done by Sparrow and Liu [69] and a semi empirical method has been used for the turbulent region.

For laminar range ($\mathrm{Re} \le \mathrm{Re}^*$)

$$j_c = 0.53(\mathrm{Re})^{-0.5}(l/D_e)^{-0.15}(s/h)^{-0.14} \tag{2.15}$$

$$f = 8.12.(\mathrm{Re})^{-0.74}(l/D_e)^{-0.41}(s/h)^{-0.02} \tag{2.16}$$

For turbulent range ($\mathrm{Re} \ge \mathrm{Re}^* + 1000$)

$$j_c = 0.21(\mathrm{Re})^{-0.4}(l/D_e)^{-0.24}(t/D_h)^{0.02} \tag{2.17}$$

$$f = 1.12.(\mathrm{Re})^{-036}(l/D_e)^{-0.65}(t/D_e)^{0.17} \tag{2.18}$$

The critical Reynolds number for heat transfer and pressure drop considerations is given by

$$\mathrm{Re}^* = 257(l/s)^{1.23}(t/l)^{0.58} D_e \left(t + 1.328 \left(\frac{\mathrm{Re}}{lD_e} \right)^{0.5} \right)^{-1} \tag{2.19}$$

The empirical correlation for j and f factors proposed by the authors were verified with experimental data on 21 heat exchanger geometries and their own observations on scaled up geometries. They were able to correlate 82% of the f data and 91% of the j data within $\pm 15\%$.

Manglik and Bergles [70] examined the heat transfer and friction data for 18 offset strip fin surfaces given by Kays and London [2], Walters [112] & London and Shah [38], and analyzed the effect of various geometrical attributes of offset strip fins. The equations that describe the asymptotic behavior of the data in the deep laminar and fully turbulent zones have been devolped.These asymptotes have been combined to give the single predictive equation for j and f which are valid for laminar, turbulent and transition zones.

$$j = 0.6522\,\mathrm{Re}^{-0.5403}(s/h)^{-0.1541}(t/l)^{0.1499}(t/s)^{-0.0678}\times \left[1+5.269\times10^{-5}\,\mathrm{Re}^{1.340}(s/h)^{0.504}(t/l)^{0.546}(t/s)^{-1.055}\right]^{0.1} \quad (2.20)$$

$$f = 9.6243\,\mathrm{Re}^{-0.7422}(s/h)^{-0.1856}(t/l)^{0.3053}(t/s)^{-0.2659}\times \left[1+7.669\times10^{-8}\,\mathrm{Re}^{4.429}(s/h)^{0.920}(t/l)^{3.767}(t/s)^{0.236}\right]^{0.1} \quad (2.21)$$

These equations predict all of the heat transfer data and approximately 90% of the friction data within $\pm 20\,\%$.

Maiti and Sarangi [45] used CFD as numerical tool for computing velocity, pressure and temperature fields in plate and fin passages. They obtained correlations for the non dimensional heat transfer coefficient,j and pressure drop characteristic ,f in terms of Reynolds number and other geometrical parameters using both computed and experimental results . Some of the constants in the correlation are found by multiple regression from the numerically computed results and the rest of the constants from experimental data on the same geometry by another worker in the laboratory. They thus combined both the experimental and computational methods. They also obtained the expression for the transition Reynolds number.

For laminar range ($\mathrm{Re} \le \mathrm{Re}^*$)

$$j = 0.36(\mathrm{Re})^{-0.51}(h/s)^{0.275}(l/s)^{-0.27}(t/s)^{-0.063} \quad (2.22)$$

$$f = 4.67(\mathrm{Re})^{-0.70}(h/s)^{0.196}(l/s)^{-0.181}(t/s)^{-0.104} \quad (2.23)$$

Turbulent range ($\mathrm{Re} \ge \mathrm{Re}^*$)

$$j = 0.18(\mathrm{Re})^{-0.42}(h/s)^{0.288}(l/s)^{-0.184}(t/s)^{-0.05} \quad (2.24)$$

$$f = 0.32(\mathrm{Re})^{-0.286}(h/s)^{0.221}(l/s)^{-0.185}(t/s)^{-0.023} \quad (2.25)$$

The critical Reynolds number for heat transfer coefficient is given by

$$\mathrm{Re}^* = 1568.58(h/s)^{-0.217}(l/s)^{-1.433}(t/s)^{-0.217} \quad (2.26)$$

The critical Reynolds number for pressure drop is given by

$$\mathrm{Re}^* = 648.23(h/s)^{-0.06}(l/s)^{0.1}(t/s)^{-0.196} \quad (2.27)$$

Mochizuki et al [71] correlations are once again a reworking of the Wieting [67] equations, with the coefficients and exponents modified to fit their own experimental data for five scaled up rectangular offset strip fin surfaces. Only fully laminar flow and fully turbulent flow are considered, with an abrupt change of flow regime at Re=2000.

Muzychka and Yovanovich [72] developed a new model to predict the heat transfer and flow friction performance of offset strip fin geometries. They considered the offset strip fins as an array of short channels or straight ducts. They developed simple analytical models for the laminar or turbulent wake regions and suitably combined the resulting asymptotic relations to create expressions for the turbulent zone. Their correlation predicted the data in Ref [2] within ± 20 % for 96% of f data and 82% of j data.

• *Hydraulic diameter*

Hydraulic diameter is given by the following definition

$$D_h = \frac{4 \times A_c}{P} = \frac{4 \times Free flow volume}{total heat transfer area} = \frac{4 \times A_c}{A/l} \quad (2.28)$$

The terms Ac, P and A have been evaluated differently by various investigators; so there are different expressions for hydraulic diameter in the literature. At least three different expressions can be identified in the literature, which are as given below

Manglik and Bergles [70]

Free flow area is taken $A_c = sh$. In evaluating the heat transfer area A; the blunt fin edges, both vertical and lateral, have been included in the channel surface area. Heat transfer area is given by the expression:

$$A = 2(sl + hl + ht) + ts$$

Therefore hydraulic diameter is given by the formula:

$$D_h = \frac{4shl}{2(sl + hl + ht) + ts} \quad (2.29)$$

Joshi and Webb [68], **and Maiti and Sarangi** [45]

Free flow area and heat transfer area are given as

Free flow area, $A_c = (s-t)h$

Heat transfer area, $A = 2(sl + hl + ht)$

Therefore hydraulic diameter is given by the formula:

$$D_h = \frac{2(s-t)h}{(sl + hl + ht)} \tag{2.30}$$

Wieting [67] **and Kays and London [2]**

Considering a rectangular channel of cross section, sh, hydraulic diameter is defined as :

$$D_h = \frac{4sh}{2(s+h)} = \frac{2sh}{(s+h)} \tag{2.31}$$

- *Critical Reynolds number and the transition zone*

Joshi and Webb [68] conducted flow visualization experiments to identify the flow structure at transition. They observed that a transition from steady laminar flow to an oscillating or vortex shedding flow occurs at higher flow rates [72, 68, 73]; the flow is generally characterized by a progression of laminar, second laminar (transitional, or vortex shedding, or oscillating flow), and turbulent flow regimes [74].They gave a wake width based definition for the critical Reynolds number and developed an expression of the critical Reynolds number in terms of Reynolds number and other geometrical parameters. Maiti and Sarangi [45] have developed the expression for the critical Reynolds number as a function of geometrical parameters only.

In all the correlations mentioned above, only established laminar or turbulent flow is considered and the transition zone is ignored. This extends over a fairly large Reynolds number of 1000 in case of Wieting[67] and Joshi and Webb[68].Mochizuki et al [71] and Dubrovsky and Vasilev[75] completely ignore the transition zone and consider an abrupt change from laminar to turbulent flow; the evidence in the data for actual cores[2,38] is contrary to this.

The change in the wake flow affects the j and f characteristics as seen in a typical j and f versus R_e plot. The departure from the log linear behavior of the j and f

curve is observed at higher mass flow rates. The intersection point of the two zones gives the critical Reynolds number.

Mullisen and Loehrke [76] reported a direct correlation between the onset of oscillating flows and the generation of audible tones. Other studies have found that the development of oscillating flows and the consequent vortex shedding are influenced by fin separation (or length) and fin offset[55,74,68].The heat exchanger core acts as a flute for certain flow arrangements and flow rates.

2.5 Secondary irreversibilities

The performance of heat exchangers is adversely affected by the following physical factors:

i) Longitudinal heat conduction along the separating wall of the two fluids in the heat exchanger.
ii) Heat transfer from or to the ambient,
iii) Flow maldistibution at the headers and due to manufacturing errors.
iv) Fluid property variation at low temperatures.

A. Effect of longitudinal heat conduction.

Most of the literature on the role of such secondary irreversibilities considers only two stream heat exchangers. The effect of axial heat conduction in two stream heat exchangers has been discussed by Barron [77] and by Shah [78]. Barron and Yeh [79] computed temperature distribution and heat exchanger effectiveness considering the effect of axial conduction along the separating walls. The temperature of the cold fluid stream was assumed to be constant and the deterioration in performance was found to depend on the axial conduction parameter.

Kays and London [2] expressed the ineffectiveness due to longitudinal heat conduction in terms of a longitudinal heat conduction parameter, λ defined as:

$$\lambda \approx \frac{kA_c}{LC_{\min}} = \frac{\delta\varepsilon}{\varepsilon}$$

Chowdhury and Sarangi [80] have obtained the expression for the efficiency of heat exchangers considering both axial conduction and lateral resistance due to the separating wall in terms of relevant non-dimensional parameters. They gave an expression for the optimum thermal conductivity of the separating wall for maximum efficiency of heat exchangers.

Hausen [81] explained the deviation of temperature profiles from that of the heat exchanger without longitudinal heat conduction assuming average temperature properties. He thus presented an approximate method of predicting the performance deterioration due to longitudinal heat conduction. The longitudinal heat conduction in a single pass counter flow heat exchanger was studied by Hahnemann [82] and complicated expressions were presented for evaluating the effectiveness of a heat exchanger subject to longitudinal heat conduction. Bahnke and Howard [83] compared their results with that of Hahnemann [82] and observed that deterioration of the heat exchanger performance is maximum when the ratio of the flow stream capacity rates is same.

The most comprehensive work on the performance degradation of heat exchanger was carried out by Kroeger [84].He solved the governing equations of a two stream counter flow heat exchanger, taking into account the effect of longitudinal heat conduction. He presented a closed form solution for finding the ineffectiveness of a balanced flow (C_r =1) heat exchanger as follows:

$$1-\varepsilon = \frac{1}{1+[N_{tu}(1+\lambda B)/(1+\lambda N_{tu})]}$$

Where

$$B = \left[\frac{\lambda N_{tu}}{1+\lambda N_{tu}}\right]^{1/2} \tanh\left[\frac{N_{tu}}{[\lambda N_{tu}/(1+\lambda N_{tu})]^{1/2}}\right] \qquad (3.7)$$

The parameter, $(1-\varepsilon)$ is also the dimensionless hot fluid exit temperature. Kroeger presented the ineffectiveness of unbalanced flow ($C_r < 1$) heat exchangers graphically as a function of N_{tu} and longitudinal heat conduction parameter, λ .While Chiou [85-86] examined its effect on the performance of cross flow heat exchangers.

In heat exchangers with large axial temperature gradient e.g. cryogenic heat exchangers, the effect of axial heat conduction on heat exchanger performance is significant, independent of number of streams. Venkatarathnam and Narayanan [87] have studied the effect of longitudinal heat conduction from outer wall to the ambient on the effectiveness of the heat exchanger. They have studied the performance of perforated plate matrix heat exchangers and found that the performance degradation due to longitudinal heat conduction through the walls separating the streams from the environment is therefore nonnegligible in such heat exchangers. They also observed that the degradation of

performance of a high effectiveness heat exchanger due to longitudinal heat conduction through the outer walls is non negligible even when the thermal resistance to heat transfer between the stream and the outer wall is 10% of that between the fluids. The effect of longitudinal heat conduction on performance of storage type heat exchangers have also been investigated by several workers [88-89].

Recently Narayanam and Venkatarathnam [90] studied the performance of high effectiveness counter flow heat exchangers subject to longitudinal heat conduction. They derived the expression for the effectiveness of very high N_{tu} heat exchangers as a function of the longitudinal heat conduction parameter, λ and heat capacity ratio, C_r

B. Effect of heat transfer to the ambient.

The performance of most heat exchangers may be seriously affected by heat exchange with the surroundings. This is particularly true for cryogenic heat exchangers because of the large temperature differences between the ambient and the operating temperatures. This problem can be reduced by using highly effective insulation. But factors like cost, weight and volume of insulation, difficulties in fabrication and ageing of insulation limit the extent to which heat transfer may be reduced.

Wood and Kern [91] have solved the governing differential equations and obtained a closed form solution for studying longitudinal heat conduction through wall and heat leak from surroundings independently. Their solution requires an iterative procedure to determine heat exchanger effectiveness considering heat loss to the surroundings and is of only limited value to the design engineer. Chowdhury and Sarangi [92] have also obtained an expression for the effectiveness considering heat loss in terms of a heat leak parameter. They give the effectiveness without an iterative procedure unlike Wood and Kern [91]. Heat transfer from the surroundings to either one or both of the fluid streams in a binary heat exchanger is expressed in dimensionless form and a direct expression for the outlet temperature has been obtained by Barron [93]. Gupta et al [94] conducted experiments on a coiled tube- in- tube heat exchanger and found that heat in - leak from the atmosphere to the cold fluid, flowing in the annular region of the tube-in-tube heat exchanger is significant. They developed a numerical model and compared the numerical results with experiment.

C. Effect of flow maldistribution :

In the design of heat exchangers, it was assumed that the fluid is uniformly distributed across the heat exchanger cores. In practice, however, it is impossible to distribute the fluid uniformly because of improper inlet configuration, imperfect design and complex heat transfer process [95]. The gross flow maldistribution and passage to passage flow nonuniformity exist in plate fin heat exchangers. Mueller and Chiou [96] summarized various types of flow maldistribution in heat exchangers and discussed the reasons leading to flow maldistribution.The combined effects of wall longitudinal heat conduction, inlet flow nonuniformity and temperature nonuniformity on compact plate fin heat exchangers using finite element method have been investigated by Ranganayakalu and Seetharamu[97].Jiao[98] investigated experimentally and analyzed theoretically the combined effects of distributors inlet angle and mass flow rate on flow maldistribution. Some distributors with different inlet angles were studied under similar conditions and optimum performance was obtained at inlet angle of 45^0.Zhang [99] proposed a structure of two stage distribution and the numerical investigation showed that the flow distribution in plate fin heat exchangers is more uniform if the ratio of outlet to inlet equivalent diameters is equal for both headers. Wen [100] employed C.F.D technique to simulate and analyze fluid flow distribution and pressure drop in the header of plate fin heat exchangers. A baffle with small sized holes is recommended to install in the header to improve the performance of flow distribution. Most of the previous works mainly focused on the effect of flow non uniformity on heat exchanger performance deterioration based on their own flow maldistribution model. Flemming [101] investigated flow maldistribution in paired channel heat exchangers and investigated the effect of flow maldistribution on performance deterioration. Jian Wen et al [102] investigated the flow characteristics of flow field in the entrance of plate fin heat exchangers by means of particle image velocimetry (PIV). PIV is an instantaneous flow field measurement technique, which uses a pulsed light sheet to illuminate a gas flow seeded with tracer particles. They investigated the effect of configuration changes on flow field uniformity.

D. The effect of variable fluid properties

The effect of variable fluid properties on the performance of cryogenic heat exchangers has been examined by Chowdhury and Sarangi [103]. The local heat transfer coefficient (h) usually varies both as a function of temperature and flow velocity. Change

in the fluid properties with temperature can alter the local heat transfer coefficient. The heat transfer coefficient also varies along the length due to boundary layer development. Shah [104] has made an extensive review of this subject and has outlined a method for incorporating the influence of these effects on two stream heat exchanger performance. Paffenbarger[105] has incorporated the effect of longitudinal heat conduction and variation of fluid properties with temperature in his computationally intensive numeric model. He has also illustrated the effect of longitudinal heat conduction on multistream heat exchanger performance through an example.

Chapter 3

Design of Plate Fin Heat Exchanger

Chapter III

DESIGN OF PLATE FIN HEAT EXCHANGER

Design or sizing of heat exchangers covers determination of the heat exchanger dimensions for the specified heat transfer and pressure drop performance. We can reduce this problem to the rating problem by tentatively specifying the dimensions and then calculating the performance for comparison with the specified performance. The heat transfer coefficient of the surface increases with increase of flow Reynolds number. But the pressure drop which is a function of flow velocity also increases. The optimum velocity is to be found out for the specified pressure drop by using the core mass velocity equation [7].

Accurate prediction of non-dimensional heat transfer coefficient, j and friction factor, f is necessary for the correct design of heat exchangers. Various correlations are available in literature for the determination of non dimensional heat transfer coefficient, j and friction factor, f. It is difficult for the designer to choose the best among them. The heat exchanger is designed by using the correlations developed by Maiti and Sarangi [45], Manglik and Bergles [70], Joshi and Webb [68], and by using Aspen –MUSE [113], the simulation software. The performance of design procedures are validated by experiment. The experimental aspect is described separately in the subsequent chapters. In the present chapter the design procedure for the plate fin heat exchanger is given.

Heat exchanger performance is deteriorated by various factors such as longitudinal heat conduction, heat loss to the surroundings, flow maldistribution at the headers, manufacturing irregularities etc. Longitudinal heat conduction through the separating wall is the major contributor to the ineffectiveness of a heat exchanger. The decrease in the effectiveness of heat exchangers due to longitudinal heat conduction is found out by using Kroeger equation [84].

The plate fin heat exchanger consists of restricted and narrow passages. The pressure drop will be high for gases passing through the heat exchanger. The headers provided in the heat exchanger helps in the uniform flow distribution of the fluid among the passages or channels. Cross sectional area of the header passages should be more

than the diameter of the tubes. Pressures at the inlet of both the fluids should be high enough to overcome the pressure losses that occur during the flow through the heat exchanger. In this way we can ensure that the flow channels are completely flooded and there is no starvation anywhere.

Factors, j and f, are strong functions of surface geometry. Increase in heat transfer performance is associated with increase in flow friction and vice versa. The ratio of j/f is often taken as a measure of the goodness of a finned surface. Though the ideal fin geometry should have high value of j/f, the selection of particular fin geometry is primarily governed by the process requirement.

3.1 Summary of the design procedure:

The main steps involved in the design procedure are as follows.

a) Determination of the optimum mass velocity.

The optimum mass velocity for the specified pressure drop, Δp is calculated by the relation:

$$G = \left[\frac{2}{(1/\rho_m)\,\mathrm{Pr}^{2/3}} \cdot \frac{\eta_o \Delta p}{n_{tu}} (j/f) \right]^{1/2} \tag{3.1}$$

Referring to figure E 9.2 in pp.625 of Fundamentals of Heat Exchanger Design by R.K.Shah [7], value of goodness factor, j/f is assumed to be 0.25 for the Reynolds number ranging from 300 to 5000 for the specified geometry to calculate the initial approximate value of G. The overall surface effectiveness of fins, η_0 is assumed to be 80 % for the first iteration unless a better value is known from the past experience. From the initial value of G calculated, individual j and f are calculated .After a number of iterations, the core mass velocity G is obtained. It is also found that change in Reynolds number has a very little effect on the ratio of j/f for the fin of particular geometry.

b) Assumptions on free flow area and frontal area.

The frontal area or the free flow area is assumed so that core mass velocity is below the optimum value calculated as above. The length of the heat exchanger is assumed.

c) Heat transfer areas

The surface areas, A_h and A_c of both the sides are then computed from the geometry.

than the diameter of the tubes. Pressures at the inlet of both the fluids should be high enough to overcome the pressure losses that occur during the flow through the heat exchanger. In this way we can ensure that the flow channels are completely flooded and there is no starvation anywhere.

Factors, j and f, are strong functions of surface geometry. Increase in heat transfer performance is associated with increase in flow friction and vice versa. The ratio of j/f is often taken as a measure of the goodness of a finned surface. Though the ideal fin geometry should have high value of j/f, the selection of particular fin geometry is primarily governed by the process requirement.

3.1 Summary of the design procedure:

The main steps involved in the design procedure are as follows.

a) Determination of the optimum mass velocity.

The optimum mass velocity for the specified pressure drop, Δp is calculated by the relation:

$$G = \left[\frac{2}{(1/\rho_m)\,\mathrm{Pr}^{2/3}} \cdot \frac{\eta_o \Delta p}{n_{tu}} (j/f) \right]^{1/2} \tag{3.1}$$

Referring to figure E 9.2 in pp.625 of Fundamentals of Heat exchanger design by R.K.Shah [7], value of goodness factor, j/f is assumed to be 0.25 for the Reynolds number ranging from 300 to 5000 for the specified geometry to calculate the initial approximate value of G. The overall surface effectiveness of fins, η_0 is assumed to be 80 % for the first iteration unless a better value is known from the past experience. From the initial value of G calculated, individual j and f are calculated .After a number of iterations, the core mass velocity G is obtained. It is also found that change in Reynolds number has a very little effect on the ratio of j/f for the fin of particular geometry.

b) Assumptions on free flow area and frontal area.

The frontal area or the free flow area is assumed so that core mass velocity is below the optimum value calculated as above. The length of the heat exchanger is assumed.

c) Heat transfer areas

The surface areas, A_h and A_c of both the sides are then computed from the geometry.

d) Fluid mean temperatures and fluid thermo physical properties

on each fluid side are calculated.

e) Calculation of heat transfer coefficient, j and friction factor, f

The Reynolds number and j and f factors on each side are calculated by using available correlations.

f) Determination of overall heat transfer coefficient.

The heat transfer coefficients on both hot and cold sides are computed. The overall heat transfer coefficient is calculated by the formula:

$$\frac{1}{(U_O A_O)_h} = \frac{1}{(\eta_{oh} h_h A_h)} + \frac{a}{K_w A_w} + \frac{1}{(\eta_{oc} h_c A_c)} \tag{3.2}$$

where

η_{0c} = overall surface effectiveness of fins

$$= 1 - \left[(a_f / a_s) \times (1 - \eta_f)\right] \tag{3.3}$$

with

n_f = fin efficiency $= \tanh(Ml_e)/(Ml_e)$

where M is a fin parameter and is defined as

$$M = \sqrt{\frac{(2 \times h)}{(K_f \times t)}} \tag{3.4}$$

g) Number of transfer units are calculated by the relation:

$$N_{tu} = \frac{UA}{C_{\min}} \tag{3.5}$$

h) Effectiveness considering longitudinal heat conduction loss.

Longitudinal heat conduction along the separating surfaces of hot and cold fluids causes serious performance deterioration. The decrease in the effectiveness of the heat exchanger is found out by using Kroeger's equation [84].

For the case of balanced operation, $C_r = 1$, Kroeger [84] has presented the solution for the ineffectiveness as :

$$1 - \varepsilon = \frac{1}{1 + [N_{tu} \times (1 + \lambda B)/(1 + \lambda \times N_{tu})]} \tag{3.6}$$

where

$$B = \left[\frac{\lambda \times N_{tu}}{1+\lambda \times N_{tu}}\right]^{1/2} \tanh\left[\frac{N_{tu}}{\left[(\lambda \times N_{tu})/(1+\lambda \times N_{tu}\right]^{1/2}}\right] \quad (3.7)$$

For the case of N_{tu} >3, the argument of the hyperbolic tangent is greater than 3, and tanh (3) = 0.995 or almost unity. For this case, the ineffectiveness given by equation (3.6) becomes

$$1-\varepsilon = \frac{1}{1+N_{tu}\times\left[\frac{1+\lambda\left[\lambda \times N_{tu}/(1+\lambda \times N_{tu})\right]^{1/2}}{1+\lambda \times N_{tu}}\right]} \quad (3.8)$$

Kroeger [84] has developed an approximation for the ineffectiveness for the case of unbalanced operation, $C_r < 1$ as :

$$(1-\varepsilon) = \frac{(1-C_r)}{\varphi \exp(r_1) - C_r} \quad (3.9)$$

where

$$r_1 = \frac{(1-C_r)\times N_{tu}}{1+(\lambda \times N_{tu} \times C_r)} \quad (3.10)$$

For the case of $C_r > 0.50$, the value of the function reduces to:

$$\varphi = \frac{(1+\phi)}{(1-\phi)} \quad (3.11)$$

$$\phi = \gamma(y/(1+y)^{1/2}\left[\frac{(1+\gamma)y}{1-\gamma(1+\gamma)y}\right] \quad (3.12)$$

$$\gamma = \frac{(1-C_r)}{(1-C_r)(1+y)} \quad (3.13)$$

$$y = \lambda \times N_{tu} \times C_r \quad (3.14)$$

3.2 Design inputs and specification of fin geometry:

The heat exchanger has to be designed for the following design conditions

A. Heat exchanger input data.

Fluid used: Nitrogen gas

Temperature of hot fluid at inlet, =310 K

Temperature of cold fluid at inlet, =83.65 K

Pressure at inlet of hot gas = 7.35 bar.

Pressure at inlet of cold gas = 1.15 bar.

Mass flow rate of both the fluids (hot and cold) = 5 g /s.

Allowable pressure drop, $\Delta p_h = \Delta p_c = 0.05$ bar

B. Fin geometry.

The heat exchanger is to be constructed of Aluminum alloy Al-3003 with rectangular offset strip fins with the following basic dimensions.

Table 3.1 Fin geometry used in heat exchanger

	Fin geometry	**High pressure Side**	**Low pressure Side**
01	Fin frequency,f	714 fins per metre	588 fins per metre
02	Length of fin, l	3 mm	5 mm
03	Fin thickness,t	0.2 mm	0.2 mm
04	Fin height,h	9.3 mm	9.3 mm
05	Number of layers	05	04

Geometrical characteristics related to selected fin geometry.

Other geometrical characteristics related to the fin geometry are calculated as follows

i) Fin spacing, s (excluding the fin thickness) $= \dfrac{(1 - p_f \times t)}{(p_f)} = 0.0012\ m$

ii) Free flow area to frontal area ratio,

$$\sigma = a_{ff} / a_{fr} = \frac{(s-t)h}{(h+t)(s+t)} = \frac{(0.0012-0.0002)\times 0.0093}{(0.0093+0.0002)(0.0012+0.0002)} = 0.6992$$

iii) Heat transfer area / fin, $a_s = 2hl + 2ht + 2sl = 0.00006672$ m^2

iv) Ratio of fin area to heat transfer area of fin,

$$\frac{2h(l+t)}{2(hl+sl+ht)} = \frac{2\times 0.0093(0.003+0.0002)}{2(0.0093\times 0.003+0.0012\times 0.003+0.0093\times 0.0002)} = 0.8920$$

v) Equivalent Diameter, $D_e = \dfrac{(4 \times Freeflowarea \times length)}{heattransferarea}$

$$= \frac{2(s-t)hl}{hl+sl+ht} = \frac{2(0.0012-0.0002)\times 0.0093\times 0.003}{(0.0093\times 0.003+0.0012\times 0.003+0.0093\times 0.0002)} = 0.001672662 \text{ m}$$

vi) Distance between plates, $b = h + t = 0.0095$ m

3.3 Correlation based design of heat exchanger

A. Design using correlation developed by Joshi and Webb[68]:

The design calculations for the given heat exchanger are as given below:

a) Desired performance of heat exchangers.

The desired effectiveness of heat exchanger is given by the formula:

$$\varepsilon = \frac{C_h(T_{hi} - T_{ho})}{C_{\min}(T_{hi} - T_{ci})} = \frac{25.9875(310 - 92.85)}{25.8835(310 - 83.65)} = 0.96$$

Heat load, $Q = C_h(T_{hi} - T_{ho}) = 25.9875(310 - 92.85) =$ 5.56 kW

b) Estimation of dimensions of heat exchanger.

i) Length of the heat exchanger = 900 mm

ii) Width of the core, W = 73 mm

iii) Total Number of layers, N = 9.

c) Calculation of heat transfer area, A

The heat transfer area for hot side is calculated as

Total area between plates, $A_{frh} = b \times N_h \times W = 0.0095 \times 5 \times 0.073 = 0.0035$ m^2

Total free flow area, $A_{ffh} = \sigma \times A_{frh} = 0.002424$ m^2

Wall conduction area on hot side, $a_{wh} = A_{frh} - A_{ffh} = 0.00104286$ m^2

Total heat transfer area, $A_h = \frac{4 \times A_{ffh} \times L}{D_e} = \frac{4 \times 0.0024246 \times 0.9}{0.00167266} = 5.2184$ m^2

Alternatively,

Total heat transfer area,

$$A_h = \frac{a_s \times p_f \times W \times L \times N_H}{l} = \frac{0.00006672 \times 714 \times 0.073 \times 0.9 \times 5}{0.003} = 5.2184 \text{ m}^2$$

Similarly free flow area and the heat transfer are calculated for the cold side.

Total wall conduction (longitudinal conduction) area, $a_{wh} + a_{wc}$ = 0.001043+0.00069736 = 0.00174 m^2

d) Properties at average temperature.

The fluid properties at the estimated mean temperatures of 202.95 K and 191.16 K for hot and cold fluid are obtained from property package, GASPAK

The properties of hot helium gas at the mean film temperature:

Specific heat, C_p =5197.5 J/kg- K

Viscosity, $\mu = 0.0000154$ Pa-s

Prandtl number, $\Pr = 0.6685$

Density, $\rho = 1.7404$ kg/m^3

The properties of cold helium gas at the mean film temperature.

Specific heat, C_p =5197.5 J/kg- K

Viscosity, $\mu = 0.0000148$ Pa-s

Prandtl number, $\Pr = 0.67$

Density, $\rho = 0.2808$ kg/m^3

e) Heat transfer coefficients and surface effectiveness of fins

The core dimensions are calculated for the side having more stringent pressure drop specification. The dimensions on the other side are then chosen such that the calculated pressure is within the specified limit. The calculations for the heat transfer coefficients for the hot and cold gas are similar. The calculations for hot fluid are given below.

i) The core mass velocity, $G = \dfrac{m}{A_{ffc}} = \dfrac{0.005}{0.002424} = 2.062$ kg/s-m^2

ii) The Reynolds number, $\mathrm{Re} = \dfrac{GD_e}{\mu} = \dfrac{2.062 \times 0.0016766}{0.0000154} = 223.98$

iii) The critical Reynolds number for pressure drop and heat transfer coefficient is given by

$$\mathrm{Re}^* = 257(l/s)^{1.23}(t/l)^{0.58} D_e \left(t + 1.328 \left(\frac{\mathrm{Re}}{lD_e} \right)^{0.5} \right)^{-1}$$

$$= 257(3/1.2)^{1.23}(0.2/3)^{0.58} \times 0.001672\left(0.2 + 1.328\left(\frac{223.98}{0.003 \times 0.001672}\right)^{0.5}\right)^{-1} = 691.75$$

iv) The Colburn j factor (for $\mathrm{Re} \le \mathrm{Re}^*$) is given by correlation proposed by Joshi and Webb [68] as

$$j_c = 0.57(\mathrm{Re})^{-0.5}(l/D_e)^{-0.15}(\alpha)^{-0.14}$$

$$= 0.57(223.98)^{-0.5}(0.003/0.0016726)^{-0.15}(0.1290)^{-0.14} = 0.04321$$

v) The convective heat transfer coefficient, h_c is given by

$$h_c = \frac{(j_c \times c_c \times G_c)}{(\mathrm{Pr})^{0.667}} = \frac{(0.04321 \times 5197.5 \times 2.062)}{(0.6685)^{0.667}} = 605.804 \text{ W/m}^2\text{-K}$$

vi) The fin parameter is given by

$$M = \sqrt{\frac{(2 \times h_c)}{(K_f \times t)}} = \sqrt{\frac{(2 \times 605.804)}{(150 \times 0.0002)}} = 200.964 \text{ m}^{-1}$$

vii) Heat loss to the ambient decreases the overall surface effectiveness of fins and finally the effectiveness of heat exchanger. In heat exchangers used for cryogenic service, the layers through which the cold fluid passes are placed in between the two hot layers .This minimizes the heat loss from the cold fluid. The number of layers through which the hot fluid passes will be more than that of cold fluid by one and are exposed more to the ambient. To take into account the heat losses to the ambient, the fin conduction lengths for the outer layers on the hot side will be taken as b whereas for the inner layers of the hot fluid, the conduction length is taken as b/2.However for the cold layers placed between the hot layers the fin conduction length is taken as b/2 for both the inner and outer layers.

l_e = effective length of fins for inner layers of hot fluid =b/2= 4.75 mm and

l_e = effective length of fins for outer layers of hot fluid = b = 9.5 mm

viii) The fin effectiveness for a straight fin is

$= \tanh(Ml_e)/(Ml_e)$ =0.7771 for inner layers.

For the outer layers of hot side the fin effectiveness is 0.50127.

ix) The overall surface effectiveness of fins on hot side is

$$\eta_{0h} = 1 - \left[(a_f / a_s) \times (1 - \eta_f) \times \frac{(N_p - 2)}{N_p} \right] - \left[(a_f / a_s) \times (1 - \eta_{fo}) \times (\frac{2}{N_p}) \right]$$

$$\eta_{0h} = 1 - \left[(0.8920) \times (1 - 0.771) \times \frac{(5-2)}{5} \right] - \left[(0.8920) \times (1 - 0.5012) \times (\frac{2}{5}) \right] = 0.7027$$

f) The overall heat transfer coefficient and number of transfer units.

The overall heat transfer coefficient is given by the formula:

$$\frac{1}{(U_O A_O)_h} = \frac{1}{(\eta_{oh} h_h A_h)} + \frac{a}{K_w A_w} + \frac{1}{(\eta_{oc} h_c A_c)}$$

where,

$A_w =$ lateral conduction area $= W \times L \times (2N_{Pc} + 2) = 0.073 \times 0.9(2 \times 4 + 2) = 0.657$ m^2

$$\frac{1}{(U_O A_O)_h} = \frac{1}{(0.7027 \times 605.8 \times 5.2184)} + \frac{0.0008}{150 \times 0.657} + \frac{1}{(0.8214 \times 524.945 \times 3.454)}$$

$= 0.00113$ K/W

$(U_O A_O)_h = 885.23$ W/K

The overall heat transfer coefficient, $U_{Oh} = \frac{(U_O Ao)_h}{A_{oh}} = \frac{885.23}{5.2184} = 169.63$ W/m^2-K

Number of transfer units, $N_{tu} = \frac{U_O A_O}{C_{\min}} = \frac{885.23}{25.883} = 34.206$

g) Effectiveness of heat exchanger, neglecting longitudinal heat conduction.

The effectiveness of heat exchanger, neglecting longitudinal heat conduction is given by the relation [77]:

$$\varepsilon = \frac{1 - e^{-N_{tu}(1 - C_r)}}{1 - C_r e^{-N_{tu}(1 - C_r)}} = \frac{1 - e^{-34.20(1 - 0.996)}}{1 - 0.996 e^{-34.20(1 - 0.996)}} = 0.9734$$

h) The effect of longitudinal heat conduction

The effect of longitudinal heat conduction is to reduce the effectiveness of heat exchanger. The decrease in the effectiveness of heat exchanger is found out using Kroeger's equation [84].

i) Wall conduction area, $a_w = 0.00174$ m^2

ii) Conductivity of fin, $K_w = 150$ W/m-K

iii) Wall conduction parameter, $\lambda = \frac{K_w a_w}{LC_{\min}} = \frac{150 \times 0.00174}{0.9 \times 25.883} = 0.0112$

iv) $y = \lambda N_{tu} Cr = 0.0112 \times 34.20 \times 0.996 = 0.3817$

v) $\gamma = \frac{(1-Cr)}{(1-Cr)(1+y)} = \frac{(1-0.996)}{(1-0.996)(1+0.3817)} = 0.00145$

vi) $\phi = \gamma(y/(1+y)^{1/2}\left[\frac{(1+\gamma)y}{1-\gamma(1+\gamma)y}\right] = 0.00029$

vii) $\varphi = \frac{(1+\phi)}{(1-\phi)} = \frac{(1+0.001011)}{(1-0.001011)} = 1.0000$

viii) $r_1 = \frac{(1-C_r)N_{tu}}{1+\lambda N_{tu} Cr} = \frac{(1-0.996)\times 34.20}{1+0.0112\times 34.20\times 0.996} = 0.09901$

ix) $(1-\varepsilon) = \frac{(1-Cr)}{\varphi \exp(r_1) - Cr} = \frac{(1-0.996)}{1\times \exp(0.09901) - 0.996} = 0.0368$

x) $\varepsilon = [1-(1-\varepsilon)] = 0.9632$

The actual effectiveness of heat exchanger taking into account longitudinal heat conduction is 0.96 and matches with the desired effectiveness. The required number of transfer units for achieving the desired performance of the heat exchangers is 34.21 and length of the heat exchanger is 900 mm.

i) Pressure drop

Since pressure drop of cold fluid is more critical, the pressure drop calculations for the cold fluid are presented here.

i) The Colburn f factor (for $\mathrm{Re} \le \mathrm{Re}^*$) proposed by Joshi correlation [68] is as

$$f = 8.12.(\mathrm{Re})^{-0.74}(l/D_e)^{-0.41}(\alpha)^{-0.02}$$
$$= 8.12.(223.98)^{-0.74}(1.7935)^{-0.41}(0.129)^{-0.02}$$
$$= 0.12138$$

ii) The pressure drop, $\Delta p = \frac{4fLG^2}{2D_e\rho_b} = \frac{4\times 0.12138\times 0.9\times (2.398)^2}{2\times 0.001672\times 0.2808} = 2675.99$ Pa

The pressure drop is less than the allowable pressure drop of $5\ kPa.$ Hence the design does meet the hydraulic requirement.

B. Design using correlation developed by Maiti and Sarangi[45]:

Maiti and Sarangi[45] used a C.F.D tool to compute the pressure, velocity and temperature fields in the plate and fin heat exchanger passages. They expressed the non dimensional heat transfer coefficient, j as a function of the Reynolds number and other geometrical properties. Some constants in the correlation have been found out by multiple regression from the numerically computed results where as the rest of the constants in the correlation are found out by fitting experimental data of Kays and London [2].

The expressions proposed by Maiti and Sarangi [45] for Colburn, j factor for laminar and turbulent flows (for $\mathrm{Re} > \mathrm{Re}^*$) are given as,

$$j = 0.36(\mathrm{Re})^{-0.51}(h/s)^{0.275}(l/s)^{-0.27}(t/s)^{-0.063} \quad (3.15)$$

$$j = 0.18(\mathrm{Re})^{-0.42}(h/s)^{0.288}(l/s)^{-0.184}(t/s)^{-0.05} \quad (3.16)$$

Maiti and Sarangi [45] gave two separate expressions for finding the critical Reynold number for transition from laminar to turbulent flow for heat transfer and pressure drop considerations.

The critical Reynolds number for heat transfer coefficient is given by

$$\mathrm{Re}^* = 1568.58(h/s)^{-0.217}(l/s)^{-1.433}(t/s)^{-0.217} \quad (3.17)$$

The critical Reynolds number for pressure drop is given by

$$\mathrm{Re}^* = 648.23(h/s)^{-0.06}(l/s)^{0.1}(t/s)^{-0.196} \quad (3.18)$$

The authors used the following definition of hydraulic diameter to calculate the Reynolds number

$$D_h = \frac{2(s-t)h}{(sl+hl+ht)} \quad (3.19)$$

The dimensions of the heat exchanger are found out for the specified performance of the heat exchanger. The length of the heat exchanger for achieving the desired effectiveness is 1020 mm.The maximum pressure drops is 0.02 bar for the cold fluid. This is well below the available pressure drop of 0.05 bar. The other dimensions of heat exchanger core are same as given earlier.

C. Design using correlation developed by Manglik and Bergles[70]:

Manglik and Bergles [70] examined the experimental data for air flows with heat transfer for 18 different cores given by Kays and London [2], Walters [112] and London and Shah [38]. They analyzed the effect of various geometrical attributes of offset strip fins and gave the following expression for j and f factor which is valid continuously for laminar, turbulent and transition zones.

$$j = 0.6522\,\mathrm{Re}^{-0.5403}(s/h)^{-0.1541}(t/l)^{0.1499}(t/s)^{-0.0678}\times \left[1+5.269\times10^{-5}\,\mathrm{Re}^{1.340}(s/h)^{0.504}(t/l)^{0.546}(t/s)^{-1.055}\right]^{0.1} \quad (3.20)$$

$$f = 9.6243\,\mathrm{Re}^{-0.7422}(s/h)^{-0.1856}(t/l)^{0.3053}(t/s)^{-0.2659}\times \left[1+7.669\times10^{-8}\,\mathrm{Re}^{4.429}(s/h)^{0.920}(t/l)^{3.767}(t/s)^{0.236}\right]^{0.1} \quad (3.21)$$

The authors have chosen the free flow or channel flow area as $A_c = sh$ with the hydraulic diameter given by the following expression

$$D_e = \frac{4A_c}{A/l} = \frac{4shl}{2(sl+hl+th)+ts} \quad (3.22)$$

The length of the heat exchanger for achieving the desired performance of 0.96 is found out to be 1008 mm .The other dimensions of the heat exchanger are given as given above. The maximum pressure drops is 0.014 bar for the cold fluid. The pressure drop is reasonably low and is within the permissible limit.

3.4 Design of heat exchanger using simulation software

The heat exchanger has also been designed by using Aspen–MUSE [113], the simulation software. The Aspen design takes into account the various losses occurring in the heat exchanger like longitudinal heat conduction, heat losses to the ambient, flow maldistribution at the headers, pressure losses in the headers etc. It has been accepted as a versatile tool for the design of plate fin heat exchangers in industrial applications.

The core length of the heat exchanger calculated by using Aspen–MUSE [113] is 1050 mm. The pressure drop of the cold fluid and the hot fluid are 0.0325 bar and

0.00781 bar including the pressure drop in the headers. This is well below the permissible pressure drop of 0.05 bar

3.5 Concluding dimensions of the heat exchanger

The selected dimension is given in tabular form as given below in Table 3.2

Table 3.2 Concluding dimensions of heat exchanger.

ITEM	DIMENSIONS	ITEM	DIMENSIONS
CORE LENGTH	900 mm	TOTAL LENGTH	1000 mm
CORE WIDTH	73 mm	TOTAL WIDTH	85 mm
CORE HEIGHT	93 mm	TOTAL HEIGHT	105 mm
PLATE THICKNESS	0.8 mm	END PLATE THICKNESS	6 mm
		END BAR THICKNESS	6 mm

Chapter 4

Rating of Plate Fin Heat Exchanger

Chapter IV

RATING OF PLATE FIN HEAT EXCHANGER

Rating of a heat exchanger consists of the steps leading to finding the thermo hydraulic performance of a given heat exchanger for known dimensions of the exchanger and given fin geometry. Since the outlet temperatures are not known in a rating problem, the mean temperatures of the fluids have to be estimated first. The heat transfer coefficient and the effectiveness of the plate fin heat exchanger are found based on different correlations available in literature. The outlet temperatures and the average fluid temperatures are calculated for an assumed effectiveness which is verified with the calculated value. This is an iterative procedure and is repeated until the calculated values of the exit fluid temperatures matches with the assumed values.

Longitudinal heat conduction along the separating surfaces of the two streams causes serious performance deterioration in heat exchangers. It is due to short conduction lengths and higher number of transfer units (N_{tu}). The effectiveness deterioration caused by longitudinal heat conduction is obtained using Kroeger equation [84]. He obtained the expression for the ineffectiveness due to longitudinal conduction as a function of longitudinal heat conduction parameter, λ, heat capacity ratio, C_r and number of transfer units, N_{tu}. Heat loss to the ambient causes an energy unbalance. Two values of effectiveness are obtained - ε_h, the effectiveness based on the hot fluid and ε_c, the effectiveness based on the cold fluid. The effectiveness considering the heat loss is obtained using simulation software, Aspen- Muse by substituting the experimentally obtained heat loss as input along with other inputs parameters. Aspen MUSE [113] after an iterative procedure gives two values of effectiveness, ε_h, the effectiveness based on the hot fluid and ε_c,the effectiveness based on the cold fluid. Besides this, the effectiveness of the heat exchanger is also affected by flow maldistribution at the headers. The manufacturing irregularities such as burred edges, separating plate roughness and bonding imperfections influence the thermo hydraulic performance of the heat exchanger.

A performance test is conducted on the given plate fin heat exchanger core. The values of the effectiveness and pressure drops obtained at different mass flow rates and at different hot inlet temperatures by experiment are compared with theoretical predictions. The details of the experimental set up are given in chapter V and performance analysis is given in chapter VI.

4.1 Details of given heat exchanger and input data

Tables 4.1 and 4.2 give the details of the given heat exchanger core along with the fin geometry used in the performance test. The thermo hydraulic performance of the given heat exchanger is to be found for the given mass flow rate. The pressures and temperatures of hot and cold fluid at inlet are as given below.

Table 4.1 Dimensions of the heat exchanger core

ITEM	DIMENSIONS	ITEM	DIMENSIONS
CORE LENGTH	900 mm	TOTAL LENGTH	1000 mm
CORE WIDTH	73 mm	TOTAL WIDTH	85 mm
CORE HEIGHT	93 mm	TOTAL HEIGHT	105 mm
PLATE THICKNESS	0.8 mm	END PLATE THICKNESS	6 mm
		END BAR THICKNESS	6 mm

The heat exchanger is constructed of Aluminum alloy Al-3003 with rectangular offset strip fins having the following basic dimensions.

Table 4.2 Fin geometry of the heat exchanger core

	Fin geometry	**High pressure Side**	**Low pressure Side**
01	Fin frequency,f	714 fins per meter	588 fins per meter
02	Length of fin, l	3 mm	5 mm
03	Fin thickness, t	0.2 mm	0.2 mm
04	Fin height, h	9.3 mm	9.3 mm
05	Number of layers	05	04

A. Geometrical characteristics related to selected fin geometry

Other geometrical characteristics related to the fin geometry are calculated from the given fin geometry .The calculations have been given in chapter III.

B. Heat exchanger input data.

Temperature at hot nitrogen gas at inlet, =368.96 K

Temperature at cold nitrogen gas at inlet, =315.24 K

Pressure at inlet of hot nitrogen gas = 1.0721 bar

Pressure at inlet of cold nitrogen gas = 1.0917 bar

Mass flow rate of hot nitrogen gas = 5.77 g/s

Mass flow rate of cold nitrogen gas = 5.77g/s

4.2 Rating of the given heat exchanger using different correlations

Effectiveness and pressure drop are obtained for given mass flow rate at the desired inlet temperatures of hot and cold fluids by using the correlations developed by Maiti and Sarangi[45], Manglik and Bergles [70] and Joshi and Webb [68]. Simulated values of the effectiveness and pressure drop are also obtained by using simulation software, Aspen- MUSE [113].They are compared with the performance parameters obtained by experiments in chapter V. The procedure for calculating the effectiveness and pressure drop using different correlations and simulation software is given below.

A. Rating of the given heat exchanger using correlations developed by Maiti and Sarangi [45]

a) Heat transfer area, A

The heat transfer area for high pressure side is calculated as follows:

Total area between plates, $A_{frh} = b \times N_h \times W = 0.0095 \times 5 \times 0.073 = 0.0035$ m^2

Total free flow area, $A_{ffh} = \sigma \times A_{frh} = 0.002425$ m^2

Wall conduction area on hot side, $a_{wh} = A_{frh} - A_{ffh} = 0.001043$ m^2

Total heat transfer area, $A_h = \dfrac{4 \times A_{ffh} \times L}{D_e} = \dfrac{4 \times 0.0024246 \times 0.9}{0.00167266} = 5.215$ m^2

Alternatively,

Total heat transfer area,

$$A_h = \frac{a_s \times p_f \times W \times L \times N_H}{l} = \frac{0.00006672 \times 714 \times 0.073 \times 0.9 \times 5}{0.003} = 5.215 \text{ m}^2$$

Similarly free flow area and the heat transfer areas are calculated for the cold side.

Total wall conduction (longitudinal conduction) area, $a_{wh} + a_{wc}$ = 0.001043+0.00069736 = 0.00174 m^2

b) Estimation of average temperature.

Since the outlet temperatures are not known for the rating problem, the mean temperatures of the fluids have to be estimated first. The fluid properties at the estimated mean temperatures of 344.15 K and 340.05 K for hot and cold fluid are obtained from property package, GASPAK.

The properties of hot nitrogen gas at the mean film temperature are:

Specific heat, C_p =1040.8 J/kg- K

Viscosity, $\mu = 0.0000199$ Pa-s

Prandtl number, $\Pr = 0.7170$

Density, $\rho = 1.046$ kg/m^3

The properties of cold nitrogen gas at the mean film temperature are,

Specific heat, $C_p = 1040.7$ J/kg- K

Viscosity, $\mu = 0.0000197$ Pa-s

Prandtl number, $\Pr = 0.717$

Density, $\rho = 1.076$ kg/m^3

c) Heat transfer coefficients and surface effectiveness of fins

The experimental set up uses atmospheric air from the compressor as the cold fluid and heated air from the heater as the hot fluid. For the hot fluid test conducted, the hot layer is sandwiched between the two outer cold layers. Therefore the number of layers through which the cold air from the compressor passes is taken as 5 where as for the hot air the number of layers is taken as 4.

The calculations for the heat transfer coefficients for the hot and cold gases are similar. The calculations are presented for the cold nitrogen gas.

i) The core mass velocity, $G = \frac{m_c}{A_{ffh}} = \frac{0.00577}{0.002425} = 2.38$ kg/s-m^2

ii) The Reynolds number, $\mathrm{Re} = \frac{GD_e}{\mu} = \frac{2.38 \times 0.001674}{0.0000197} = 202.3$

iii) The critical Reynolds number for heat transfer coefficient is given as:

$$\mathrm{Re}^* = 1568.58(h/s)^{-0.217}(l/s)^{-1.433}(t/s)^{-0.217}$$

$$= 1568.58(7.743)^{-0.217}(2.498)^{-1.433}(0.1665)^{-0.217} = 399.77$$

iv) The Colburn factor, j (for $\mathrm{Re} > \mathrm{Re}^*$) is given by correlation proposed by Maiti and Sarangi [45] as:

$$j_c = 0.18(\mathrm{Re})^{-0.42}(h/s)^{0.288}(l/s)^{-0.184}(t/s)^{-0.05}$$

$$= 0.18(202.298)^{-0.42}(7.743)^{0.288}(2.498)^{-0.184}(0.1665)^{-0.05} = 0.03685$$

v) The convective heat transfer coefficient is given as:

$$h_c = \frac{(j_c \times c_c \times G_c)}{(\mathrm{Pr})^{0.667}} = \frac{(0.03685 \times 1040.71 \times 2.3804)}{(0.7169)^{0.667}} = 113.95 \text{ W/m}^2\text{K}$$

vi) The fin parameter is calculated as:

a. $M = \sqrt{\frac{(2 \times h_c)}{(K_f \times t)}} = \sqrt{\frac{(2 \times 113.954)}{(170 \times 0.0002)}} = 81.87 \text{ m}^{-1}$

vii) The hot layer is sandwitched between the two outer cold layers. The cold layers are exposed more to the atmosphere and for calculating the fin effectiveness, fin conduction lengths for the outer layers on the cold side will be taken as b to take into account the heat losses from the ambient whereas for the inner layers the conduction length is taken as b/2.However for the hot layers sandwiched between the two cold layers, The fin conduction length is taken as b/2 for both inner and outer layers.

$l_c =$ height of fins for the inner layers of the cold fluid =b/2= 4.75 mm.

$l_c =$ height of fins for outer layers of the cold fluid = b = 9.5 mm

$l_h =$ height of fins for both inner and outer layers of the hot fluid = b/2 = 4.75 mm

viii) The fin effectiveness for a straight fin is

$$n_f = \tanh(Ml_c)/(Ml_c) = 0.9525 \quad \text{for inner layers.}$$

For the outer layers of cold side the fin effectiveness is 0.8375

ix) The overall surface effectiveness of fins on cold side is:

$$\eta_{0c} = 1-(a_f / a_s)\times(1-\eta_{fi})(\frac{(N_P-2)}{N_P}-(a_f/a_s)\times(1-\eta_{fo})(\frac{2}{N_P})$$

$$\eta_{0c} = 1-(0.8920)\times(1-0.9524)(\frac{(5-2)}{5}-(0.8920)\times(1-0.8375)(\frac{2}{5})$$

=0.9166.

The overall surface effectiveness of fins on hot side is:

$$\eta_{0h} = 1-(a_f / a_s)\times(1-\eta_f) = 1-(0.8656)(1-0.9626) = 0.9676$$

d) The overall heat transfer coefficient and number of transfer units

The overall heat transfer coefficient is given as:

$$\frac{1}{(U_O A_O)_h} = \frac{1}{(\eta_{oh} h_h A_h)} + \frac{a}{K_w A_w} + \frac{1}{(\eta_{oc} h_c A_c)}$$

where,

$A_w =$ lateral conduction area $= W \times L \times (2N_P + 2) = 0.073 \times 0.9(2\times 4+2) = 0.657$ m^2

$$\frac{1}{(U_O A_O)_h} = \frac{1}{(0.9676\times 88.464\times 3.452)} + \frac{0.0008}{170\times 0.657} + \frac{1}{(0.9166\times 113.954\times 5.215)}$$

$= 0.00522$ K/W

$(U_O A_O)_h = 191.32$ W/K

Overall heat transfer coefficient, $U_{Oc} = \frac{(U_O Ao)_c}{A_{oc}} = \frac{191.32}{5.215} = 36.68$ W/m^2-K

Number of transfer units, $N_{tu} = \frac{U_O A_O}{C_{\min}} = \frac{191.32}{6.0084} = 31.84$

e) Effectiveness of heat exchanger, neglecting longitudinal heat conduction

The effectiveness of heat exchanger, neglecting longitudinal heat conduction is given by the relation [77]:

$$\varepsilon = \frac{1-e^{-N_{tu}(1-C_r)}}{1-C_r e^{-N_{tu}(1-C_r)}} = \frac{1-e^{-31.84(1-0.9998)}}{1-0.9998e^{-31.84(1-0.996)}} = 0.9696$$

f) The effect of longitudinal heat conduction

The effect of longitudinal heat conduction is to reduce the effectiveness of heat exchanger. The decrease in the effectiveness of heat exchanger is determined using Kroeger's equation [84].

i) Wall conduction area, $a_w = 0.00174$ m^2

ii) Conductivity of fin, $K_w = 170$ W/m-K

iii) Wall conduction parameter, $\lambda = \frac{K_w a_w}{LC_{\min}} = \frac{170 \times 0.00174}{0.9 \times 6.0084} = 0.05467$

iv) $y = \lambda N_{tu} Cr = 0.05467 \times 31.843 \times 0.996 = 1.741$

v) $\gamma = \frac{(1-Cr)}{(1-Cr)(1+y)} = \frac{(1-0.996)}{(1-0.996)(1+1.7408)} = 1.928 \times 10^{-5}$

vi) $\phi = \gamma (y/(1+y)^{1/2} \left[\frac{(1+\gamma)y}{1-\gamma(1+\gamma)y} \right] = 2.675 \times 10^{-5}$

vii) $\varphi = \frac{(1+\phi)}{(1-\phi)} = \frac{(1+2.675 \times 10^{-5})}{(1-2.675 \times 10^{-5})} = 1.0000$

viii) $r_1 = \frac{(1-C_r)N_{tu}}{1+\lambda N_{tu} Cr} = \frac{(1-0.996) \times 31.84}{1+0.05467 \times 31.84 \times 0.996} = 0.001228$

ix) $(1-\varepsilon) = \frac{(1-Cr)}{\varphi \exp(r_1) - Cr} = \frac{(1-0.996)}{1 \times \exp(0.001228) - 0.996} = 0.0761$

x) $\varepsilon = [1-(1-\varepsilon)] = 0.9238$

This is the value of the actual effectiveness of heat exchanger after considering longitudinal heat conduction. Outlet temperatures of fluids based on this value of effectiveness are calculated as follows:

The outlet temperature of hot fluid is computed as:

$$T_{ho} = T_{hi} - \frac{\varepsilon C_{\min}(T_{hi} - T_{ci})}{C_h} = 368.96 - \frac{0.9238 \times 6.0084(368.96 - 315.24)}{6.0084} = 319.34K$$

The outlet temperature of cold fluid is computed as:

$$T_{co} = T_{ci} + \frac{\varepsilon C_{\min}(T_{hi} - T_{ci})}{C_c} = 315.24 + \frac{0.9238 \times 6.0084(368.96 - 315.24)}{6.0084} = 364.87K$$

Mean temperatures of hot and cold fluid are given by

Mean temperature of hot fluid, $T_{hm} = \frac{T_{hi} + T_{ho}}{2} = \frac{368.96 + 319.34}{2} = 344.15\,\text{K}$

Mean temperature of cold fluid, $T_{cm} = \frac{T_{ci} + T_{co}}{2} = \frac{315.24 + 364.87}{2} = 340.05\,\text{K}$

g) Calculation of pressure drop, Δp

Since pressure drop of cold fluid stream is more critical, the pressure drop calculations for the cold fluid are presented here.

i) The critical Reynolds number for pressure drop is given calculated as:

$$\text{Re}^{**} = 648.23(h/s)^{-0.06}(l/s)^{0.1}(t/s)^{-0.196}$$

$$= 648.23(7.7435)^{-0.06}(2.5)^{0.1}(0.1667)^{-0.196} = 892.77$$

ii) The friction factor

If Re>Re**,

$$f = 0.32(\text{Re})^{-0.286}(h/s)^{0.221}(l/s)^{-0.185}(t/s)^{-0.023}$$

$$= 0.32(202.298)^{-0.286}(7.743)^{0.221}(2.5)^{-0.185}(0.1665)^{-0.023}$$

$$= 0.1731$$

iii) The pressure drop, $\Delta p = \frac{4fLG^2}{2D_e\rho_b} = \frac{4 \times 0.1732 \times 0.9 \times (2.3804)^2}{2 \times 0.001674 \times 1.07551} = 980.67$ Pa

Since the pressure drop is less than the allowable pressure drop of 5 kPa, the design does meet the hydraulic requirement.

Thus the value of the effectiveness of the heat exchanger obtained using the correlations developed by Maiti and Sarangi[45] after considering the longitudinal conduction losses is 0.9238 and the pressure drops in the cold and hot fluids are 0.0098

bar and 0.00746 bars respectively. This is well below the allowable pressure drop of 0.05 bar.

B. Rating of the given heat exchanger using correlations developed by Manglik and Bergles[70]

The rating of the given heat exchanger is also done by correlations developed by Manglik and Bergles [70] using the same procedure as given above. For better readability, the (Equations 3.20, 3.21 and 3.22) of Manglik and Bergles [70] are rewritten as

The non-dimensional heat transfer coefficient,j and friction factor,f are given by the following expressions

$$j = 0.6522\,\mathrm{Re}^{-0.5403}(s/h)^{-0.1541}(t/l)^{0.1499}(t/s)^{-0.0678}\times \left[1+5.269\times10^{-5}\,\mathrm{Re}^{1.340}(s/h)^{0.504}(t/l)^{0.546}(t/s)^{-1.055}\right]^{0.1}$$

$$f = 9.6243\,\mathrm{Re}^{-0.7422}(s/h)^{-0.1856}(t/l)^{0.3053}(t/s)^{-0.2659}\times \left[1+7.669\times10^{-8}\,\mathrm{Re}^{4.429}(s/h)^{0.920}(t/l)^{3.767}(t/s)^{0.236}\right]^{0.1}$$

Hydraulic diameter is given by the following expression

$$D_e = \frac{4A_c}{A/l} = \frac{4shl}{2(sl+hl+th)+ts}$$

The effectiveness of the heat exchanger obtained using the correlation developed by Manglik and Bergles [70] and after considering the longitudinal conduction losses is 0.9424 and the pressure drops in the cold and hot fluids are 0.0064 bar and 0.005 bar respectively. This is well below the allowable pressure drop of 0.05 bar

C Rating of the given heat exchanger using correlations developed by Joshi and Webb[68]

Joshi and Webb [68] used the same expression for the hydraulic diameter as defined by Maiti and Sarangi [45]. The non dimensional heat transfer coefficient, j and friction factor, f are given by the following expressions.

The Colburn, j factor and friction factor, f (for $\mathrm{Re} \le \mathrm{Re}^*$) are given by correlations developed by Joshi and Webb [68].

$$j_c = 0.57(\mathrm{Re})^{-0.5}(l/D_h)^{-0.15}(\alpha)^{-0.14} \quad (4.1)$$

$$f = 8.12.(\mathrm{Re})^{-0.74}(l/D_h)^{-0.41}(\alpha)^{-0.02} \quad (4.2)$$

The effectiveness of the heat exchanger obtained using the Joshi and Webb [68] correlation and after considering the longitudinal conduction losses is 0.9303 and the pressure drops in the cold and hot fluids are 0.0074 bar and 0.0053 bar respectively. This is well below the allowable pressure drop of 0.05 bar

4.3 Rating of the given heat exchanger using simulation software, Aspen-MUSE {113].

Aspen MUSE [113] is the simulation software which is being increasingly used for the industrial design of heat exchangers. It takes into consideration the various losses that affect the thermo hydraulic performance of the heat exchanger while simulating for the given inputs. The value of the effectiveness using simulation software is 0.89. The pressure drops of the cold and hot fluid are 0.008 bar and 0.00525 bar respectively.

Table 4.3 and Table 4.4 show the predicted value of the effectiveness and pressure drop of the cold fluid calculated using different correlations and by simulation software, Aspen MUSE [113].

Table 4.3.The predicted value of the effectiveness using different correlations for a mass flow rate of 5.77 g/s operating between 315 K and 369 K.

SL. No	**Mass flow rate,g/s**	**Effectiveness**			
		Maiti and Sarangi correlation	Manglik and Bergles correlation	Joshi and Webb correlation	Aspen-MUSE
1	5.77	0.9238	0.9434	0.9303	0.89

Table 4.4.The predicted value of the pressure drop of the cold fluid using different correlations for a mass flow rate of 5.77 g/s operating between 315 K and 369 K.

SL. No	**Mass flow rate,g/s**	**Pressure drop**			
		Maiti and Sarangi correlation	Manglik and Bergles correlation	Joshi and Webb correlation	Aspen-MUSE
1	5.77	0.0098	0.00637	0.0074	0.008

4.4 Effect of heat transfer to the ambient.

The performance of cryogenic heat exchangers may be seriously affected by heat exchange with the surroundings. Because of the large temperature difference between the ambient and operating temperature, the quantity of heat leak is quite high. This reduces the effectiveness of the heat exchangers. This problem can be reduced by using highly effective insulation, but the amount of insulation to be used may be too high. Cryogenic heat exchangers are essentially placed in the vacuum chamber to minimise the heat loss.

In this analysis the hot test method is used to study the performance of the given plate fin heat exchanger. The flow direction is reversed so that the hot layers (layers through which the hot fluid passes) are placed inside the two outer cold layers. In this experiment several layers of glass wool and thermocole insulations are used on the heat exchanger to eliminate the heat transfer to the surroundings. A resistance temperature detector is placed on the outer surface of the insulation to indicate the temperature difference for assessment of heat losses to the surroundings.

Energy balance between the hot and cold fluids is lost if there is a heat loss to the surroundings. The temperature difference between the two fluids at the hot end and that at the cold end are noted down. The difference in the values of temperatures at hot end and cold end indicates the loss of energy. Hence two values of effectiveness - ε_h, the effectiveness based on the hot fluid and ε_c, the effectiveness based on the cold fluid are obtained.

Chapter 5

Experimental Apparatus

Chapter V

THE EXPERIMENTAL APPARATUS

The experimental set up used in this experiment consists of a counter flow plate fin heat exchanger. Cold air from the compressor is made to flow through one channel where as hot air coming from a heating unit is made to flow through the second channel in a counter flow direction. This chapter presents the measurement principle, layout of the experimental set up, description of the different components of the set up, calibration procedure of the instruments used, and an analysis of possible experimental errors.

5.1 Experimental set up and the operation

The experimental rig comprises of the air supply system, the heating unit, heat exchanger core and the instrumentation / measurement system as shown in Figures 5.1 and 5.2. In this apparatus a counter flow type of heat exchanger is used as the test section.

Air is used as a working fluid in this experiment. The heat exchanger is connected to a screw compressor which is capable of continuously supplying dry air. A control valve is used to regulate the flow rate through the heat exchanger. The cold air enters the heat exchanger from the bottom and gets heated as it passes through the exchanger. The air coming out then passes through the heating unit and gets further heated. The hot air coming out of the heater is fed into the heat exchanger from the top end. The amount of hot air entering the heater is regulated by a valve located at the inlet of the heater. The bypass valve will be closed for the balanced case, i.e, when the mass flow rates of both the fluids are equal. The heat supplied to the heater is controlled with the help of variacs.

Pressure gauges are provided to measure the pressures at inlet of both the hot and cold fluids. The pressure taps are located on the upstream and downstream of heat exchanger to measure the pressure drop across the heat exchanger. These pressure taps are connected to a U tube manometer to give the value of pressure drop. The inlet and outlet temperatures of both the fluids are measured by using resistance temperature

detector (RTD). For balanced flow, a rotameter at the exit of the heat exchanger is used for measuring the flow rate of the fluids directly in the circuit. In case of unbalanced flow, orifice plates are used for measuring the flow rate of both the fluids. Rotameter also helps in calibrating the flow rate of the orifice meters as and when required.

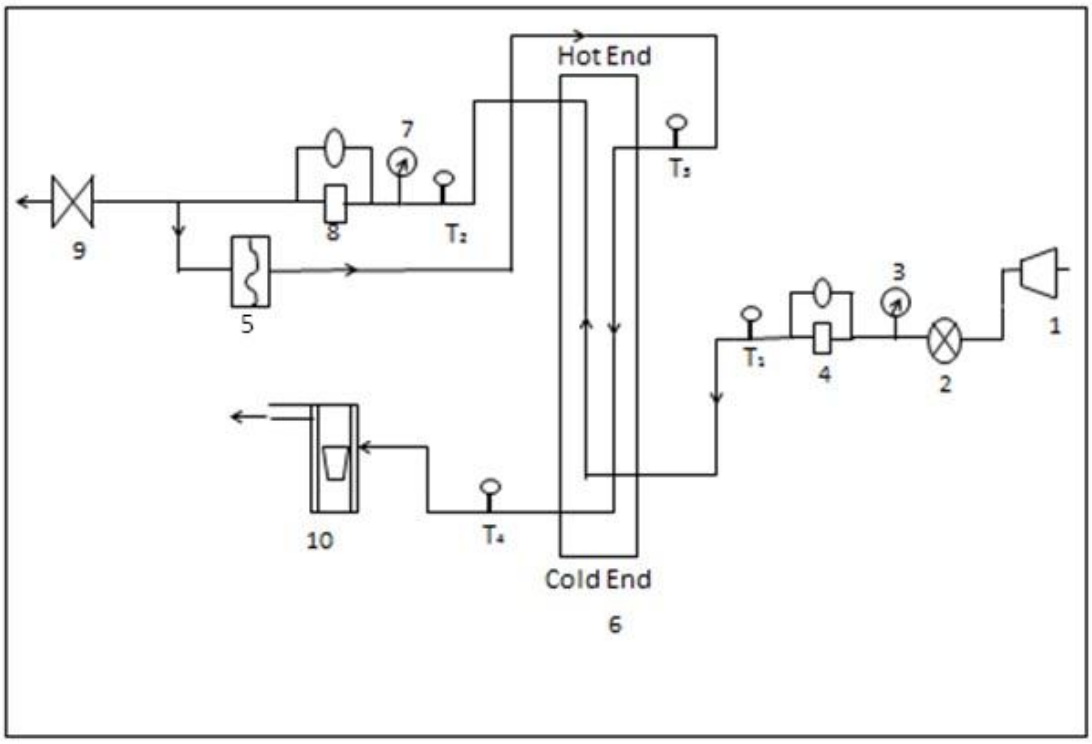

Figure 5.1: Schematic P&I diagram of the experimental test rig

1: Compressor	2: Control Valve	3,7: Pressure Taps
4,8: U- Tube manometer	5: Heater	6:Test section
T_1, T_2, T_3, T_4 are RTD's	9: Bypass valve	10: Flowmeter

The test section is carefully insulated by using glass wool and thermocole (polystyrene foam) sheets to eliminate heat losses from the system to the surroundings. Nearly 80 mm of glass wool insulation is used as shown in Figure 5.3. A resistance temperature detector is placed on the outer surface of the insulation to indicate the temperature difference for assessment of heat losses to the surroundings.

The by pass valve is closed for the balanced flow rate operation. The flow rate through the test section is set at the desired value. The volume flow rate through the test section can be observed in a rotameter placed at the exit of the heat exchanger test rig at balanced condition. The variac is kept at a low value initially and then increased

gradually according to the desired hot inlet temperature. Pressures at the inlet of both the fluids are noted from pressure gauges. Temperature of hot air at inlet of the heat exchanger is maintained at the desired temperature by adjusting the wattage of the variac. The system is allowed to run until the steady state conditions are reached. The inlet and outlet temperatures of both the fluids are noted down from the measurement of resistance temperature detectors (RTD). Pressure drop of both the fluids are read from the U–tube mercury manometers.

Figure 5.2: Photograph of the experimental set up

The performance parameters of the heat exchangers such as the effectiveness and pressure drop of the fluids are calculated. The values of the effectiveness, pressure drops of the fluids are also found out using the various correlations available in literature and also from well known simulation software, Aspen MUSE [113]. The performance parameters obtained by experimentation and that obtained by simulation are compared with the theoretical values for analyzing the various losses.

Figure 5.3: Photograph of the experimental set up (with insulation)

5.2 Calculation procedure

In the steady state experiment, measurement of temperature and mass flow rates in the two sides provides the required information to compute the heat exchanger effectiveness. For the flow rate of 300 liter/min operating between 315 K and 369 K, the calculations of the performance parameters are given as below

i) For a balanced mass flow rate of hot and cold fluids, the effectiveness is given by

$$\varepsilon = \frac{(T_2 - T_1)}{(T_3 - T_1)} = \frac{(T_3 - T_4)}{(T_3 - T_1)} \qquad (5.1)$$

where

T_1 =Temperature at inlet of cold fluid = 315.2 K

T_2 =Temperature at outlet of cold fluid = 360.2 K

T_3 =Temperature at inlet of hot fluid = 368.96 K

T_4 =Temperature at outlet of hot fluid = 321.1 K

we get

ε_h = Effectiveness of hot fluid = 0.89

ε_c = Effectiveness of cold fluid = 0.84

ii) Mass flow rate of the fluids flowing through the heat exchanger is measured by a rotameter placed at the exit of the heat exchanger test rig.

Mass flow rate, $m = \rho_4 \times Q$ (5.2)

where

ρ_4 =Density of the hot fluid at exit =1.1542 kg/m^3

Q = Volume flow rate measured by the rotameter = 0.005 m^3/sec

Mass flow rate, $m = 1.1542 \times 0.005 = 5.77$ g/s.

iii) The pressure taps are located on the upstream and downstream of heat exchanger to measure the pressure drop across the heat exchanger. The minor pressure loss due to flow through elbows and pressure loss in the headers have to be subtracted from the measured pressure drop to get the pressure drop in the heat exchanger core. The pressure loss in the headers is found out by simulation with and without headers.

Pressure drop in the core = measured pressure drop –minor losses-pressure loss in the headers

= 0.012-0.001-0.0056

= 0.0054 bar

The non-dimensional heat transfer coefficient, j and friction factor, f are calculated using the correlations developed by Maiti and Sarangi [45], Manglik and Bergles [70], and Joshi and Webb [68]. The theoretical or the predicted values of the effectiveness are calculated by using the rating procedure outlined in chapter IV. The theoretical value of the effectiveness calculated using the above correlations and that calculated using simulation software, Aspen-MUSE [113] are compared with the effectiveness value obtained from experiment.

5.3 Effect of heat transfer from the ambient

The performance of heat exchangers may be seriously affected by heat leak from the surroundings. Because of the large temperature difference between the ambient and operating temperatures, the quantity of heat leak is quite high. This problem can be reduced by using highly effective insulation. But factors like cost, weight and volume of insulation, difficulties in fabrication and ageing of insulation limit the extent to which heat transfer may be reduced. Heat transfer from the surroundings is manifested as a reduction in the effectiveness of heat exchangers. In this experiment

several layers of glass wool and thermocole insulation are used on the heat exchanger to eliminate the heat transfer from the surroundings. This can be ascertained from the reading on the temperature detector placed on the outer surface of insulation.

5.4 Description of various equipment and instruments

A. Plate fin heat exchanger.

The test section consists of a counter flow plate fin heat exchanger with offset strip fin geometry. The design procedure of the given plate fin heat exchanger has been given in chapter III. Figure 5.4 shows the plate fin heat exchanger with all its dimensions and arrangements of inlet and outlet ports. The cold layers (layers through which the cold fluid passes) are sandwiched in between the two outer hot layers of the plate and fin heat exchangers used in cryogenic applications. Table 5.1 shows the flow arrangement for the hot and cold fluids intended for cryogenic applications. However for the performance test conducted (Hot test), the flow direction has been reversed. The cold fluid from the compressor is made to flow through the high pressure side (having 5 layers) whereas the hot fluid passes through the low Pressure side (having 4 layers).Thus a hot layer is sandwiched between the two outer cold layers. The Tables 5.2 and 5.3 provide the details of core dimensions and fin geometry used in the given heat exchanger. The Table 5.4 gives the design data of the given heat exchanger.

Table 5.1: Flow arrangement for the designed heat exchanger

	HIGH PRESSURE SIDE (HOT SIDE)	**LOW PRESSURE SIDE (COLD SIDE)**
FIN	OSF	OSF
NO. OF PASSAGE	5	4
NO. OF PASS	1	1
FLOW RATE	COUNTER FLOW	COUNTER FLOW

Table 5.2: Core dimensions of the test heat exchanger

CORE LENGTH	900 mm	TOTAL LENGTH	1000 mm
CORE WIDTH	73 mm	TOTAL WIDTH	85 mm
CORE HEIGHT	93 mm	TOTAL HEIGHT	105 mm

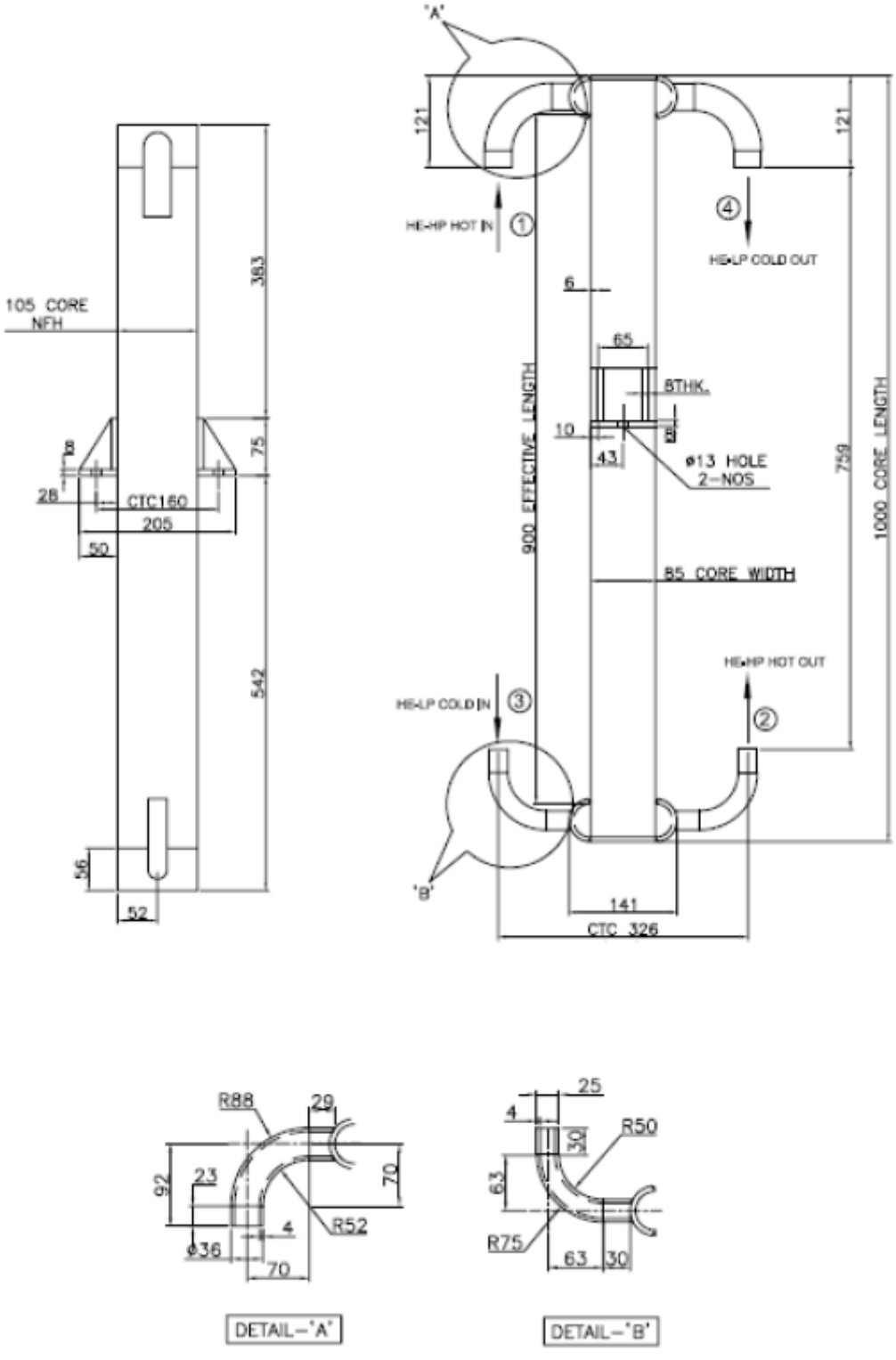

Figure 5.4: Plate fin heat exchanger

Table 5.3: Fin geometry in the given heat exchanger

	Fin geometry	**High pressure Side**	**Low pressure Side**
01	Fin frequency, f	714 fins per metre	588 fins per metre
02	Length of fin, l	3 mm	5 mm
03	Fin thickness ,t	0.2 mm	0.2 mm
04	Fin height, h	9.3 mm	9.3 mm
05	Number of layers	05	04

Table 5.4: Design data of the given heat exchanger

HEAT LOAD	5.5 KW	
	HOT SIDE	COLD SIDE
FLUID	HELIUM (HP)	HELIUM (LP)
FLOW RATE	5 g/s	4.8 g/s
INLET TEMP.	310 K	83.65 K
OUTLET TEMP.	92.85 K	301.67 K
ALLOWABLE PRESSURE DROP	0.05 bar	0.05 bar
PRESSURE AT INLET	7.35 bar	1.15 bar

B. Twin screw compressor

The air supply system consists of a twin screw rotary compressor which is a positive displacement type. In this oil flooded rotary compressor lubricating oil bridges the space between the rotors, providing a hydraulic seal and transferring mechanical energy between the driving and driven rotors. Gas enters at the suction side and meshing rotors force the gas through the threads as the screws rotate. Screw compressors have relatively high rotational speed compared to other types of positive displacement machines which make them compact. Sufficient amount of oil provided gives the cooling effect to maintain the temperature nearly constant. They have the ability to maintain high volumetric efficiencies over a wide range of operating pressure and flow rates. It has long service life and high reliability.

The Compressor specification is given below:

Table 5.5 Compressor Specifications:

Make:	Kaeser (Germany)
Model:	BSD 72
Profile of screw:	Sigma
Free air delivery:	336 m3 /hr
Suction pressure:	Atmospheric
Maximum Pressure:	11 bar
Operating temperature:	75- 100^0C
Motor:	37kW, 74amps, 3Φ, 50Hz, 415V±10%, 3000rpm
Oil capacity:	24 L
Cooling:	Air

C. Heating device

This heating element was fully designed and developed in our laboratory. It consists of a shell containing a number of heating elements. The cold fluid enters the shell from one side and moves over the heater to leave at the other end of the shell. The heating elements are arranged in a particular pattern which also acts as baffles for better heat transfer. There are seventeen number of heating tubes each having a capacity of 1500 W (220/230V, 50 Hz).

D. Resistance Temperature Detectors (RTDs)

Resistance thermometers also called as resistance temperature detectors (RTD) or resistive thermal devices are temperature sensors that exploit the predictable change in electrical resistance of some materials with changing temperature. It is a positive coefficient device, which means that the resistance increases with temperature. So the material whose resistance increases with temperature is used for making the RTD. Typical elements used for RTD include nickel (Ni), copper (Cu), but platinum (Pt) is by far the most common, because it has the best accuracy and stability in comparison to other RTD materials. For platinum RTD the resistance versus temperature curve is fairly linear and the temperature range is widest and has a very high resistivity. It means that only a small amount of platinum is required to fabricate a sensor and making platinum costs competitive with other RTD materials. The RTD's are slowly replacing the use of

thermocouples in many industrial applications below 600 ^{0}C, due to higher accuracy and reliability.

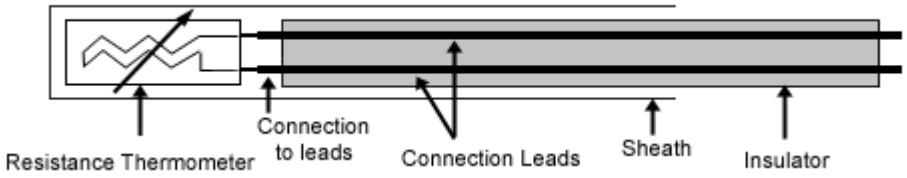

Figure 5.5: RTD's construction

Figure 5.5 shows the construction of a RTD. RTDs are constructed by one of two different manufacturing configurations. First one is the wire wound RTD which are constructed by winding a thin wire into a coil. Second type, thin fin element is a more common configuration, which consists of a very thin layer of metal laid out on a plastic or ceramic substrate. Thin-film elements are cheaper and more widely available because they can achieve higher nominal resistances with less platinum. In order to protect the RTD, a metal sheath encloses the RTD element and lead wires are connected to it. RTD's are available with three different lead wire configurations. The selection of a particular configuration depends on the desired accuracy and instruments to be used for the measurement.

(a) Two wire configuration
(b) Three wire configuration and
(c) Four wire configuration.

RTDs are popular because of their excellent stability and exhibit the most linear signal with respect to temperature when compared to any other electronic temperature sensor. They are generally more expensive than alternatives, however, because of the careful construction and use of platinum, RTDs are also characterized by a slow response time and low sensitivity; and because they require current excitation, they can be prone to self heating. And there main limitation is that they cannot be used for measurement of temperature above 660 ^{0}C and below -270 ^{0}C. Also they are less sensitive to very small temperature changes.

RTD's are commonly categorized by their nominal resistance at 0^{0}C. By far the most common RTD used in the industry have a nominal resistance of 100 Ohms at 0^{0}C

are called as the PT-100 sensors. The relationship between resistance and temperature is nearly linear and follows the equation,

For $< 0\ ^0C$ $\quad R_T = R_0\,[1+ aT+bT^2+cT^3\ (T-100)]$ (5.4)

For $> 0\ ^0C$ $\quad R_T = R_0\,[1+ aT+bT^2]$ (5.5)

Where,

R_T = resistance at temperature T

R_0 = resistance at nominal temperature

a, b, and c are the constants used to scale the RTD.

Four numbers of RTDs are used for the measurement of inlet and exit temperature of both the fluid streams. For accurate measurement of temperature, these RTD'S are to be calibrated with a single known temperature. Water is heated in a beaker with the help of induction type heater. The resistance temperature detectors to be calibrated are immersed in the water .The water is heated slowly and is stirred with the help of stirrer for uniform distribution of heat. The temperatures indicated in a 16 channel temperature indicator are noted down.

The variation of temperature detector readings T_2, T_3 and T_4 are plotted with respect to temperature indicator reading T_1The thermometer is also inserted to observe the temperatures and it acts as a reference thermometer. The calibration graph and the measured values are shown in fig 5.7 and Table 5.6.The set up used for calibration of resistance temperature detectors is shown in fig 5.6.

Figure 5.6: Photograph of the set up used for calibration

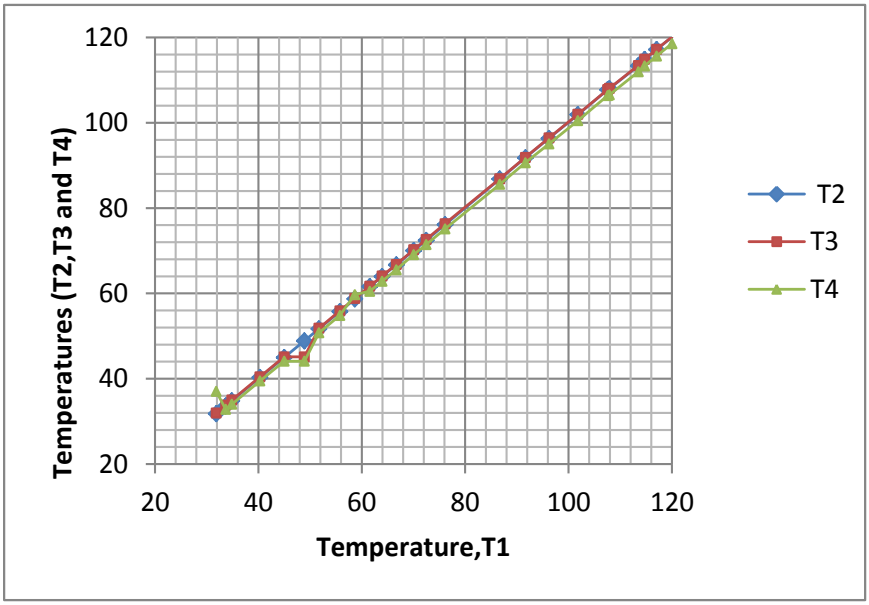

Figure.5.7: RTD Calibration graph

Table 5.6 Calibration Chart

THERMOMETER(^{0}C)	RTD1(^{0}C)	RTD2(^{0}C)	RTD3(^{0}C)	RTD4(^{0}C)
30.5	31.85	31.8	31.98	37.04
32.8	33.67	33.64	33.82	32.84
34	34.87	34.84	35.01	34.03
39	40.31	40.31	40.46	39.48
43.5	44.98	44.98	45.13	44.11
47	48.9	48.89	45.13	44.11
50	51.72	51.69	51.84	50.76
54	55.76	55.74	55.92	54.85
57	58.66	58.7	58.82	59.71
60	61.55	61.6	61.69	60.51
62.8	63.93	63.98	64.07	62.87
65	66.67	66.71	66.78	65.54
68	70.04	70.06	70.24	69.1
71	72.45	72.43	72.63	71.44
74.5	76.1	76.12	76.34	75.12
85	86.69	86.81	86.87	85.57
90	91.64	91.79	91.89	90.64
94.5	96.21	96.34	96.45	95.04
100	101.8	101.91	101.99	100.51
105.5	107.55	107.73	107.77	106.38
107.5	107.9	108.01	108.08	106.55
110.5	113.5	113.36	113.42	111.95
112.5	114.71	114.85	114.89	113.33
115	117.04	117.18	117.22	115.65
117	120	120.07	120.12	118.54

E. Orifice mass flow meter

A flow meter or flow sensor is an instrument used in process instrumentation to measure the flow rate of liquid or gas. Its working is based on the Bernoulli's principle which says that there is a relationship between the pressure and the velocity of a fluid stream. When the velocity increases, the pressure decreases and vice versa.

An orifice plate is basically a thin plate with a hole in the middle. It is usually placed in a pipe in which fluid flows. When the fluid reaches the orifice plate, with the hole in the middle, the fluid is forced to go through the small hole of varying cross section causing the change in both the velocity and pressure of the fluid. The point of maximum convergence actually occurs shortly at downstream of the physical orifice and is called as the point of vena contracta. Beyond the vena contracta, the fluid expands and the velocity and pressure change to normal. The volumetric and mass flow rates are obtained from the Bernoulli's equation by measuring the difference in fluid pressure between the normal pipe section and at the vena contracta, as shown in figure 5.7.The pressure recovery is limited for an orifice plate and the permanent pressure loss depends primarily on the area ratio. For an area ratio of 0.5, the head loss is about 70 - 75% of the orifice differential.

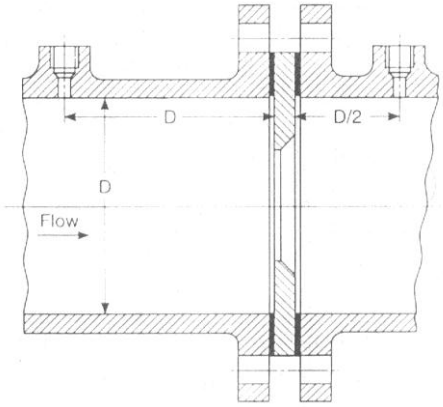

Fig.5.7 Orifice plate [114]

The volume flow rate, Q can be calculated from the formula given below:

$$Q = CC_d\sqrt{2gh_a} \tag{5.6}$$

Where, C = area constant = $\dfrac{A_2}{\sqrt{1-(\frac{A_1}{A_2})^2}}$

C_d = coefficient of discharge and h_a = head of air = $h_w(\dfrac{\rho_w}{\rho_a}-1)$

Mass flow rate, m = $\rho_a \times Q$

F. Variac or Autotransformer

A variac, also called as an autotransformer is an electrical transformer with only one winding. The auto prefix refers to the single coil acting on itself rather than any automatic mechanism. In an autotransformer portions of the same winding act as both the primary and secondary. The winding has at least three taps where electrical connections are made. In India, autotransformers are used to step up or step down between voltages in the 220-230-240-volt range. The autotransformers are used to regulate the voltage of the heating element to get the desired temperature of the heater unit.

5.5 Error analysis:

The total uncertainty in an observable or measurable quantity is decomposed into two parts: *random errors* and *systematic errors*. A random error is defined as the uncertainty detected by repeating the measurement procedure under the same conditions, while a systematic error is that which cannot be detected through this method and is usually associated with bias in experimental data. Random errors are generally caused by the imprecision of the measuring instruments and fluctuations in environmental conditions. They can, in general, be bound within desired limits by using precision instruments and by controlling environmental factors. But systematic errors are inherent in the experimental process and a high degree of subjective judgment is necessary to estimate these errors. For example, faulty design of the test system or lack of homogeneity in the heat exchanger core leads to errors in velocity distribution, which translate to errors in Re and f. Even if the replicated measurements give identical results, this intrinsic defect will yield results that may not replicate in future. Calibration of the experimental system can eliminate some of these errors.

The following major sources of systematic errors are identified in this experimental system:

1. Errors inherent in the design and execution of the test system: Faulty design of the test system leads to error in velocity distribution, which leads to errors in j and f values. This can contribute up to $\pm 1\%$ in j and f data, as observed by Kays and London [2].This in turn effect the measurement of the effectiveness.

2. Errors in calibration of pressure transducers and temperature sensors. The uncertainty in calibration of the sensors is estimated to be of the order of $\pm 1\%$ for pressure transducers and $\pm 0.5\%$ for temperature sensors.
3. Lack of homogeneity in test core construction such as uneven accumulation of brazing alloy at the roots of the fins and compression of flow passages results in errors in both friction factor and heat transfer measurements. The level of uncertainty is of the order of $\pm 1\%$ as reported by Kays and London [2].

The result R of an experiment is calculated from a set of measurements, for example, $x_1, x_2, x_3 \ldots\ldots x_n$. Thus,
$R=R(x_1, x_2, x_3 \ldots\ldots x_n)$

Let δR be the overall uncertainty in the result, representing the range (on both the sides of R) in which the true value may lie, and $\delta x_1, \delta x_2, \delta x_3 \ldots\ldots \delta x_n$ the uncertainties in the independent variables $x_1, x_2, x_3 \ldots\ldots x_n$ respectively. In a simplistic way, the overall uncertainty may be calculated, by adding the uncertainties caused by all independent variables.

$$\delta R = \left|\frac{\partial R}{\partial x_1}\delta x_1\right| + \left|\frac{\partial R}{\partial x_2}\delta x_2\right| + \ldots\ldots + \left|\frac{\partial R}{\partial x_n}\delta x_n\right| \tag{5.7}$$

In this expression, errors in $x_1, x_2, x_3 \ldots\ldots x_n$, with the same sign and the maximum magnitude for each term, are combined in the worst possible way, resulting in an overestimation of the experimental inaccuracy. This can happen only when the variables are not really independent. A more realistic expression for the overall uncertainty can be predicted by the root mean square error: [106-111]

$$\delta R = \left[\left(\frac{\partial R}{\partial x_1}\delta x_1\right)^2 + \left(\frac{\partial R}{\partial x_2}\delta x_2\right)^2 + \ldots\ldots\left(\frac{\partial R}{\partial x_n}\delta x_n\right)^2\right]^{0.5} \tag{5.8}$$

The effectiveness of the heat exchanger is given by

$$\eta = \frac{m_1(T_2 - T_1)}{m_2(T_3 - T_1)}$$

$$\frac{\partial \eta}{\partial m_1} = \frac{(T_2 - T_1)}{m_2(T_3 - T_1)} \tag{5.9}$$

$$\frac{\partial \eta}{\partial m_2} = \frac{-m_1(T_2 - T_1)}{m_2{}^2(T_3 - T_1)} = \frac{-1(T_2 - T_1)}{m(T_3 - T_1)} = \frac{(T_1 - T_2)}{m(T_3 - T_1)} \tag{5.10}$$

$$\frac{\partial \eta}{\partial T_1} = \frac{m_2(T_3 - T_1)\dfrac{\partial\left(m_1(T_2 - T_1)\right)}{\partial T_1} - m_1(T_2 - T_1)\dfrac{\partial}{\partial T_1}\left(m_2(T_3 - T_1)\right)}{m_2{}^2(T_3 - T_1)^2}$$

$$\frac{\partial \eta}{\partial T_1} = \frac{m_2(T_3 - T_1)(-m_1) - m_1(T_2 - T_1)(-m_2)}{m_2{}^2(T_3 - T_1)^2}$$

$$= \frac{(m_2T_3 - m_2T_1)(-m_1) - (m_1T_2 - m_1T_1)(-m_2)}{m_2{}^2(T_3 - T_1)^2}$$

$$= \frac{-m_1m_2T_3 + m_1m_2T_1 + m_1m_2T_2 - m_1m_2T_1}{m_2{}^2(T_3 - T_1)^2}$$

$$= \frac{m_1(T_2 - T_3)}{m_2(T_2 - T_1)^2} \tag{5.11}$$

$$\frac{\partial \eta}{\partial T_2} = \frac{\partial}{\partial T_2}\left(\frac{m_1(T_2 - T_1)}{m_2(T_3 - T_1)}\right)$$

$$= \frac{\partial}{\partial T_2}\left(\frac{m_1T_2}{m_2(T_3 - T_1)} - \frac{m_1T_1}{m_2(T_3 - T_1)}\right)$$

$$\frac{\partial \eta}{\partial T_2} = \frac{1}{(T_3 - T_1)} \tag{5.12}$$

$$\frac{\partial \eta}{\partial T_3} = \frac{\partial}{\partial x}\left(\frac{m_1(T_2 - T_1)}{x}\right)\frac{\partial x}{\partial T_3}$$

$$\frac{\partial \eta}{\partial T_3} = \left(\frac{-m_1(T_2 - T_1)}{m_2(T_3 - T_1)^2}\right) \tag{5.13}$$

$$\delta\eta = \sqrt{(\frac{\partial \eta}{\partial m_1}\delta m_1)^2 + (\frac{\partial \eta}{\partial m_2}.\delta m_2)^2 + \left(\frac{\partial \eta}{\partial T_1}.\delta T_1\right)^2 + \left(\frac{\partial \eta}{\partial T_2}.\delta T_2\right)^2 + \left(\frac{\partial \eta}{\partial T_3}\delta T_3\right)^2} \tag{5.14}$$

Where

δm_1 and δm_2 are the errors in mass flow rates

$\delta T_1, \delta T_2$ And δT_3 are the errors in temperatures which are equal to 0.1 K for RTD.

The mass flow rate is measured by a rotameter placed at the exit of the hot fluid. The accuracy of the rotameter has been specified as ± 12 liter/min by the instrument supplier. However the readings of the rotameter were checked by a thermal mass flow meter. The least count of RTD is 0.05 K as specified by the supplier. In this experiment the temperature difference is measured. Thus the total least count is addition of individual least counts which comes to 0.1 K.

The error in mass flow rate = the error in volume flow rate $\times$ density of hot fluid at outlet

$$= 0.0002 \times 1.15$$

$$= 0.000231 \text{ kg /sec}$$

For the mass flow rate of 5.77 g/s operating between 315.4 K and 369.13 K, The error terms in equation (5.14) are obtained by substituting the temperature and mass values in equation (5.9) to (5.13).

The error terms in the equation are obtained as 145.09, 145.09, 0.00303, 0.0186 and 0.01558 and the errors in mass and temperatures to get the error in effectiveness as

$$\delta\eta = \sqrt{(\frac{\partial \eta}{\partial m_1}\delta m_1)^2 + (\frac{\partial \eta}{\partial m_2}.\delta m_2)^2 + \left(\frac{\partial \eta}{\partial T_1}.\delta T_1\right)^2 + \left(\frac{\partial \eta}{\partial T_2}.\delta T_2\right)^2 + \left(\frac{\partial \eta}{\partial T_3}\delta T_3\right)^2}$$

$$\delta\eta = \sqrt{\begin{matrix}(145.09 \times 0.000234)^2 + (145.09 \times 0.000234)^2 + (0.00303 \times 0.1)^2 + (0.01861 \times 0.1)^2 \\ + (0.015578 \times 0.1)^2\end{matrix}}$$

= 0.0475

Hence for an effectiveness of $\eta = 89\%$, the percentage of uncertainty is 4.75%.

Chapter 6

Performance Analysis

Chapter VI

PERFORMANCE ANALYSIS

Hot fluid test is conducted to determine the performance parameters such as effectiveness and pressure drop, Δp across the core for both the fluids and compare them with the theoretical or predicted values. The experiment is conducted at different mass flow rates (5.7 g/s to 14.2 g/s) and at different hot fluid inlet temperature to study the variation of the performance parameters. The amount of air entering the heat exchanger is controlled by a control valve placed at the inlet of the heat exchanger. The temperature of the hot air at inlet is maintained at the desired value by using the auto transformer. The values of the experimentally observed data have been tabulated in Tables 6.1 to 6.4.

Table 6.1.Experimentally observed data at different mass flow rates for the hot fluid inlet temperature of 369 K

Flow rate, Q (litr/min)	Pressure at cold inlet,P_1(kg/cm^2)	Pressure at hot inlet,P_2(kg/cm^2)	Pressure drop, cold fluid, mm of Hg	Pressure drop, hot fluid, mm of Hg	Cold fluid inlet temperature,T_1(K)	Cold fluid outlet temperature, T_2 (K)	Hold fluid inlet temperature, T_3 (K)	Hold fluid outlet temperature, T_4(K)
300	0.08	0.06	9	6	315.24	360.22	368.96	321.1
400	0.14	0.12	15	12	311.35	359.94	367.91	316.95
500	0.2	0.17	25	22	311.93	361.38	368.88	317
550	0.24	0.20	30	26	312.82	361.71	369.45	317.35
588	0.28	0.24	31	27	313.41	361.33	368.96	317.86
650	0.32	0.26	40	35	314.16	360.74	368.72	318.08

Table 6.2.Experimentally observed data at different mass flow rates for the hot fluid inlet temperature of 359 K

Flow rate ,Q (litr /min)	Pressure at cold inlet,P_1(kg/cm^2)	Pressure at hot inlet,P_2 (kg/cm^2)	Pressure drop, cold fluid, mm of Hg	Pressure drop, hot fluid, mm of Hg	Cold fluid inlet temperature,T_1(K)	Cold fluid outlet temperature, T_2 (K)	Hold fluid inlet temperature, T_3 (K)	Hold fluid outlet temperature, T_4(K)
300	0.09	0.06	12	10	313.94	352.08	358.83	319.3
400	0.14	0.1	15	13	313.6	352.88	358.86	318.43
500	0.2	0.16	24	20	312.7	353.05	358.69	317.35
550	0.24	0.19	30	26	315.08	353.06	358.86	318.99
588	0.28	0.23	34	31	316.55	353.16	358.83	320.3
650	0.34	0.28	38	35	315.75	352.39	359.32	319.06

Table 6.3.Experimentally observed data at different mass flow rates for the hot fluid inlet temperature of 349 K

Flow rate,Q (litr /min)	Pressure at cold inlet,P_1	Pressure at hot inlet,P_2	Pressure drop, cold fluid, mm of Hg	Pressure drop, hot fluid, mm of Hg	Cold fluid inlet temperature,T_1(K)	Cold fluid outlet temperature, T_2 (K)	Hold fluid inlet temperature, T_3(K)	Hold fluid outlet temperature, T_4(K)
300	0.08	0.06	8	7	313.32	343.27	348.86	317.78
400	0.13	0.11	15	13	314.13	344.11	348.98	317.85
500	0.2	0.16	23	21	316.18	344.66	348.88	319.5
550	0.24	0.19	30	26	316.1	344.52	348.71	319.44
588	0.28	0.24	33	31	316.62	344.63	348.88	319.59
650	0.34	0.28	39	34	316.6	344.16	348.8	319.18

Table 6.4.Experimentally observed data at different mass flow rates for the hot fluid inlet temperature of 339 K

Flow rate ,Q (litr /min)	Pressure at cold inlet,P_1 (kg/cm^2)	Pressure at hot inlet,P_2 (kg/cm^2)	Pressure drop, cold fluid, mm of Hg	Pressure drop, hot fluid, mm of Hg	Cold fluid inlet temperature,T_1(K)	Cold fluid outlet temperature, T_2 (K)	Hold fluid inlet temperature, T_3(K)	Hold fluid outlet temperature, T_4(K)
300	0.08	0.06	8	6	313.92	335.01	339.31	316.94
400	0.14	0.11	16	14	315.77	335.86	339.26	318.45
500	0.2	0.16	24	22	312.51	335.42	338.9	315.55
550	0.24	0.19	30	26	316.46	336.01	338.83	318.86
588	0.28	0.23	33	31	312.99	335.34	338.8	315.57
650	0.34	0.28	37	34	315.72	335.67	339.16	317.93

6.2 Variation of effectiveness with the mass flow rate:

The figures 6.1 to 6.4 show the comparison of the effectiveness values obtained by various correlations and the simulation software with the experimental values at different mass flow rates and at different hot inlet temperatures. The difference in the values of temperatures at hot end and cold end indicates a loss of energy. In an ideal situation without heat leak from the surroundings, the temperature drop in hot stream must be equal to the temperature gain in cold stream. There is always some amount of energy imbalance even with sufficient insulation. Hence two values of effectiveness - ε_h, the effectiveness based on the hot fluid and ε_c, the effectiveness based on the cold fluid are obtained.The energy imbalance is minimum when the heat exchanger is operated at 500-550 litre/min (10.44 to 11.72 g/s). It is observed from experiment that hot effectiveness, ε_h (effectiveness measured on the basis of hot fluid) increases with the mass flow rate where as the cold effectiveness, ε_c (the effectiveness based on the cold fluid) increases up to certain mass flow rate, remains constant and then decreases with

further increase in mass flow rate. The mean of these effectiveness values is also found out and variation of the mean effectiveness with mass is shown.

The effectiveness values obtained by using the correlations developed by Maiti and Sarangi [45], Joshi and Webb [68] have found to increase up to the mass flow rate of 11.72g/s and then remain constant. The values of effectiveness obtained by simulation using Aspen MUSE [113] and the experimental mean effectiveness have also shown the same trend. The effectiveness is directly related to $NTU(hA/mc_p)$.With increase in mass flow rate, the Reynold number increases and thus increases the heat transfer coefficient as per the correlation at a faster rate than the mass flow rate. This increases NTU which gives higher effectiveness .Further increase in mass flow rate, gives saturated condition where the heat transfer coefficient increases slowly compared to the mass flow rate. The effectiveness thus increases very slowly or remains nearly constant at higher mass flow rate.

The values of the effectiveness obtained by different correlations are without the heat loss considerations and are hence compared with the mean experimental value. The actual experimental values that may have been obtained without the heat loss may be slightly higher (nearer to the hot effectiveness line) than these mean experimental values. The percentage deviation between the mean experimental values and the predicted values given by Maiti and Sarangi[45] varies from 6.42 % to 4.57%, while for Manglik and Bergles[70],the variation is from 8.27% to 4.97 % and for Joshi and Webb[68], the variation is from 7.07 % to 5.54 % when the inlet temperature of the hot fluid is 369 K. The experimental values agree with the values obtained by simulation. The percentage deviation between the mean experimental values and the simulated values is from 3.83% to 2.6%. It can be seen that the percentage deviation between the effectiveness values obtained by various correlations and the experimental values decreases with increase in mass flow rate and with the increase in hot inlet temperature.

The effectiveness values with heat losses are also obtained using simulation software, Aspen MUSE [113]. The amount of heat loss obtained from the experiments is given as an input in the simulation software along with other inputs. Simulation gave two values of the effectiveness, the hot effectiveness and the cold effectiveness. These are compared with the respective hot and cold effectiveness value obtained from the experiments as shown in figure 6.5. The percentage deviation between the effectiveness value obtained by simulation software, Aspen (with heat leak considered) and the

experimental value varies from 2.26 % to 2.75 % at the hot inlet temperature 369 K. This is well within the error band of the measurement error. More detailed description is given in the next section.

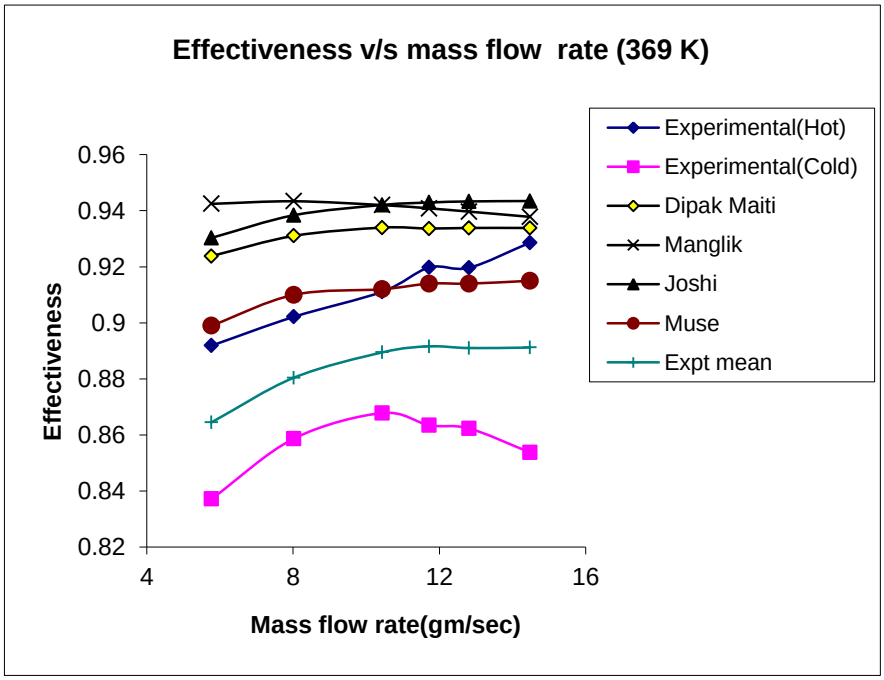

Figure 6.1: Variation of effectiveness with mass flow rate (hot inlet temperature=369 K)

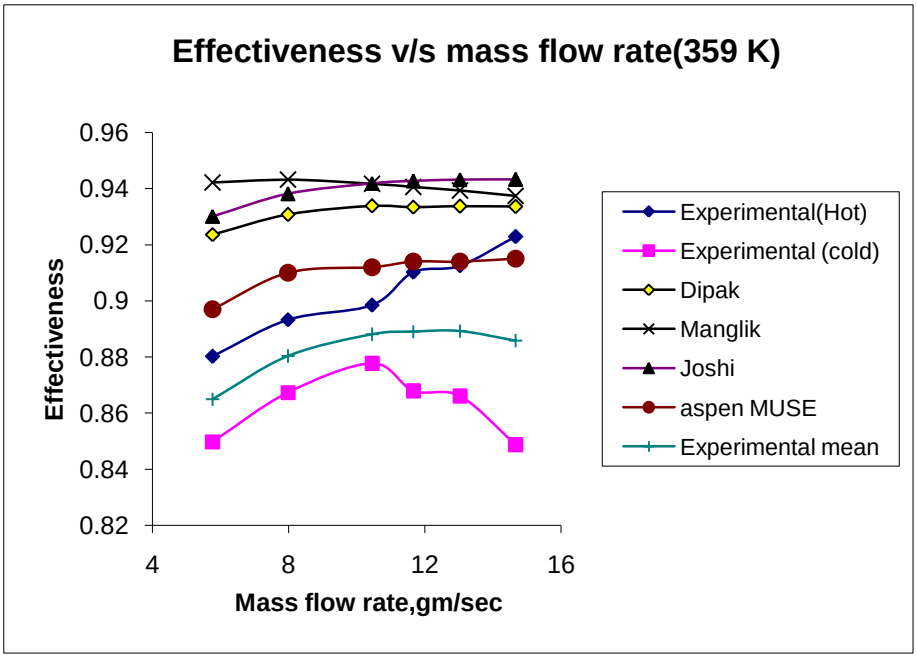

Figure 6.2: Variation of effectiveness with mass flow rate (hot inlet temperature=359 K)

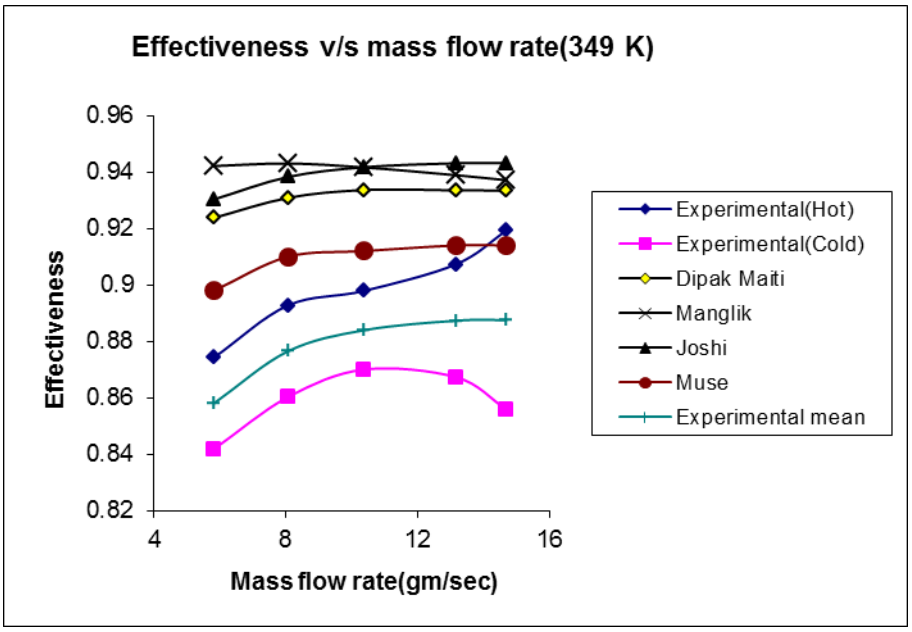

Figure 6.3: Variation of effectiveness with mass flow rate (hot inlet temperature=349 K)

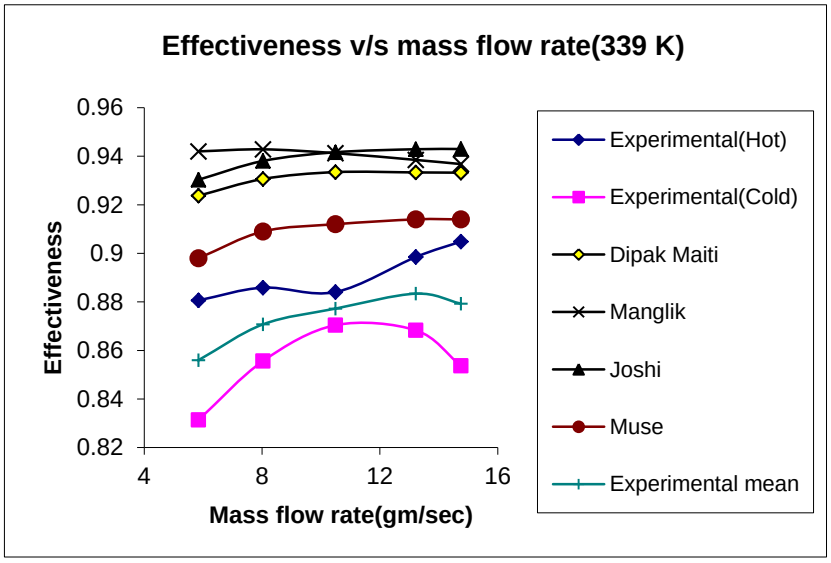

Figure 6.4: Variation of effectiveness with mass flow rate (hot inlet temperature=339 K)

6.3 Effect of heat transfer to the ambient

Energy balance between the hot and cold streams is lost if there is a heat loss to the surroundings. The temperature difference between the two fluids at the hot end and that at the cold end are noted down. The difference in the values of these temperatures at hot end and cold end indicates a loss of energy. Hence there are two values of

effectiveness - ε_h, the effectiveness based on the hot fluid and ε_c, the effectiveness based on the cold fluid. For balanced flow condition, the heat unbalance of the two streams is given as,

$$mc_p\left[(T_3 - T_2) - (T_4 - T_1)\right]$$

$$= 5.77 \times 1.04 \times (8.75 - 5.82) = 17.582\,\text{W}.$$

Substituting the input heat value as 17.58 W and for the mass flow rate of 5.77 gm/sec operating between 369 K and 315.3 K, simulation by Muse gave the two values of effectiveness, the hot effectiveness and the cold effectiveness. These effectiveness followed the same trend as the respective experimental values as shown in the figure 6.5.

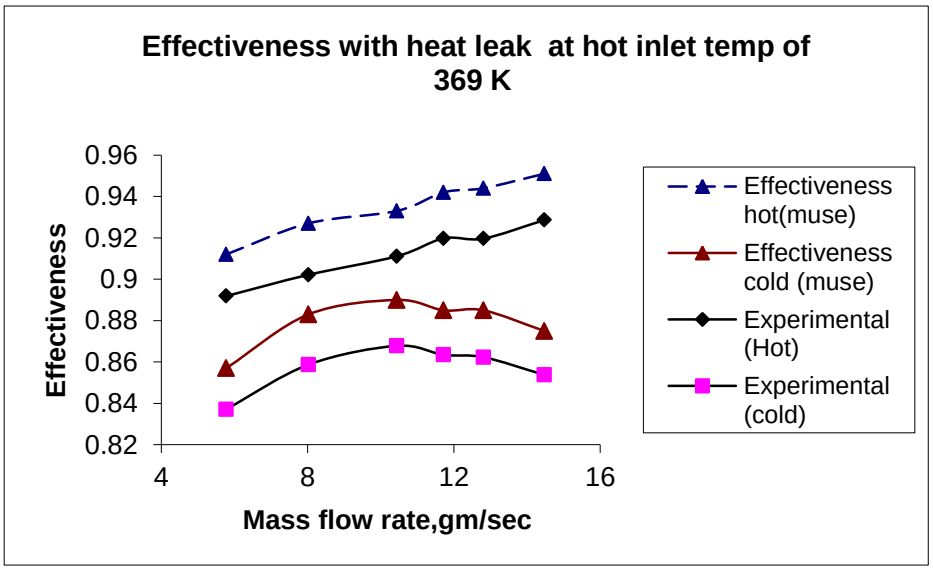

Figure 6.5: Comparison of effectiveness obtained by experiment and by simulation with heat leak at different mass flow rates.

The percentage deviation between the effectiveness values obtained by simulation software, Aspen MUSE [113] (with heat leak considered) and the experimental value varies from 2.26 % to 2.75 % at the hot inlet temperature 369 K.

6.4 Comparison of effectiveness obtained with and without heat loss

Figure 6.6 shows the comparison of the effectiveness values obtained by simulation software aspen-MUSE [113] with and without heat loss for the mass flow rate of 5.77 g/s operating between 369 K and 315.3 K. As explained earlier, heat loss to the ambient causes an energy imbalance between the hot and cold streams. Energy lost by the hot fluid is not equal to energy gained by the cold fluid. By substituting the heat leak

in the simulation software, Aspen- MUSE[113], two values of the effectiveness are obtained effectiveness - ε_h, the effectiveness based on the hot fluid and ε_c,the effectiveness based on the cold fluid. The mean of these effectiveness is calculated and variation of this mean effectiveness with mass flow rate is shown in figure 6.6.

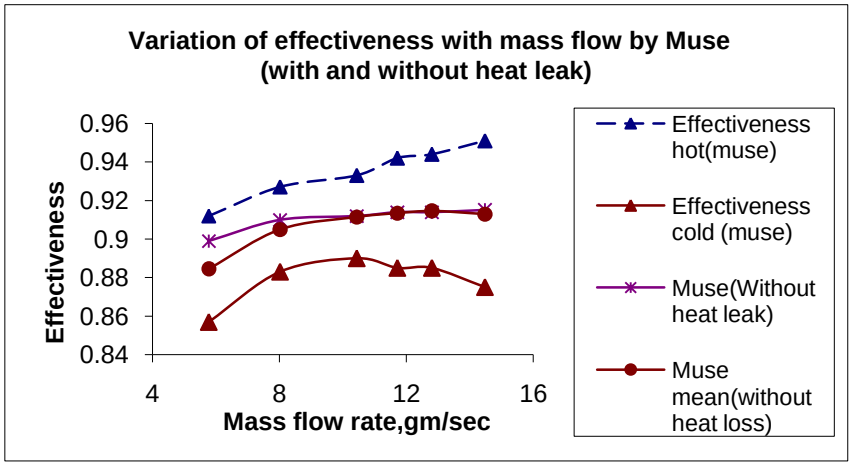

Figure 6.6: Variation of effectiveness with mass flow rate including heat leak (hot inlet temperature=369 K)

The mean effectiveness is compared with the effectiveness obtained without heat loss for the same mass flow rate. The comparison shows that the effectiveness obtained without heat loss is slightly more than the mean effectiveness. Hot end of the heat exchanger gets more affected by the heat loss to the surroundings. This means that the effect of heat loss on effectiveness of the cold fluid is more compared to that on hot fluid.

The effectiveness obtained by experiments is with heat loss while the predicted values of the effectiveness obtained by different correlations are without heat loss. For analysis purpose the mean of the experimental hot and cold effectivenesses can be approximated as the effectiveness without heat loss. The mean experimental value is compared with the predicted value of the effectiveness to find the percentage deviation between the predicted and the experimental value of the effectiveness. Actual deviation may be slightly lower than this deviation when there is no heat leak.

6.5 Error estimation in experimental results

The errors in the measurement of effectiveness have been estimated from the measurement of individual variables for one set of data. Equations 5.9 to 5.14 of chapter-V are used to calculate the uncertainty in the measurement of effectiveness.

Table 6.5 shows the uncertainties in the value of effectiveness obtained at different mass flow rates when the inlet temperature of hot fluid is 369 K. It is found that the uncertainties decrease with increase in mass flow rate.

Table 6.5. Uncertainties obtained at different mass flow rates for the hot fluid inlet temperature of 369 K

Mass flow rate, g/s	T_1(K)	T_2(K)	T_3(K)	T_4(K)	$\frac{\partial \eta}{\partial m_1} = \frac{\partial \eta}{\partial m_2}$	$\frac{\partial \eta}{\partial T_1}$	$\frac{\partial \eta}{\partial T_2}$	$\frac{\partial \eta}{\partial T_3}$	uncertainty
5.77	315.24	360.22	368.96	321.1	145.1	0.0030	0.0186	0.01557	0.04807
8.02	311.35	359.94	367.91	316.95	107.07	0.0025	0.0177	0.01518	0.03661
10.44	311.93	361.38	368.88	317	83.125	0.0023	0.0175	0.01523	0.0297
11.72	312.82	361.71	369.45	317.35	73.67	0.0024	0.0177	0.01525	0.02663
12.81	313.41	361.33	368.96	317.86	67.32	0.0025	0.018	0.01552	0.0253
14.48	314.16	360.74	368.72	318.08	58.96	0.0027	0.0183	0.01564	0.02284

6.6 Variations of pressure drop of cold fluid with the mass flow rate:

Figures 6.7 to 6.10 show the comparison of the pressure drop values obtained by various correlations and the simulation software with the experimental values at different mass flow rates and at different hot inlet temperatures. It is seen that the pressure drop increases continuously with mass flow rate. The pressure drop of cold fluid is below the allowable pressure drop of 0.05 bar up to the Reynolds number of 550. The pressure drop exceeds 0.05 bar when the Reynolds number of the flow exceeds 600.

A large amount of deviation is observed between the experimental and theoretical pressure drops obtained by various correlations. The variation between the pressure drops obtained by experiments and by simulation is also large. However the pressure drop is not a serious concern since it is within the allowable limit.

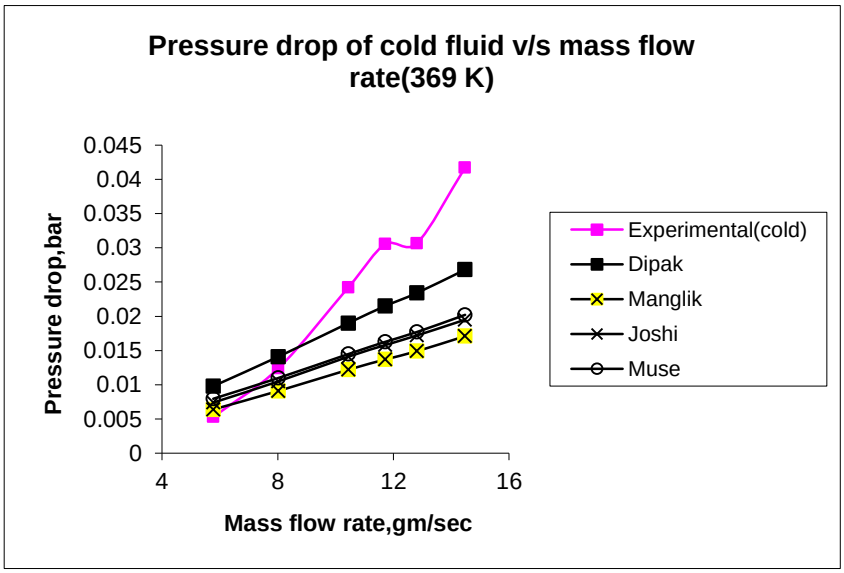

Figure 6.7: Variation of pressure drop of cold fluid with mass flow rate (hot inlet temperature = 369 K)

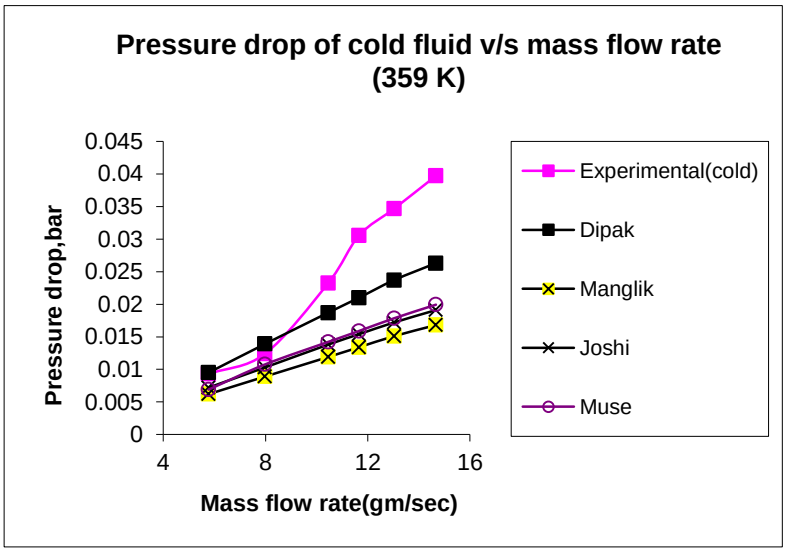

Figure 6.8: Variation of pressure drop of cold fluid with mass flow rate (hot inlet temperature =359 K)

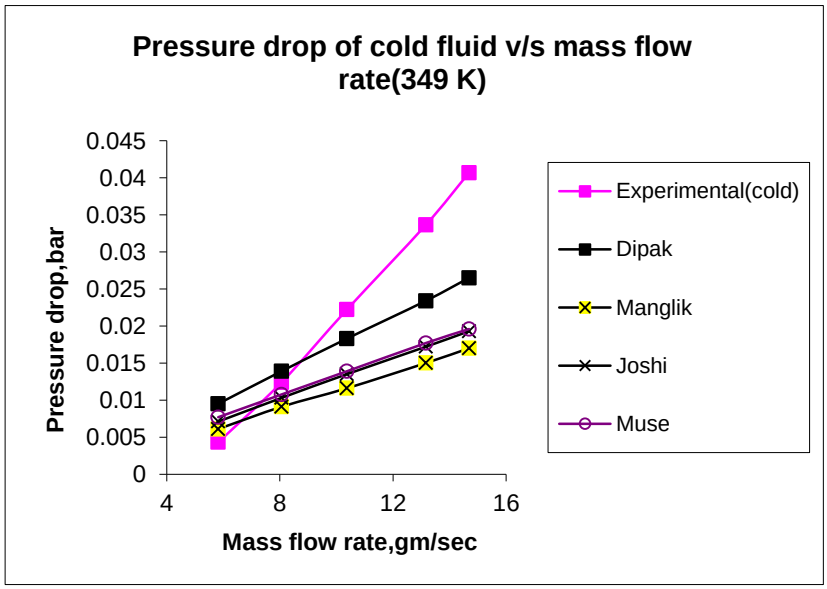

Figure 6.9: Variation of pressure drop of cold fluid with mass flow rate (hot inlet temperature=349 K)

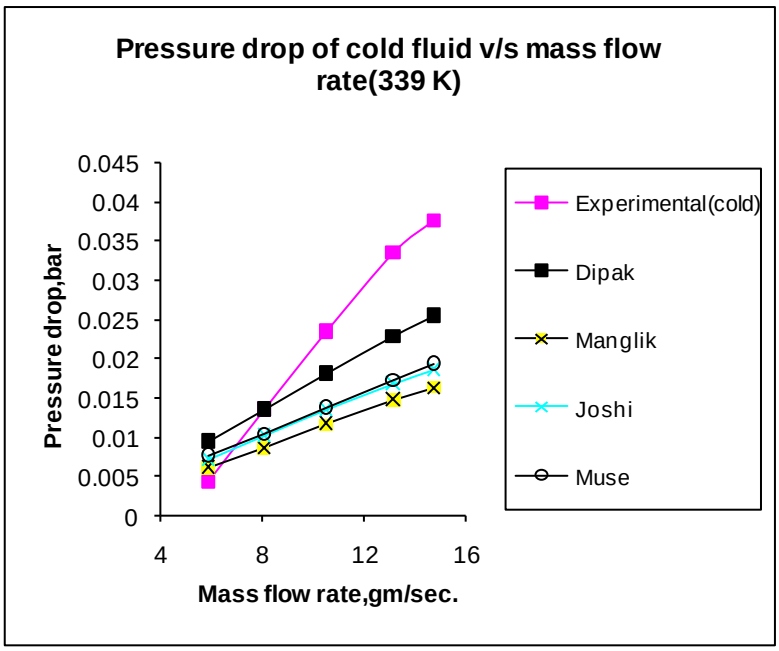

Figure 6.10: Variation of pressure drop of cold fluid with mass flow rate (hot inlet temperature=339 K)

6.7 Variations of pressure drop of hot fluid with the mass flow rate:

Variation of pressure drop of hot fluid with mass flow rate is also shown in Figures 6.11 to 6.14. It is seen that the pressure drop increases continuously with the mass flow rate. The pressure drop is below the allowable pressure drop of 0.05 bar over the entire range of mass flow rate.

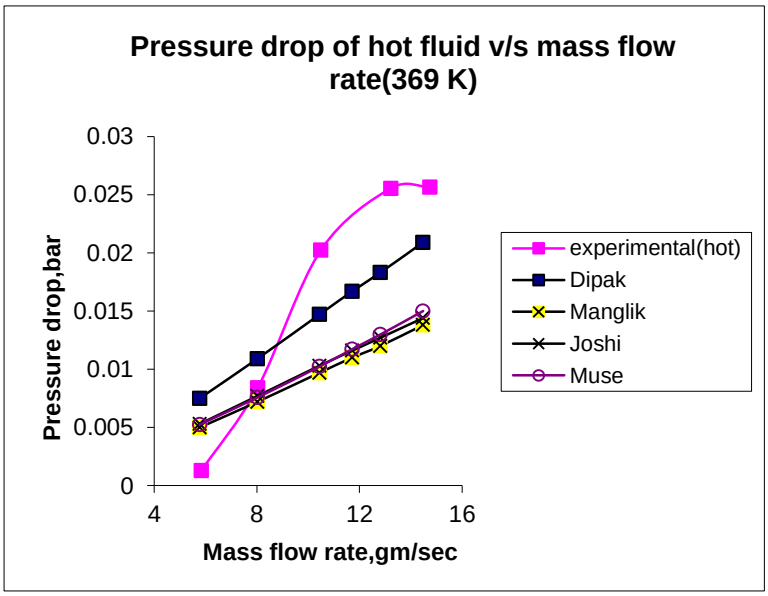

Figure 6.11: Variation of pressure drop of hot fluid with mass flow rate (hot inlet temperature=369 K)

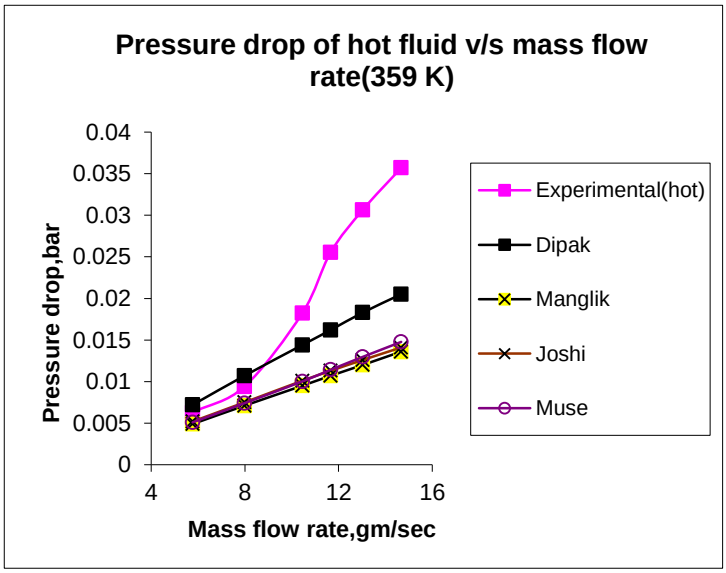

Figure 6.12: Variation of pressure drop of hot fluid with mass flow rate (hot inlet temperature=359 K)

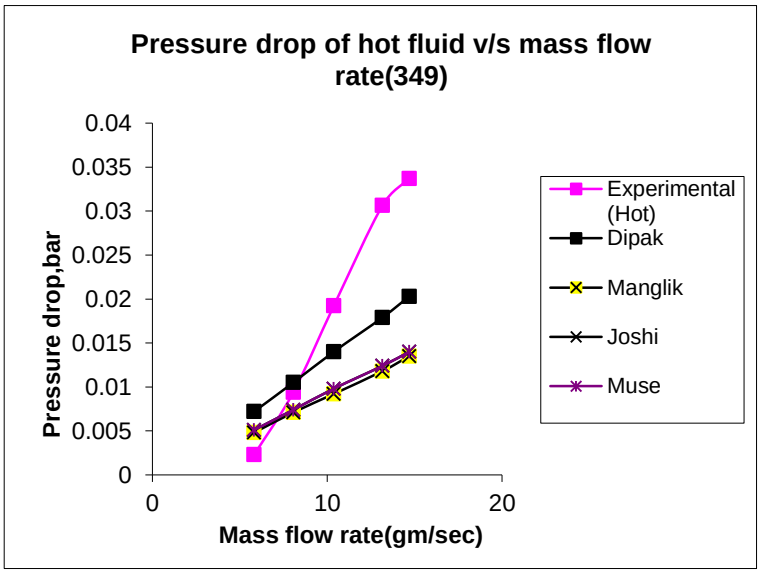

Figure 6.13: Variation of pressure drop of hot fluid with mass flow rate (hot inlet temperature = 349 K)

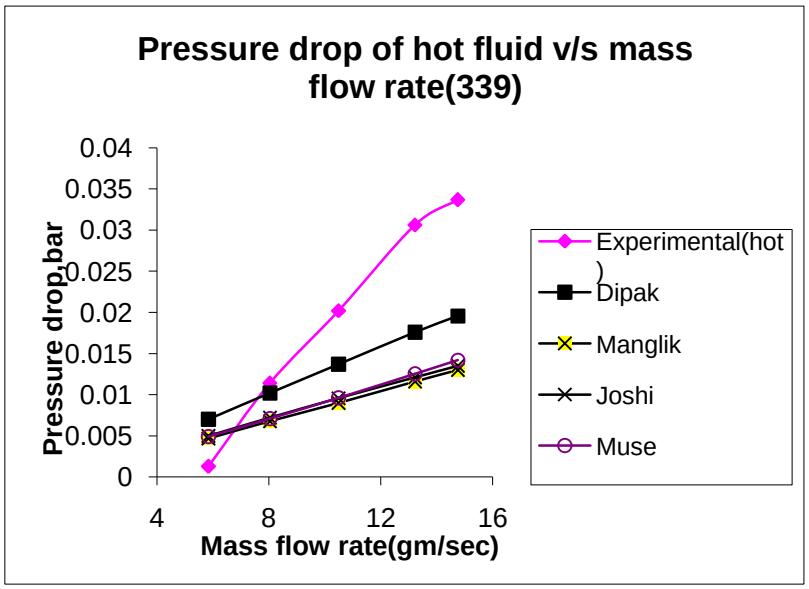

Figure. 6.14 Variation of pressure drop of hot fluid with mass flow rate (hot inlet temperature=339 K)

6.8 Results and discussion

The values of effectiveness obtained from experiments agree with the values obtained by simulation software, Aspen-MUSE[113].The percentage deviation between the effectiveness values obtained by simulation software, Aspen-MUSE (with heat leak considered) and the experimental values varies from 2.26 % to 2.75 % at the hot inlet

temperature 369 K. This is well within the band of the measurement error. The percentage deviation between the mean experimental values (estimated as obtained without heat loss) and the predicted values given by various correlations shows that correlations developed by Maiti and Sarangi[45] are in better agreement with the experimental data compared to the other correlations, the percentage deviation between the experimental values and the predicted values given by Maiti and Sarangi [45] varying from 6.42 % to 4.57%. The value of uncertainties varies from 4.75 % to 2.28 % for the variation of mass flow rate from 5.77 g/s to 14.48 g/s.

The heat loss to the ambient causes an energy imbalance between the hot and cold fluids. Two values of effectiveness are measured, the hot effectiveness, ε_h (effectiveness based on the hot fluid) and the cold effectiveness, ε_c (Effectiveness based on the cold fluid).The mean value of the hot and cold effectiveness obtained from the experiments is estimated as the effectiveness value obtained without heat loss and is compared with the predicted values of effectiveness obtained by different correlations as they are without heat loss consideration. The heat loss to the ambient causes the decrease in effectiveness based on both the fluids, the cold fluid flowing in the outer layers suffering the most. Normally heat exchangers are placed in a vacuum insulated cold box to completely eliminate the heat loss when operated at cryogenic temperatures.

The pressure drop increases continuously with the mass flow rate. The pressure drop of cold fluid is below 0.05 bar up to the Reynolds number of 550 and thereafter the pressure drop increases rapidly. A large amount of deviation is obtained between the pressure drop obtained by experiment and the pressure drop obtained by various correlations or the simulation software, Aspen-MUSE [113].

Manufacturing irregularities such as burred edges, separating plate roughness and bonding imperfections influence the heat transfer and fluid flow in heat exchanger cores. Burred fin ends causes an effective increase in fin thickness and therefore in form drag. Top and bottom surface roughness may cause an increase in both heat transfer and flow friction. Irregularities may not be uniform over the entire length of the heat exchanger. Heat transfer and pressure drop is also affected by the vortices leaving the trailing edges of the fin segments and their interaction with the fins downstream. Analytical modeling consists of solving the energy and momentum equations on the unit cell of the geometry. The unit cell is an idealization of the actual geometry considered because it neglects the possible burrs on the fin ends and also the roughness on the top

and bottom of the channel. Numerical solution also depends upon certain simplifying assumptions made.

The correlations for j and f factors developed experimentally are based on the experimental technique of Kays and London [2]. The experimental set up used by Kays and London [2] consists of a small N_{tu} heat exchanger with cross flow arrangement of fluids of steam and air (with no header losses) or a channel of heat exchanger. The arrangement may be an ideal arrangement for the measuring the j factors but not for friction factors. It does not give a real estimate of pressure drop although pressure drop per unit length is used for determining the friction factor. Any small deviation in friction factor between the predicted and the experimental value will get reflected as a large deviation in the pressure drop as the pressure drop is a function of mass velocity, equivalent diameter and length of heat exchanger in addition to the friction factor. Pressure drop also depends on density which varies with temperature.

Chapter 7

Conlusion

Chapter VII

CONCLUSION

7.1 Concluding remarks

An experimental set up has been built in the laboratory to test the plate fin heat exchanger. A hot fluid test is conducted to determine the thermo hydraulic performance of the given heat exchanger at different mass flow rates (5.8 g/s to 14.5 g/s) and at different hot inlet temperatures. The values of the effectiveness and pressure drops obtained are compared with the values obtained by using the correlations developed by Maiti and Sarangi [45], Manglik and Bergles [70], Joshi and Webb [68].The effectiveness values are also compared with the values obtained by simulation software, Aspen-MUSE [113]. The following points are noted from comparison of the experimental with the predicted and the simulated values.

i) The value of the effectiveness obtained by the experiments agree with the values obtained by simulation software, Aspen-MUSE[113].The percentage deviation between the effectiveness value obtained from Aspen-MUSE [113] (with heat leak considered) and the experimental value varies from 2.26 % to 2.75 % at the hot inlet temperature of 369 K. This is well within the measurement error band.

ii) The percentage deviation between the mean experimental values and the predicted values of effectiveness given by Maiti and Sarangi[45] varies from 6.42 % to 4.57%, while for Manglik and Bergles[70],the variation is from 8.27% to 4.97 % and for Joshi and Webb[68], the variation is from 7.07 % to 5.54 % when the inlet temperature of the hot fluid is 369 K. The experimental values agree with the values obtained by simulation. The percentage deviation between the mean experimental values and the simulated values is from 3.83% to 2.6%.

iii) Correlations developed by Maiti and Sarangi [45] are in better agreement with the experimental data compared to the other correlations.

iv) The pressure drop of the fluids is below the allowable pressure drop of 0.05 bar up to the Reynolds number of 500 and thereafter the pressure drop increases rapidly. A large amount of deviation is observed between the experimental and theoretical pressure drops obtained by various correlations. The variation between the pressure drops obtained by experiments and by simulation is also large.

The experiment suggests that the plate fin heat exchanger is ideal for low Reynold number applications (up to the Reynold number of 500-550).Correlations developed by Dipak Maiti [45] are in better agreement with experimental data although with correlation developed by Joshi and Webb [68], the deviation is slightly higher and both the correlations can be used for the design of heat exchangers. Manglik and Bergles [70] has neglected the thickness of fins while calculating the free flow area and correlation developed by them can also be used if the correction is made for the same. Now as regarding the pressure drop considerations, the plate fin heat exchanger should be used for low Reynold number applications.

All the correlations including the simulation software, Aspen MUSE [113] have under- predicted the pressure drop. A large amount of deviation observed between the experimental and the theoretical pressure drops calls for alternative experimental set up for determining the friction factor. The correlations developed by using the experimental technique of Kays and London have predicted the j factors reasonably well but have under- estimated the pressure drop. The experimental set up used by Kays and London consisting of a cross flow heat exchanger (with no header losses) and small N_{tu} seems to be ideal for predicting the j factors but not the friction factors. In addition to the pressure drop taking place in the narrow and intricate passages of an exchanger, pressure drop also takes place in the headers, while flowing through elbows and connecting piping. Manufacturing irregularities such as burred edges, separating plate roughness and bonding imperfections influence heat transfer and flow friction in heat exchanger cores. The pressure drop occurring through the heat exchanger should be estimated correctly and friction factor should be determined accurately. This is because any small deviation in friction factor between the predicted and the experimental value will bring about a large deviation in the pressure drop as the pressure drop is a function of mass velocity, equivalent diameter and length of heat exchanger in addition to the friction factor.

Maiti and Sarangi [45] have suggested a new approach to develop heat transfer and flow friction correlations by combining computational and experimental data. While numerical results are used to find the effect of fin geometry on j and f, experimental data compensate the error due to simplifying assumptions taken in numerical simulation. This method reduces the volume of experiments to be done and can use the available computing resources in the laboratory. The approach provides a workable solution and can be used for the generation of j and f factors. For finding friction factors, experimental set up used in this thesis can be used to generate the correlation for f factors. The experimental arrangement used in the thesis gives a real estimate of the pressure drop occurring in a practical heat exchanger set up. The hot test method is simple compared to testing of plate fin heat exchanger at cryogenic temperature. The heat exchanger used in this test rig will be applied to cryogenic temperature. Since the heat exchanger performance is satisfactory at hot test, it can be presumed that satisfactory result is expected at cryogenic temperature. It is because the dimensionless parameters are same in both hot and cold tests.

7.2 Scope for future work

Various correlations are available in literature for predicting the non-dimensional heat transfer and pressure drop characteristics of plate fin heat exchanger. The thesis presents an experimental set up for finding the thermo hydraulic performance of a specific plate fin heat exchanger and to check the validity of these correlations. Following are some of the activities that are proposed to be taken in our laboratory in the near feature:

- All the correlations developed so far have predicted the j factors reasonably well but have under predicted the friction factors considerably. The experimental set up used in this thesis can be used for developing the correlations for friction factors. The experimental set up used is a practical heat exchanger set up with header and piping connections and gives a real estimate of the pressure drop.
- Most of the available correlations for j and f factors have been developed by using the experimental technique of Kays and London [2] for fluids at or above room temperatures. Cold fluid test has to be conducted using fluids at cryogenic temperatures to check the validity of these correlations at cryogenic temperatures.
- It is found from the hot fluid tests that even with sufficient insulation, heat loss could not be eliminated completely. Plate fin heat exchanger presents a large

surface area through which the heat gets dissipated to the surroundings. The heat loss from the plate fin heat exchanger has to be obtained only experimentally. Experiments have to be conducted on plate fin heat exchangers of different geometries and heat loss has to be determined at different temperature levels and at different mass flow rates. Heat loss to the surroundings has to be taken into account while calculating the effectiveness of heat exchanger using different correlations.

References

References

1. **Barron, R.F.** Cryogenic systems, Oxford University Press (1985)

2. **Kays, W.M. and London, A.L.** Compact Heat exchangers, McGraw-Hill, New York (1984)

3. **Kern, D.Q., Kraus, A.D.** Extended Surface Heat Transfer, McGraw-Hill, New York (1972)

4. **Frass,A.P.**, Heat Exchanger Design, 2nd ed., Wiley-Inter science (1989)

5. **Ozisik, M.N.**, Heat Transfer-A Basic Approach, McGraw-Hill (1985)

6. **Incropera, F.P., Dewitt, D.P.** Fundamentals of Heat Transfer 2nd ed. John Wiley, New York, 1985

7. **Shah, R.K., Dusan,P., Sekulic,D.P.** Fundamentals of Heat Exchanger Design, John Wiley & Sons, (2003)

8. **Shah, R.K.** Compact Heat Exchangers & Enhancement Technology, Begell House Publication, (1999)

9. **Kakac,S., Bergles, A.E., Mayinger, F.** Heat Exchangers, Thermal-Hydraulic Fundamentals and Design, by Hemisphere Publication (1980)

10. **Shah, R.K., Subbarao, E.C. Mashelkar, R.A.** Heat Transfer Equipment Design edited by R.K.Shah, Publishing Corporation, Washington, DC, (1988)

11. **Taborek, J., Hewitt, G.F. and Afgtan,N** Heat Exchangers-Theory and Practice(Eds.) Hemisphere Publishing, New York (1983)

12. **Taylor, M.A.** Plate Fin Heat Exchangers: Guide to their Specification and Use HTFS, Oxon, UK (1987)

13. **Sunden, B., Faghiri, M.** Computer Simulations in Compact Heat Exchangers 1st ed. by Computational Mechanics Publications (1998)

14. **Applied Thermal Engineering**, Editor-In-Chief D.A. Reay(http://www.elsvier.com)

15. **Experimental Thermal and Fluid Science**, Editor-In-Chief I. Kennedy and L. Kennedy (http://www.elsevier.com)

16. **Journal of Heat Transfer**, Editor-In-Chief V.K. Dhir (http://www.asme.org)

17. **International Journal of Heat and Mass transfer**, Editor-In-Chief J. Harnet and W. Minkowycz (http://www.elsevier.com)

18. **Heat Transfer Engineering**. Editor-In-Chief Afshin J. Ghajar (http://www.tandf.co.uk./journals/titles/01457632.asp)

19. **International Journal of Heat Exchangers**, Editor-In-Chief Bengt Sunden (http://www.edwardspub.com/journals/IJHEX)

20. **London, A.L.** A Brief History of Compact Heat Exchanger Technology, in Compact Heat Exchangers, History, Technological Advancement and Mechanical Design Problems edited by R.K. Shah et al (1980) HTD-Vol.10 1-4

21. **Mori, Y. Nakayama, W.** Recent Advances in Compact Heat Exchangers in Japan, History, Technological Advancement and Mechanical Design Problems edited by R.K. Shah et al (1980) HTD-Vol.10 5-16

22. **Cowel, T., Achaichia,N.** Compact Heat Exchangers in the Automobile Industry Proceedings of the International Conference on Compact Heat Exchangers in the Process Industries (1997) 11-28

23. **Lenfestey, A.G.** Low Temperature Heat Exchangers, Progress in Cryogenics Heywood & Co. (1961) 25-47

24. **Butt, A.G.** Mechanical Design of Cryogenic heat exchangers Compact Heat Exchangers-history, Technical Advancement and Mechanical Design Problems(Eds. Shah,R.K. et al) (1980)HTD-Vol10 161-190

25. **Panitsidis, H., Gresham, R.D. and Westwater, J.W.** Boiling of liquids in a compact plate fin heat exchangers, International Journal of Heat and Mass Transfer, 18, 37-42, (1975)

26. **Robertson, J.M.**, Boiling heat transfer with liquid nitrogen in brazed-aluminum plate-fin heart exchangers, American Institute of Chemical Engineers Symposium Series, san diego, 75, 151-164 (1979)

27. **ALPEMA**, The Standards for the Brazed Aluminium Plate Fin Heat Exchanger Manufactures' Association (http://www.alpema.org/)

28. www.chart-ind.com

29. www.kobelco.co.jp/eneka

30. www.linde.com

31. www.nordon-cryogenie.com

32. www.spp.co.jp

33. www.htfs.comj

34. www.htri.com

35. **Kohlweiler,W.** http://www.brazetec.de/brazetec/content_en/articles/brazing_aluminium.pdf

36. **Giannettoni,R., Tirloni,A., Tonini,G.** A technique for vacuum aluminum brazing: development of a high vacuum furnace for aluminum brazing http://www.tav-alto-vuoto.it/brazin.htm (2000)

37. **Kays, W.M. and London, A.L.** Description of Test equipment and method of Analysis for basic Heat transfer and flow friction test of high rating heat exchanger surfaces Technical Report No. 2, Department of Mechanical Engineering, Stanford University (1948)

38. **London, A.L., and Shah,R.K.** Offset Rectangular Plate –fin surfaces-Heat Transfer and Flow Friction Characteristics, Transactions of the ASME,Journal of Engineering for Power (1968) 90 218-228.

39. **Shah, R.K.** Assessment of Modified Wilson Plot Techniques for obtaining Heat Exchanger Design Data Proceedings of 9th International Conference (1990) 5 51-56

40. **Davenport, C.J.** Heat Transfer and Flow Friction Characteristics of Louvered Heat Exchanger, Heat Exchangers-Theory and Practice edited by J. Taborek, G.F.Hewitt, N.Afgan, McGraw –Hill, New York (1983) 387-412.

41. **Sunden, B., and Svantesson, J.** Heat Transfer and Pressure Drop from Louvered Surfaces in Automotive Heat Exchangers, Experimental Heat Transfer (1991) 4 111- 125.

42. **Wang, J., Hirs, G.G., Rollmann, P.** The Performance of a New Gas to gas Heat Exchanger with Strip Fin, Energy Conservation and Management (1999) 40 1743-1751.

43. **Lozza, G., Merlo, U.** An Experimental Investigation of Heat Transfer and Friction Losses of Interrupted and Wavy Fins for Fin and Tube Heat exchangers, International Journal of Refrigeration (2001) 24 409-416.

44. **Indranil Ghosh,** Experimental and Computational Studies on Plate Fin Heat Exchanger. PhD Dissertation, Indian Institute of Technology, Kharagpur (2004)

45. **Maiti, D.K.,and Sarangi.S.K.** Heat Transfer and Flow Friction Characteristics of Plate Fin Heat Exchanger Surfaces- A Numerical Study PhD Dissertation, Indian Institute of Technology, Kharagpur (2002)

46. **Freund,S., Kabelac,S.** Investigation of local heat transfer coefficients in plate heat exchangers with temperature oscillation IR thermography and CFD, International Journal of Heat and Mass Transfer, 2010; 53: 3764-3781.

47. **Pucci, P.F., Howard, C. P. And Piersall, C.H.** The single blow Transient Testing Technique for Compact Heat Exchanger Surfaces, Transactions ASME Journal of Engineering for Power 89(A) 29-40 (1967)

48. **Mondt, J.R. and Siegla, D.C.** Performance of Perforated Heat Exchanger Surfaces, Transactions ASME Journal of Engineering for Power 96(A) 81-86 (1974)

49. **Shah, R. K** Compact Heat Exchangers in S. Kakak, A.E. Bergles and F.Maylingar (Eds) Heat Exchangers –Thermal Hydraulic Fundamentals and Design, Hemisphere Publishing Corp Washington DC, 111-151 (1981)

50. **Patankar, S.V.** Numerical prediction of flow and heat transfer in compact heat exchanger passages, in Compact Heat Exchangers edited by R.K.Shah, A.D.Kraus and D.Metzger, Hemisphere Publishing Corp New York (1990) 191-204.

51. **Bilir, L., B. Ozerdem, A. Erek and Z. Ilken**. Heat Transfer and Pressure Drop Characteristics of Fin-Tube Heat Exchangers with Different Types of Vortex Generator Configurations, Journal of Enhanced Heat Transfer, 17(3), 243-256 (2010)

52. **Jacobi, A.M., and Shah, R.K.** Air Side Flow and Heat transfer in Compact Heat Exchangers: A Discussion of Enhancement Mechanisms, Heat Transfer Engineering (1998) 19 (4), 29-41.

53. **Shah, R.K., Heikal, M.R., Thonon,B.,Touchon,P**.Progress in numerical analysis of compact heat exchanger surfaces, Advances in Heat Transfer (2001) 34 363-442.

54. **Patankar, S.V., Liu, C.H., and Sparrow, E.M.** Fully Developed Flow and Heat Transfer in Ducts Having Stream wise-Periodic Variations of Cross-Sectional Area, Transactions of the ASME Journal of Heat Transfer (1977) 99 180-186.

55. **Patankar, S.V., and Prakash, C.** An Analysis of the Effect of Plate Thickness on Laminar Flow and Heat Transfer in Interrupted–plate passages, International Journal of Heat and Mass Transfer, (1981) 24(11)1801-1810.

56. **Suzuki, K., Hirai, E., Miyake, T.** Numerical and Experimental Studies on a Two-dimensional Model of an Offset-strip-fin Type Compact Heat Exchanger Used at Low Reynolds Number, International Journal of Heat and Mass Transfer, (1985) 28(4)823-836

57. **Zhang, L.W., Tafti, D.K., Najjar, F.M., and Balachandar, S.** Computations of Flow and Heat Transfer in Parallel-Plate Fin Heat Exchangers on the CM-5: Effects of Flow Unsteadiness and Three-Dimensionality, International Journal of Heat and Mass Transfer (1997) 40 (6) 1325-1341

58. **Achaichia, A. and Heikal, M. R., Sulaiman, Y. and Cowell, T.A.** Numerical Investigation of Flow and Friction in Louvered Fin Arrays, in Proc. 10th International Heat Transfer Conference, Brighton (1994)

59. **Ha, M.Y., Kim, K.C., Koak,S.H., Kim,K.H., Kim,K.I., Kang,J.K.and Park,T.Y.** Fluid Flow and Heat Transfer Characteristics in Multi-louvered Fin Heat Exchangers, SAE Paper No 950115 (1995)

60. **Atkinsona, K.N., Drakulic, R., Heikal, M.R. and Cowell, T.A.** Two and Three Dimensional Numerical Models of Flow and Heat Transfer over Louvered Fin Arrays in Compact Heat Exchangers, International Journal of Heat and Mass Transfer, **41** 4063-4080 (1998).

61. **Achaichia, A. and Cowell, T.A.** Heat transfer and pressure drop characteristics of Flat tube and louvered plate fin surfaces, Experimental Thermal and Fluid Science **1** 147-157 (1988).

62. **Springer, M.E. and Thole, K.A.** Experimental design for flow field studies of louvered fins, Experimental Thermal and Fluid Science **18** 258-269 (1998)

63. **Tafti, D.K., Zhang, L.W. and Wang,G.** Time-Dependent Calculation Procedure for Fully developed and developing Flow and Heat Transfer in Louvered Fin Geometries, Numerical Heat Transfer Part A **35** 225-249 (1999)

64. **Tafti, D.K., Wang,G. and Lin, W.** Flow Trasition in a Multilouvered Fin Array, International Journal of Heat and Mass Transfer, **43** 901-919 (2000)

65. **Manson, S. V.,** Correlation of Heat Transfer Data and of friction Data for Interrupted Plane fins Staggered in Successive rows, NACA Tech. Note 2237, National Advisory Committee for Aeronautics, Washington, DC, December 1950.

66. **Kays, W.M.,** Compact Heat Exchangers, AGARD lecture Serr. No 57 on Heat exchangers, AGARD-LS-57-72, NATO, Paris, 1972.

67. **Wieting, A. R.** Empirical Correlations for Heat Transfer and Flow Friction Characteristics of Rectangular Offset-fin Plate-fin Heat Exchangers, ASME Journal of Heat Transfer (1975) 97 488-490.

68. **Joshi, H.M. and Webb, R.L.** Heat Transfer and Friction in the Offset Strip-fin Heat Exchanger, International Journal of Heat and Mass Transfer, (1987) 30 (1) 69-84

69. **Sparrow, L.U. and Liu, C.H.** Heat Transfer, Pressure Drop and Performance relations for in-line, Staggered and Continuous Plate Heat Exchangers, International Journal of Heat and Mass Transfer, (1979) 22 1613-1625

70. **Manglik, R. M., and Bergles, A.E**. Heat Transfer and Pressure Drop Correlations For the Rectangular Offset strip Fin Compact Heat Exchanger, Experimental Thermal and Fluid Science (1995) 10 171-180

71. **Mochizuki, S., Yagi, Y., and Yang, W.J.,** Transport phenomena in stacks of Interrupted parallel plate surfaces, Experimental Heat Transfer 1, 127-140, 1987

72. **Muzychka, Y.S. and Yovanovich, M.M.** Modeling the f and j Characteristics for transverse flow through an offset strip fin at low Reynolds number, Journal of Enhanced Heat Transfer (2001) 8 261-277

73. **Mochizuki, S., Yagi, Y., and Yang, W.J.,** Flow pattern and turbulence intensity in stacks of interrupted parallel plate surfaces, Experimental Thermal and Fluid Science -1, 51-57, 1988

74. **Mochizuki, S., Yagi, Y.,** Characteristics of vortex shedding in plate arrays , in Flow visualization II, Merzkirch, Ed, pp- 99-103, Hemisphere, Washington, D.C, 1982

75. **Dubrovsky, E.V., and Vasileiev,V.Y,** Enhancement of convective heat transfer in reactangular ducts of interrupted surfaces, International Journal of Heat and Mass Transfer, 31 807-818 (1988)

76. **Mullisen, R.S., and Loehrke, R.I.,** Study of the Flow Mechanisms Responsible for Heat Transfer Enhancement in Interrupted –Plate Heat Exchangers**,** Transactions of the ASME Journal of Heat Transfer 108,377-385, 1986

77. **Barron, R.F.** Cryogenic Heat Transfer, Taylor &Francis (1999) 311-318

78. **Shah, R.K.** A Review of Longitudinal Wall Heat Conduction in Regenerators, Journal of Energy, Heat and Mass Transfer (1994) **16** 15-25

79. **Barron, R.L. and Yeh, S.L.** Longitudinal Conduction in a Three-Fluid Heat Exchanger, (1976) ASME Paper, 76-WA, HT-9 2-7

80. **Chowdhury, K., Sarangi, S.** Effect of finite thermal conductivity of the separating wall on the performance of counter flow heat exchangers, Cryogenics (1983) 23 212-216

81. **Hausen .H,** Heat transfer in counter flow, parallel flow and cross flow, New York: Mc Graw Hill, 1983.

82. **Hahnemann. H.W,** Approximate calculation of thermal ratios in heat exchangers including heat conduction in direction of flow; National Gas Turbine Establishment Memorandum, 1948:36.

83. **Bahnke. G.D., Howard. C.P.,** The effect of longitudinal heat conduction on periodic flow heat exchanger performance, ASME Journal of Engineering for Power 1964: 86: 105-20.

84. **Kroeger,P.G.** Performance deterioration in high effectiveness heat exchanger due to Axial Conduction Effect, Advances in Cryogenic Engineering, Vol.12, pp. 363-372, 8 (1966)

85. **Chiou, J. P.** The Effect of Longitudinal Heat Conduction on Cross flow Heat Exchanger, Transactions ASME, Journal of Heat Transfer (1978) **100** 436-441

86. **Chiou, J. P.** The Advancement of Compact Heat Exchanger Theory considering the Effects of Longitudinal Heat Conduction and Flow Non-uniformity in Compact Heat Exchangers, History, Technological Advancement and Mechanical Design Problems edited by R.K. Shah et al) (1980) HTD-Vol.10 101-121

87. **Venkatarathnam, G., Narayanan, S.P.** Performance of a counter flow heat exchanger with longitudinal heat conduction through the wall separating the fluid streams from the environment, Cryogenics (1999) **39** 811-819.

88. **Mondt, J.R.** Correlating the Effects of Longitudinal Heat Conduction on Heat Exchanger performance in Compact Heat Exchangers, History, Technological) Advancement and Mechanical Design Problems edited by R.K. Shah et al) (1980) HTD-Vol.10 123-134

89. **Shah, R.K.** A Correlation for Longitudinal Heat Conduction Effects in Periodic flow Heat Exchangers, Transactions ASME Journal of Engineering for Power (1975) **97** 453- 454

90. **Narayanan. S. P, Venkatrathnam. G** Performance degradation due to longitudinal heat conduction in very high N_{tu} counter flow heat exchangers, Cryogenics 1998: 38; 927-30

91. **B.M.Wood and J.Kern**," Design of Heat exchangers with heat loss to the Surroundings,"paper No 17, Second National Meeting of the South African Institute of Chemical Engineers(S-123), Johnnesburg (1976).

92. **Chowdhury, K., Sarangi, S.** Performance of Cryogenic Heat Exchangers with Heat leak from the Surroundings in Advances in Cryogenics Engineering (1984) **29** 273-280

93. **Barron, R.F.** Effects of Heat Transfer from Ambient on Cryogenic Heat Exchangers Performance in Advances in Cryogenics Engineering (1984) **29** 265-272

94. **Gupta, P., Atrey, M. D.** Performance evaluation of counter flow heat exchangers considering the effect of heat in leak and longitudinal conduction for low-temperature applications, Cryogenics (2000) **40** (7) 469-474

95. **Kitto, J.B, Robertson, J.M.** Effects of Maldistribution of Flow on Heat Transfer Equipment Performance, Heat Transfer Engineering 1989; 10(1): 18-25.

96. **Mueller A. C, Chiou J. P** Review of various Types of Flow Maldistribution in Heat Exchangers, Heat Transfer Engineering 1988; 9(2); 36-50.

97. **Ranganayakulu Ch, Seetharamu. K.N.** The combined effects of wall longitudinal heat conduction, inlet fluid flow nonuniformity and temperature nonuniformity in compact tube fin heat exchanger: A finite element method, International Journal of Heat and Mass Transfer, 1999; 42: 263.73.

98. **Jiao AJ, Li YZ, Chen CZ, Zhang R.** Experimental investigation on fluid flow maldistribution in plate fin heat exchangers, Heat Transfer Engineering 2003; 24(4): 25-31.

99. **Zhang Z, Li YZ**. CFD simulation on inlet configuration of plate-fin heat exchanger, Cryogenics (2003) 43: **(**12) 673-678.

100. **Wen J, Li Y.** Study of flow distribution and its improvement on the header of plate fin heat exchanger, Cryogenics (2004) 44: 8 23-31.

101. **Fleming, R. B.** The effects of flow distribution in parallel channels of counter flow heat exchangers, Advanced Cryogenic Engineering 1967 (December): 352.

102. **Jian Wen, Yanzhong Li, Aimin Zhou, Ke Zhang.Jiang Wang.** PIV experimental investigation of entrance configuration on flow maldistribution in plate fin heat exchanger, Cryogenics (2006) 46 37-48.

103. **Chowdhury, K., Sarangi, S.** The Effect of Variable specific Heat of the working Fluid on the Performance of counter flow Heat Exchangers, Cryogenics (1984) 2**4** 679-680

104. **Shah, R.K.** Non Uniform Heat Transfer Coefficients for Heat Exchanger Thermal Design in Aerospace Heat Exchanger Technology edited by R. K.Shah and A. Hashem (1993) 417-445.

105. **Paffenbarger, J.** General Computer Analysis of Multistream Plate Fin Heat Exchangers Compact Heat Exchangers –A Festschrift for A.L. London, (Eds. Shah, R.K., Kraus, A.D, and Metzger, D) Hemisphere Publishing New York (1990) 727-746

106. **Taylor, R.P., Hodge, B.K., James, C.A**. Estimating uncertainty in thermal systems analysis and design, Applied Thermal Engineering, (1999) **19** 51-73

107. **Moffat, R.J.** Describe the Uncertainties in Experimental Results, Experimental Thermal and Fluid Science (1988) **1** (1)3-17

108. **Evans, D.M.** The Role of Probable Uncertainty in the Design and Testing of Compact Heat Exchanger in Compact Heat Exchangers, History, Technological

Advancement and Mechanical Design Problems edited by R.K. Shah et al) (1980) HTD-Vol.**10** 135-143

109. **Lestina, T. Scott, B.** Assessing the Uncertainty of Thermal Performance Measurements of Industrial Heat Exchangers Proceedings of the International Conference on Compact Heat Exchangers in the Process Industries (1997) 401-416.

110. **Clarke, D.D., Vasquez, V.R., Whiting, W.B., Greiner, M.** Sensitivity and uncertainty analysis of heat exchanger designs to physical properties estimation, Applied Thermal Engineering 2001 (21) 993-1017

111. **Brown, K.K., Coleman, H.W., Steele W.G.,** A Methodology for Determining Experimental Uncertainties in Regressions, Proceedings of the ASME Fluids Engineering Division, ASME (1996) FED-Vol. **242** 263-273

112. **Walters, F.M.,** Hypersonic Research Engine Project –phase II A, category I Test report on fin Heat transfer and pressure drop testing, Data item No. 63.02, Ai Research Manufacturing co., Doc, AP-69-5348, 1969

113. **Aspen Muse Reference guide**, Cambridge, Massachusetts: Aspen Technology, Inc. V2006

114. **Fribance, Austine.** Industrial Instrumentation Fundamentals, McGraw-Hill (1962)

.

Curriculum Vitae

SIDRAMAPPA ALUR

E-mail: s.alur@rediffmail.com

Permenant Address: At Post Mannur
Tq Afzalpur.
Dist Gulbarga.
Pin Code – 585246
Karnataka, India

Education:

2012	Dissertation submitted
1995	M.E, Gulbarga University, Gulbarga.
1989	B.E, Gulbarga University, Gulbarga.

Personal Information:

Date of Birth	29-09-1966
Nationality	Indian

Employment:

1990 – 1992	**Lecturer,** M.C.E, Nilanga, Latur, Maharashtra.
1995 – 1997	***Lecturer***, R.E.C, Bhalki, Bidar, Karnataka.
1997 – Till Date	***Lecturer*****, Senor lecturer and Asst Professor, H.I.T**, Nidasoshi, Belgaum, Karnataka.

Publications:

1. **S.A.Alur., Balaji Kr Choudhury., R.K.Sahoo., Sunil Kr. Sarangi**., Simulation of Turboexpander Based Nitrogen Liquefier. Proceedings of the 20th National and 9th International ISHMT-ASME Heat and Mass Transfer Conference.January 4-6, 2010, Mumbai, India.
2. **S.A.Alur., Balaji Kr Choudhury., R.K.Sahoo., Sunil Kr. Sarangi.,** Design of High Expansion Ratio Turboexpander for nitrogen Liquefier. Proceedings of the 3rd International Conference on Advances in Mechanical Engineering, January 4-6, 2010., S.V. National Institute of Technology, Surat, India.
3. **Balaji Kr Choudhury., S.A.Alur., R.K.Sahoo., Sunil Kr. Sarangi.** Optimization Analysis of Liquefaction Cycles for Nitrogen., Indian Journal of Cryogenics**,** 37 (1-4), pp 34, 2012.
4. **S.A.Alur., Balaji Kr Choudhury., R.K.Sahoo., Sunil Kr. Sarangi**., Performance Analysis of plate fin heat exchanger at low Reynolds number. *23rd National Symposium on cryogenics (NSC-23).* October 26-30, 2010, National Institute of technology, Rourkela-769008, Orissa, India.

5. **S.A.Alur., Balaji Kr Choudhury., R.K.Sahoo., Sunil Kr. Sarangi**., Performance Analysis of plate fin heat exchanger. Asian conference on Applied Super conductivity and cryogenics, November 16-18, 2011, I.U.A.C, .New Delhi.

Papers Communicated:

1. **S.A.Alur., Balaji Kr Choudhury., R.K.Sahoo., Sunil Kr. Sarangi**.,Thermo hydraulic Performance of plate fin heat exchanger using hot fluid test at and above room temperature, Experimental thermal and Fluid Sciences, International journal of experimental heat transfer, Thermodynamics and Fluid Mechanics.